

AWARD NUMBER: W81XWH-07-1-0169

TITLE: Resetting the T Cell Repertoire in Prostate Cancer Bearing Host

PRINCIPAL INVESTIGATOR: Pan Zheng, M.D., Ph.D.

CONTRACTING ORGANIZATION: University of Michigan
Ann Arbor, MI 48109

REPORT DATE: March 2009

TYPE OF REPORT: Annual

PREPARED FOR: U.S. Army Medical Research and Materiel Command
Fort Detrick, Maryland 21702-5012

DISTRIBUTION STATEMENT: Approved for Public Release;
Distribution Unlimited

The views, opinions and/or findings contained in this report are those of the author(s) and should not be construed as an official Department of the Army position, policy or decision unless so designated by other documentation.

REPORT DOCUMENTATION PAGE

Form Approved
OMB No. 0704-0188

Public reporting burden for this collection of information is estimated to average 1 hour per response, including the time for reviewing instructions, searching existing data sources, gathering and maintaining the data needed, and completing and reviewing this collection of information. Send comments regarding this burden estimate or any other aspect of this collection of information, including suggestions for reducing this burden to Department of Defense, Washington Headquarters Services, Directorate for Information Operations and Reports (0704-0188), 1215 Jefferson Davis Highway, Suite 1204, Arlington, VA 22202-4302. Respondents should be aware that notwithstanding any other provision of law, no person shall be subject to any penalty for failing to comply with a collection of information if it does not display a currently valid OMB control number. **PLEASE DO NOT RETURN YOUR FORM TO THE ABOVE ADDRESS.**

1. REPORT DATE 1 March 2009		2. REPORT TYPE Annual		3. DATES COVERED 5 February 2008 – 4 February 2009	
4. TITLE AND SUBTITLE Resetting the T Cell Repertoire in Prostate Cancer Bearing Host				5a. CONTRACT NUMBER	
				5b. GRANT NUMBER W81XWH-07-1-0169	
				5c. PROGRAM ELEMENT NUMBER	
6. AUTHOR(S) Pan Zheng, M.D., Ph.D. E-Mail: panz@umich.edu				5d. PROJECT NUMBER	
				5e. TASK NUMBER	
				5f. WORK UNIT NUMBER	
7. PERFORMING ORGANIZATION NAME(S) AND ADDRESS(ES) University of Michigan Ann Arbor, MI 48109				8. PERFORMING ORGANIZATION REPORT NUMBER	
9. SPONSORING / MONITORING AGENCY NAME(S) AND ADDRESS(ES) U.S. Army Medical Research and Materiel Command Fort Detrick, Maryland 21702-5012				10. SPONSOR/MONITOR'S ACRONYM(S)	
				11. SPONSOR/MONITOR'S REPORT NUMBER(S)	
12. DISTRIBUTION / AVAILABILITY STATEMENT Approved for Public Release; Distribution Unlimited					
13. SUPPLEMENTARY NOTES					
14. ABSTRACT This is the second annual report on the grant "Resetting the T cell repertoire in prostate cancer bearing host". A major obstacle to effective anti-tumor immune response is immune tolerance to tumor antigens, mostly caused by the defective cancer-reactive T-cell repertoire and increased immune suppression by regulatory T cells. We proposed to reset the immune system of cancer-bearing host by rescuing cancer-reactive T cells and by eliminating the generation and survival of Treg. In the past funding period, we have published two papers that summarized our results from specific aim 2 in modulating Treg production in anti-tumor immunity. We have submitted the third paper in the role of lymphotoxin and its receptor in T cell negative selection. We applied the lymphotoxin receptor beta IgG Fc fusion protein to TRAMP prostate cancer mice and achieved the cancer preventive effect.					
15. SUBJECT TERMS Tumor immunology, costimulatory molecules, tumor antigens, immunotherapy					
16. SECURITY CLASSIFICATION OF:			17. LIMITATION OF ABSTRACT	18. NUMBER OF PAGES	19a. NAME OF RESPONSIBLE PERSON
a. REPORT	b. ABSTRACT	c. THIS PAGE			19b. TELEPHONE NUMBER (include area code)
U	U	U	UU		

Table of Contents

Introduction.....	4
Body.....	5
Key Research Accomplishments.....	10
Reportable Outcomes.....	11
Conclusions.....	13
References.....	None
Appendices.....	15

(4) Introduction

This is the revised second annual report (or Final Report) on the grant “**Resetting the T cell repertoire in prostate cancer bearing host**”.

A major obstacle to effective anti-tumor immune response is immune tolerance to tumor antigens, mostly caused by the defective cancer-reactive T-cell repertoire and increased immune suppression by regulatory T cells. It has been realized that T cell development in thymus is a continuous process throughout life span and androgen blockade results in the complete regeneration of the thymic function and restoration of peripheral T cell phenotype and function, both in mice and in human. We have demonstrated in the transgenic mouse prostate cancer (TRAMP) model that T cells reactive to tissue specific tumor antigens are deleted in the thymus. Our preliminary studies further indicated that lymphotoxin (LT)-*aire* pathway likely controls the expression of tumor antigens and the clonal deletion of T cells specific for tumor antigens in the thymus. We have also shown that costimulatory molecules are required for the generation of regulatory T cells (Treg). We proposed to reset the immune system of cancer-bearing host by rescuing cancer-reactive T cells and by eliminating the generation and survival of Treg.

In our proposal, we have proposed: (1). To rescue cancer-reactive T cells by preventing clonal deletion of tumor-reactive T cells in the thymus. (2). To block the Treg production using anti-B7 antibodies and to optimize the immunotherapy of prostate cancer using antibodies and fusion proteins. In the past funding period, we have published two papers that summarized our results from specific aim 2 in modulating Treg production in anti-tumor immunity. We have submitted the third paper in the role of lymphotoxin and its receptor in T cell negative selection for the specific aim 1. We applied the lymphotoxin receptor beta IgG Fc fusion protein to TRAMP prostate cancer mice and achieved the cancer preventive effect.

(5) Body of Annual Report**Task I. Rescuing cancer-reactive T cells by preventing clonal deletion of tumor-reactive T cells in the thymus. (Month 1-36). (Finished).**

*I-A. We will evaluate the contribution of *aire* and *LT*, the two major regulators of peripheral antigen expression in the thymus and of clonal deletion of tumor-reactive T cells in the thymus, using mice with targeted mutations of *aire*, lymphotoxin alpha, and lymphotoxin beta receptor. (Month 1-12) (Finished)*

- a. We have obtained the *aire* and *LT* alpha knock out mice from our collaborator, Dr. Yang-Xin Fu at the University of Chicago. We have started to breed the TRAMP mice with mice with targeted mutations. Two generations of cross will be needed to generate TRAMP+ *aire* (-/-) and TRAMP+ *LT* alpha (-/-). We are in good progress in this step and expect to have the right genotypic mice within 3-4 months. (Month 1-4). (Finished)*
- b. Analyze the mice at 8-12 weeks to obtain information on peripheral antigen expression profile from thymus by real time PCR. (Month 3-8). (Finished)*
- c. Analyze the effects of targeted mutations of *aire*, *LT* alpha and *LT* beta receptor on the thymic expression of peripheral tissue antigens and tumor associated antigens. (Month 5-12). (Finished).*

The work proposed in Task I-A was mainly to breed different genetic modified mice. We have finished this part. We tested the effects of targeted mutation of *Aire* gene on the thymic expression of peripheral tissue antigens as shown in Fig. 1. We found that the expression of mouse probasin gene was drastically decreased in *Aire* KO mice.

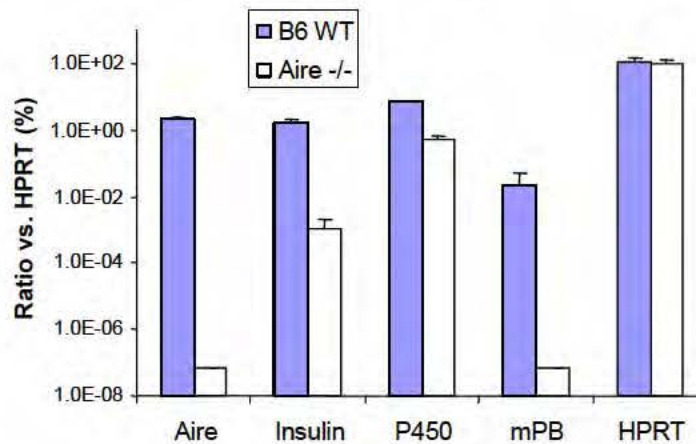


Fig. 1. Targeted mutation of *aire* abrogates expression of probasin gene in the thymus. Thymus tissues from WT and *aire*-deficient mice were homogenized and analyzed for the expression of several tissue-specific genes. Data shown are means and S.D. of triplicates and represent two independent experiments.

I-B. We will inhibit the expression of peripheral antigens in the thymus by using a soluble LT receptor that blocks membrane-bound LT and evaluate its effect in clonal deletion and mouse susceptibility to the spontaneously arisen prostate cancer in TRAMP mice (Month 1-36). (Finished).

- a. Backcross the three strains of knock out mice to B10.BR background at least 5 generations. We are currently in 4th generation in heterozygous state. We will backcross another generation (Month 1-6). (Finished)*
- b. Breed the mice generated in Task I-B-a with T cell receptor transgenic mice TgB. Two generations of cross will be needed to generate TgB+ aire (-/-) and TgB+ LT alpha (-/-) mice. (Month 6-18). (Finished).*

We have generated TgB+ aire (-/-) mice in past year. However, an unexpected genetic makeup of the LT alpha gene prevented us in generating TgB+ LT alpha (-/-) mice. The purpose of the breeding is to replace the H-2^b background of LT alpha (-/-) mice to H-2k for the B10.BR-TGB mice to present H-2^k related SV40 large T antigen epitope. After several months of frustration, we realized that LT alpha gene is in the same chromosome as H-2 (MHC gene). We will not be able to obtain the mice we expected.

We recently obtained the TCR-I transgenic mice that is in C57BL/6 background and recognize the H2-D^b-restricted SV40 large tumor antigen epitope I (residues 206-215) from Jackson Laboratory. We will breed this mice to LT alpha (-/-) mice to get TCR-I (+) LT alpha (-/-) mice.

- c. Generate TRAMP x TgB F1 mice that carry different target mutations. (Month 12-21). (Finished).*
- d. To study the impact of LT-aire pathway mutations on the tumor antigen expression and clonal deletion of the tumor antigen specific T cells in the thymus. (Month 18-24). (Finished).*

This part of work has been summarized in our manuscript “Targeting Lymphotoxin-mediated Negative Selection to Prevent Prostate Cancer in Mice with Genetic Predisposition”.

In summary, we have found that **targeted mutation of LT α limits clonal deletion of SV40 T antigen-specific T cells**. The figures correlated to this part are presented in Appendix 3, Fig. 1 A to D.

In our previous work that supported by DAMD17-03-0013 “Rescuing High Avidity T Cells for Prostate Cancer Immunotherapy”, we have shown that the profound immune tolerance to tumor antigen SV40 large T antigen in mouse prostate cancer TRAMP model was caused by thymic clonal deletion of high avidity tumor antigen specific T cells in the mice. The current proposal will consider different methods to reverse and break the immune tolerance and to enhance the anti-tumor immunity. Here we tested the idea that lymphotoxin pathway plays an important role in T cell development in thymus. We found that mutations in lymphotoxin alpha gene (through LTa KO mice) broke the negative selection of the tumor antigen reactive T cells in the thymus. Without LTa mutation, the TRAMP/TCR double transgenic mice have a very small thymus (10% of normal size) with extremely low tumor antigen specific, transgenic T cells. However, the one copy mutation of LTa increased the thymus size and led to the

increase numbers of tumor antigen specific T cells, and the both copy mutations of LTa (LTa knockout) drastically increased the thymus size to almost normal size and a large proportion of mature T cells are tumor antigen specific. Thus the target mutation of LTa abrogates the clonal deletion of the tumor antigen specific T cells.

- e. To study the function of rescued high avidity T cells in the TRAMP x TgB model. (Month 24-36). (Finished).*
- f. To study the function of rescued high avidity T cells in the TRAMP model. (Month 24-36). (Finished).*

The most impressive finding on this part is the MRI images taken from 30 weeks old TRAMP mice that carry targeted mutation of LTa. TRAMP mice developed spontaneous, aggressive prostate cancer beginning at 15-20 weeks. The wild type TRAMP mice at 30 weeks of age have almost 100% prostate cancer indicated by MRI image with much enlarged prostate gland. Many of the mice have metastasis in lung and liver. We found that targeted mutation of LTa inhibited the development of prostate cancer and the cancer metastasis in TRAMP mice. The data is presented in Appendix 3, Fig. 2 A to C.

- g. Using soluble LT beta receptor Ig fusion protein to treat TRAMP x TgB F1 mice to examine the effect of fusion protein on tumor antigen expression and T cell clonal deletion in the thymus. (Month 13-24). (Finished).*

LT beta receptor Ig fusion protein treatment had strong effect on rescuing tumor antigen specific T cells from negative selection. This part of data is presented in Appendix 3, Fig. 4 A to H to Fig. 5.

The effect of fusion protein treatment on thymic antigen expression is not remarkable as showed here as Fig. 2.

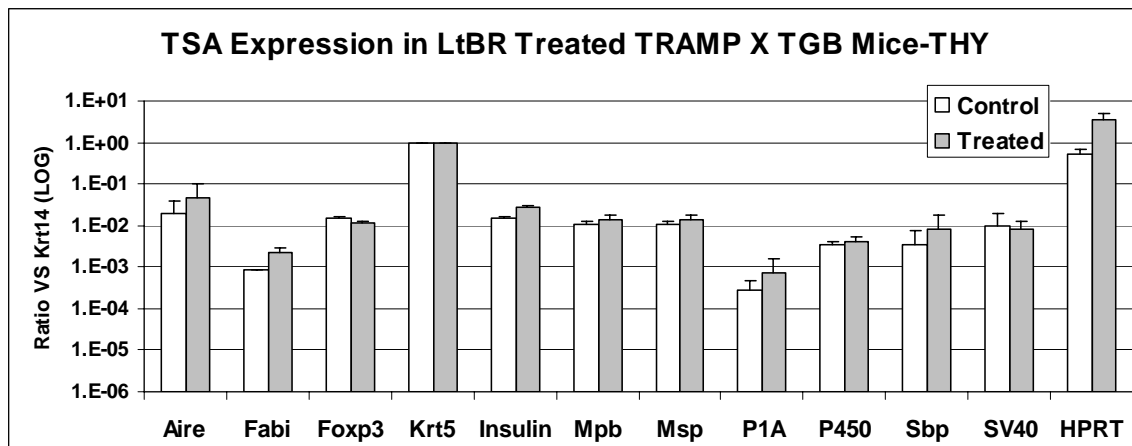


Fig. 2. The effect of LT beta receptor Ig fusion protein treatment on thymic expression of auto-antigens and tumor antigens. The fusion protein was administrated by IP with 100 ug/mouse/injection either LTbIgFc or human Ig-Fc to 8 weeks old TRAMP/TGB double transgenic mice. Total 5 injections, every other days. Two weeks after last injection, the

mRNA was isolated from thymic tissue and real time Q-PCR were performed. Five mice per group.

- h. Using soluble LT beta receptor Ig fusion protein to treat TRAMP mice to examine the effect of fusion protein on tumor antigen expression and T cell clonal deletion in the thymus. (Month 13-24). (Finished).*
- i. Long term survival surveillance on the mice that treated with fusion protein, record the tumor incidence, tumor size, metastasis and autoimmune side effect. (Month 18-36). (Finished).*

This part of data is presented in Appendix 3, Fig. 5 and 6 for effect of LT beta receptor Ig fusion protein treatment on TRAMP mice.

I-C. We will explore the combination of androgen ablation and soluble LT beta receptor Ig fusion protein and evaluate the effect on thymic regeneration and rescuing tumor antigen specific T cells in older TRAMP mice (Month 1-36). (We request modification).

The progress in this sub-aim is delayed due to the approval of animal surgical castration procedure. It was reviewed and considered to cause excessive pain to mice in surgical castration by DOD ACURO committee. It took me a long time for back and forth communication with ACURO. Since the tumor preventive effect is strong by administration of LT beta receptor Ig fusion protein, we considered that the proposed combination experiments were no longer informative.

I-D. The impact of soluble LT beta receptor Ig fusion protein on autoimmune inflammation.

- a. We will systemically examine the effect of soluble LT beta receptor Ig fusion protein in inducing autoimmune side effects. Wild type mice age week 4, 6, 8, 16, 24, 36 will be injected with soluble LT beta receptor Ig fusion protein and short-term (within two weeks) and long-term (three months) side effect will be studied. Histological sections will be prepared and the lymphocytic infiltration will be examined in skin, colon, stomach, heart, lung, liver and kidney. Immunofluorescence staining will be done on frozen section of kidney and skin tissue to detect IgG and C3 deposits. (Month 13-36). (Finished).*
- b. All the above mentioned (Aim I-B, I-C) mice that were treated with soluble LT beta receptor Ig fusion protein will be examined vigorously as described above. (Month 1-36). (Finished).*

This part of data is presented in Appendix 3, Fig. 3 and Table 1. We have found that the treatment of fusion protein induced lymphocyte infiltration to multiple organs if the age of the mice was less than 6 weeks. When the fusion protein was given to older mice, there was no lymphocyte infiltration in different organs.

II. Transient blockade of Treg production and immunotherapy of prostate cancer (Month 1-36). (Finished).

- II-A. We will develop the immunotherapy of prostate cancer by transient B7 blockade. We will identify an optimal blockade condition that reduces Treg development without blocking activation of effector T cells. (Month 9-24) (**Finished**)
- a. To perform adoptive transfer experiments to examine the short-term and long-term effect of costimulatory blockade on Treg and the effect on the tumor antigen specific T cell activation. (Month 9-15). (**Finished**)
 - b. To study the activation, differentiation of tumor antigen specific T cells after the release of Treg blockade. (Month 11-17). (**Finished**)
 - c. To study the recruitment of T cells into prostate tissue (Month 12-24). (**Finished**).

The manuscript “B7 Blockade Re-Balances Regulatory T cells and Tumor-reactive T Cells for Prevention and Therapy of Prostate Cancer” was published and is attached as Appendix 1.

- II-B. We will explore combination therapy targeting at regenerating thymic function, reducing Treg and rescuing cancer-reactive T cells. (Month 13-36). (**In progress**).
- a. To study the impact of LT beta receptor Ig fusion protein on the development of Treg. (Month 13-18). (**Finished**).
 - b. To modify the combination therapy (surgical castrated, soluble LT beta receptor Ig fusion protein treatment, anti-B7 antibody treatment) in the TRAMP x TgB mouse model (Month 15-24). (**In progress**).
 - c. To modify the combination therapy (surgical castrated, soluble LT beta receptor Ig fusion protein treatment, anti-B7 antibody treatment) in the TRAMP mouse model (Month 25-36). (**In progress**).

(6) Key Research Accomplishments

- We have found that B7-1 and B7-2 are required for the production of regulatory T cells. Anti-B7 antibodies significantly reduced the number of Treg in the thymus and in the spleen. **(Appendix 2, paper published).**
- We have shown that anti-B7 antibody treatment in adult TRAMP mice prolonged the mice survival for more than 10 weeks.
- We have established that expression of tissue-specific antigen/tumor antigen in the thymus and clonal deletion of tumor-reactive T cells can be modulated in the TRAMP mice.
- We have established collaboration with Department of Radiology in University of Michigan to successfully measure prostate glands and prostate tumors with MRI.
- We demonstrated that temporary blockade of B7-1 and B7-2 reduced the number of regulatory T cells and conveyed considerable therapeutic effects in TRAMP mice with spontaneous prostate cancer. To our knowledge, this is the first time that the prostate cancer in the TRAMP mice can be effectively treated when the large tumors can be demonstrated.
- Mechanistically we showed that transient blockade of B7-1/2 resets the balance of Treg and cancer reactive T cells to confer prevention and therapy of prostate cancer. A second major advantage is that the data can be easily translated into human use as the drug that blocks B7-1 and B7-2 (FDA approved CTLA4Ig) has already been approved for the treatment of autoimmune diseases. It is possible to dramatically shorten the path of clinical development for the novel immunotherapy. **(Appendix 1, paper published)**
- We showed that the development of NKT cells are defect in the mice with targeted mutations of B7-1/2 and CD28. The percentage of $\text{TCR}_\beta^+ \text{NK1.1}^+$, as well as $\text{TCR}_\beta^+ \alpha\text{-Galcer/CD1d}^+$ (iV α 14 NKT) cells population are significantly reduced in the thymus, spleen and liver in the mice with targeted mutations of B7-1/2 and CD28.
- We have shown the mice with target mutation of costimulatory molecules have defect NKT cell function. B7 and CD28 deficient mice develop much less severe ConA induced hepatitis, which is known mediated by NKT cells. **(Paper published in PLoS ONE and attached as Appendix 4).**
- We have shown that targeted mutation of the *LT α* gene efficiently rescued tumor-reactive T cells, drastically reduced cancer incidence and almost completely ablated metastasis.
- We have shown that, remarkably, short-term treatments with LT β RIg interrupted clonal deletion, reduced the size of primary cancer and completely prevented metastasis later in life, thus providing an easily translatable immune prevention for those with genetic predisposition to cancer. **(Appendix 3).**

•
(7) Reportable Outcomes:

Manuscripts:

1. Penghui Zhou, Xincheng Zheng, Huiming Zhang, Yang Liu and Pan Zheng. B7 Blockade Re-Balances Regulatory T cells and Tumor-reactive T Cells for Prevention and Therapy of Prostate Cancer. *Clinical Cancer Research*. 2009. 15:960-970. (Appendix 1).
2. Proietto AI, van Dommelen S, Zhou P, Rizzitelli A, D'Amico A, Steptoe RJ, Naik SH, Lahoud MH, Liu Y, Zheng P, Shortman K, Wu L. Dendritic cells in the thymus contribute to T-regulatory cell induction. *Proc Natl Acad Sci U S A*. 2008. 105:19869-74. (Appendix 2).
3. Penghui Zhou, Xianfeng Fang, Ping Yu, Mingzhao Zhu, Yang-Xin Fu, Lizhong Wang, Yang Liu and Pan Zheng. Targeting Lymphotoxin-mediated Negative Selection to Prevent Prostate Cancer in Mice with Genetic Predisposition. 2009. Submitted. (Appendix 3).
4. Zheng X, Zhang H, Yin L, Wang CR, Liu Y, **Zheng P**. 2008. Modulation of NKT cell development by B7-CD28 interaction: an expanding horizon for costimulation. *PLoS ONE*. 3(7):e2703. (Appendix 4).

Graduate students supported by this grant:

Penghui Zhou: Successfully finished his PhD thesis in December, 2008.

Manuscripts with Penghui Zhou as first author or co-author:

1. Proietto AI, van Dommelen S, **Zhou P**, Rizzitelli A, D'Amico A, Steptoe RJ, Naik SH, Lahoud MH, Liu Y, Zheng P, Shortman K, Wu L. Dendritic cells in the thymus contribute to T-regulatory cell induction. *Proc Natl Acad Sci U S A*. 2008. 105:19869-74.
2. **Penghui Zhou**, Xianfeng Fang, Ping Yu, Mingzhao Zhu, Yang-Xin Fu, Lizhong Wang, Yang Liu and Pan Zheng. Targeting Lymphotoxin-mediated Negative Selection to Prevent Prostate Cancer in Mice with Genetic Predisposition. 2009. Submitted.
3. Liu R, Wang L, Chen C, Liu Y, **Zhou P**, Wang Y, Wang X, Turnbull J, Minassian BA, Liu Y, Zheng P. 2008. Laforin negatively regulates cell cycle progression through GSK-3{beta} dependent mechanisms. *Mol Cell Biol*. 28:7236-44.

4. May KF Jr, Chang X, Zhang H, Lute KD, **Zhou P**, Kocak E, **Zheng P**, Liu Y. 2007. B7-deficient autoreactive T cells are highly susceptible to suppression by CD4(+)CD25(+) regulatory T cells. *J Immunol.* 178(3):1542-52.5.
5. **Penghui Zhou**, Xincheng Zheng, Huiming Zhang, Yang Liu and Pan Zheng. B7 Blockade Re-Balances Regulatory T cells and Tumor-reactive T Cells for Prevention and Therapy of Prostate Cancer. *Clinical Cancer Research.* 2009. 15:960-970.

Chong Chen: Successfully finished his PhD thesis in December, 2008.

Manuscripts with Chong Chen as first author or co-author:

1. **Chen C**, Liu Y, Liu R, Ikenoue T, Guan KL, Liu Y, Zheng P. 2008. TSC-mTOR maintains quiescence and function of hematopoietic stem cells by repressing mitochondrial biogenesis and reactive oxygen species. *J Exp Med.* 205(10):2397-408.
2. Liu R, Wang L, **Chen C**, Liu Y, Zhou P, Wang Y, Wang X, Turnbull J, Minassian BA, Liu Y, Zheng P. 2008. Laforin negatively regulates cell cycle progression through GSK-3{beta} dependent mechanisms. *Mol Cell Biol.* 28:7236-44.
3. Liu RH, Wang LZ, Chen G, Katoh H, **Chen C**, Liu Y, Zheng P. 2009. FOXP3 Up-regulates p21 Expression by Site-specific Inhibition of Histone Deacetylase 2/4 Association to the Locus. *Cancer Res* 69:2252-2259.
4. **Chen C**, Liu Y, Liu Y, Zheng P. 2009. The axis of mTOR-mitochondria-ROS and stemness of the hematopoietic stem cells. *Cell Cycle* 8(8): 1158-1169.
5. Chen GY, **Chen C**, Wang L, Chang X, Zheng P, Liu Y. 2008. Broad expression of the FoxP3 locus in epithelial cells: a caution against early interpretation of fatal inflammatory diseases following in vivo depletion of FoxP3-expressing cells. *J Immunol.* Cutting edge. 180(8):5163-6.

Patent filed:

U of M Ref. No. 3960; HDP Ref. No. 2115-003960/US/PS1; Title: Rebalance Regulatory and Effector T Cells With B7 Blockade for Cancer Immunotherapy.

(8) Conclusions:

In summary, in this funding period, we have demonstrated that a short-term anti-B7 blockade re-balances regulatory T cells and tumor-reactive T cells for prevention and therapy of prostate cancer.

It is generally agreed that immunotherapy is very inefficient for treatment of established tumors. This can be more challenging in transgenic tumor models where malignant tumor cells continue to arise due to transgenic expression of oncogenes. Our data demonstrated that even when administered at a time when the TRAMP mice show more than three fold enlargement of prostate size, transient blockade of B7-1 and B7-2 dramatically reduced the rate of tumor growth. Thus, at eight weeks after initiation of the treatment, the prostate of the control Ig-treated expanded by five fold in volume. In contrast, those from anti-B7-treated mice expanded by less than two fold during the same period. When the palpable tumors were used as endpoint, the anti-B7 treatment at 25 weeks reduced tumor development by 7 weeks. Nevertheless, perhaps because of the continuous production of new cancer cells from the germline insertion of SV40 large T antigen and waning of antibodies, short term treatment did not completely eradicate the tumors. However, consider the relatively simplicity of the treatment, it may show greater efficacy when apply to human prostate cancer patients as the cancer growth rate is expected to be slower than oncogene transgenic mice such as TRAMP mice.

Identification of genetically susceptible individuals calls for preventive measures to minimize the life-long cancer risk of these high risk populations. Immune prevention is made necessary by the anticipated health threat but only possible by predictability of antigens. Lack of enough high affinity of T cells against tumor-associated antigens and unpredictability of tumor antigen make antigen-based immune prevention untenable for cancer. To address this issue, we explored a non-antigen-based cancer immune prevention using the TRAMP mice that spontaneously develop prostate cancer with 100% penetrance. We show that targeted mutation of the *LT α* gene efficiently rescued tumor-reactive T cells, drastically reduced cancer incidence and almost completely ablated metastasis. Remarkably, short-term treatments with LT β RIg interrupted clonal deletion, reduced the size of primary cancer and completely prevented metastasis later in life, thus providing an easily translatable immune prevention for those with genetic predisposition to cancer.

**(9) References:
None.**

B7 Blockade Alters the Balance between Regulatory T Cells and Tumor-reactive T Cells for Immunotherapy of Cancer

Penghui Zhou,¹ Xincheng Zheng,² Huiming Zhang,¹ Yang Liu,¹ and Pan Zheng¹

Abstract Purpose: In prostate cancer bearing host, regulatory T (Treg) cells restrain activity of tumor antigen specific T cells. Because B7:CD28 interactions are needed for both function of CD4⁺CD25⁺ Treg cells and CD8⁺ effective T cells, targeting this pathway may help to overcome the immunotherapy barriers.

Experimental Design: The anti B7 1/B7 2 monoclonal antibodies were administered to a transgenic mouse model of prostate cancer (TRAMP) ectopically expressing SV40 large T antigen in different tumor development stages for prevention and therapy of prostate cancer. The treatment was also tested in treating transplanted MC38 colon adenocarcinoma in mice.

Results: Here, we showed that short term administration of anti B7 1/B7 2 monoclonal antibodies in TRAMP mice leads to significant inhibited primary tumor growth and the size of metastatic lesions. The treatment is effective to inhibit MC38 colon cancer growth. Correspondingly, this treatment results in a transient reduction of Treg in both thymus and the periphery. *In vivo* cytotoxicity assay revealed T antigen specific CTL effectors in anti B7 treated but not control IgG treated TRAMP mice.

Conclusions: Transient blockade of B7 1/B7 2 alters the balance between Treg and cancer reactive T cells to enhance cancer immunotherapy.

Many of tumor antigens identified thus far are self antigens (1–4) and may therefore trigger immune tolerance. Logically, mechanisms that mediate self tolerance may contribute to inadequacy of tumor immunity. The best characterized mechanism of self tolerance is clonal deletion (5, 6). In this context, we have shown that tumor antigen controlled by tissue specific promoter is also expressed in the thymus to trigger clonal deletion (7).

In addition to clonal deletion, CD4⁺CD25⁺ regulatory T (Treg) cells play a pivotal role in the maintenance of peripheral self tolerance (8–12). Accumulating evidence also support a role for Treg in restrained cancer immunity. Thus, cancer patients have elevated numbers of Treg cells in the blood of malignant effusions (13–15). Treg cells are also recruited and

accumulated at tumor sites in animal models and in cancer patients (16–18). Correlation between the number of CD4⁺CD25⁺ Treg cells and clinical outcomes in some, although not all, cancer patients supported the hypothesis that Treg may suppress the effector function of tumor antigen specific T cells, allowing tumor growth in the presence of tumor antigen specific T cells (19, 20). Consistent with this concept, the removal of CD4⁺CD25⁺ Treg cells by an anti CD25 antibody promoted rejection of transplanted tumor cells (21). However, this approach has shown little efficacy in animals with spontaneous tumors, which better reflect the challenge of cancer immunotherapy. In a recent study using a transgenic model of prostate dysplasia, anti CD25 monoclonal antibody (mAb) treatment at age 12 weeks caused only 25% reduction in the prostate mass at 20 weeks, although extended observation has not been carried out to document long term effect (22).

Alternatively, it is worth considering conditions that are selectively required for the generation and maintenance of Treg. CD28^{-/-} and B7 1/B7 2^{-/-} mice have markedly decreased numbers of CD4⁺CD25⁺ Treg cells in the thymus as well as in the periphery (23–25). Meanwhile, we and others have reported a significant role for B7:CD28 interaction in clonal deletion of some, although not necessarily all, self antigens (26, 27). As such, transient blockade of B7 1/B7 2 may reduce Treg while increase the frequency of cancer reactive T cells, thus overcoming the two major barriers to effective cancer immunity.

Transgenic mouse model of prostate cancer (TRAMP) is a well established mouse model for prostate cancer with clearly defined progression of prostate cancer that resembles the human disease (28). Metastasis to periaortic lymph nodes and lungs can be detected frequently (29). By the time the mice are 24 to 30 weeks old, the prostate cancer becomes palpable in

Authors' Affiliations: ¹Department of Surgery and Pathology, University of Michigan Medical Center, Program of Molecular Mechanism of Diseases and Comprehensive Cancer Center, Ann Arbor, Michigan and ²OncImmune, Inc., Columbus, Ohio

Received 6/24/08; revised 10/7/08; accepted 10/7/08.

Grant support: Department of Defense and American Cancer Society (P. Zheng) and NIH grants AI064350 and CA12001 (Y. Liu).

The costs of publication of this article were defrayed in part by the payment of page charges. This article must therefore be hereby marked *advertisement* in accordance with 18 U.S.C. Section 1734 solely to indicate this fact.

Note: Supplementary data for this article are available at Clinical Cancer Research Online (<http://clincancerres.aacrjournals.org/>).

P. Zhou and X. Zheng contributed equally to this study.

Requests for reprints: Pan Zheng, Department of Surgery and Pathology, University of Michigan Medical Center, Program of Molecular Mechanism of Diseases and Comprehensive Cancer Center, BSRB 1810, 109 Zina Pitcher Place, Ann Arbor, MI 48109. Phone: 734-615-3464; Fax: 734-763-2162; E-mail: panz@umich.edu.

©2009 American Association for Cancer Research.

doi:10.1158/1078-0432.CCR-08-1611

Translational Relevance

Despite the conceptual advances in cancer immunotherapy, clinical development has been slow. Immunotherapy has thus far failed to show clear cut effect once cancers are established in advance stage. In this article, we showed that temporary blockade of B7 1 and B7 2 reduced the number of regulatory T cells and conveyed considerable therapeutic effects in transgenic mouse model of prostate cancer mice with spontaneous prostate cancer. To our knowledge, this is the first time that the prostate cancer in the transgenic mouse model of prostate cancer mice can be effectively treated when the large tumors can be shown. Mechanistically, we showed that transient blockade of B7 1/B7 2 resets the balance of regulatory T cells and cancer reactive T cells to confer prevention and therapy of prostate cancer. A second major advantage is that the data can be easily translated into human use as the drug that blocks B7 1 and B7 2 (Food and Drug Administration approved CTLA4Ig) has already been approved for the treatment of autoimmune diseases. It is possible to dramatically shorten the path of clinical development for the novel immunotherapy.

the abdomen. We have adopted the TRAMP mouse model to test our hypothesis while facing the challenge of treating established spontaneous tumors. We report here that transient blockade of B7 1/B7 2 with mAbs resulted in temporal deletion of Treg and rescue of cancer reactive T cells from clonal deletion. These effects associated with increased effector function of CTLs. Remarkably, the relatively simple treatment confers prevention and therapy of the spontaneous prostate cancer and transplantable colon cancer. Because recombinant protein that blocks B7 1 and B7 2 has already been approved for human use, the path for translating our observation into patient care is considerably shorter than most therapeutic approach.

Materials and Methods

Experimental animals. C57BL/6 mice and TRAMP mice expressing the SV40 T antigen (TAg) controlled by rat probasin regulatory elements in the C57BL/6 background were purchased from The Jackson Laboratory. The mice were bred at the animal facilities of the Ohio State University and the University of Michigan. All animal experimental procedures were reviewed and approved by The Ohio State University and University of Michigan Institutional Animal Care and Use Committees. Mice were typed for SV40 TAg by isolation of mouse tail genomic DNA. The PCR based screening assay was described previously (7). Transgenic mice expressing T cell receptor (TCR) specific for SV40 large TAg (TGB) have been described (30). Generation of TRAMP mice expressing TGB TCR (TGB TRAMP) was also described (7).

Antibody treatment of the TRAMP mice. TRAMP mice were treated with anti B7 1 and anti B7 2 antibodies at two different stages. In the first regiment, 4 to 6 week old TRAMP male mice were injected intraperitoneally with five injections of anti B7 1 (rat anti mouse CD80, clone 3A12; ref. 31) and anti B7 2 (hamster anti mouse CD86, clone GL 1; American Type Culture Collection; ref. 32) antibodies or control hamster/rat IgG (Sigma) at 100 µg/antibody/injection every other day. Long term prostate cancer incidence was recorded by physical examination. In the second regiment, 25 week old TRAMP male mice

without palpable prostate cancer were treated intraperitoneally with the anti B7 or control IgG at 100 µg/antibody/injection for five injections every other days. The magnetic resonance imaging (MRI) examination was carried out before treatment and 8 weeks later at age 33 weeks. In a separate experiment, 25 week old TRAMP male mice were treated with one intraperitoneal injection of 1 mg anti CD25 (PC61) or control rat IgG (33). The efficiency of anti CD25 depletion was examined by flow cytometry with staining PBL using conjugated anti CD4, anti CD25 (clone 7D4; American Type Culture Collection), and anti Foxp3. The MRI examination was carried out before treatment and 5 weeks later at age 30 weeks. For long term prostate cancer incidence study, anti B7 and control IgG treated mice were examined at least weekly for palpable tumor at lower abdomen and were euthanized when they either become moribund or with tumor size exceeding 5% of body weight.

Six to 8 week old TRAMP or TRAMP/TGB mice were sublethally irradiated (500 rad) on day 0 and the treatment started on day 1 with either anti B7 1/B7 2 mAbs (100 µg/each) or control rat/hamster IgG (100 µg/each) intraperitoneally. The mice were treated six times every other days. One week after the last treatment, the mice were sacrificed and the total thymocytes and splenocytes were harvested and stained with fluorochrome conjugated antibodies anti CD4 (RM4.5), anti CD8 (53 6.7), and anti Vβ8.1+8.2 (MR5 2; BD).

For transplantable tumor model, MC38 murine colon carcinoma cells were grown in RPMI with 5% fetal bovine serum and subcutaneously injected to male C57BL/6 mice (5×10^5 per mouse). Ten days after injection, mice were divided evenly into two groups based on the tumor sizes and administered intraperitoneally with either anti B7 or control IgG three times every other day. Peripheral blood was collected at 0 and 6 days (0 day is the day before the administration of antibodies) and the splenocytes were collected at 14 days and stained with anti CD4, CD8, CD25, and Foxp3 antibodies (BD).

Proliferation of T cells to antigenic peptides. Total spleen cells (3×10^5 per well) from control immunoglobulin or anti B7 treated TRAMP \times TGB ($H 2^{b*}$) F_1 mice were cultured with the given concentrations of SV40 TAg K560 568 peptide or control HSV gB peptide in Click's Eagle's Hank's amino acid medium for 72 h. The proliferation of T cells was determined by incorporation of [3 H]thymidine pulsed (1 µCi/well) during the last 6 h of culture. The data presented are means of triplicates with variation from the means <15%.

Peptide synthesis. All peptides used were synthesized by Research Genetics. The peptides were dissolved in DMSO at a concentration of 10 mg/mL and diluted in PBS or culture medium before use. Peptides used were SV40 TAg 560 568 SEFLLEKRI (7) and HSV gB peptide gB498 505 SSIEFARL (34).

Immunohistochemistry. Mouse organs were fixed with 10% buffered formalin. Tissue sections were stained with H&E and examined under a microscope. Frozen sections were prepared and stained with 2 µg/mL antibodies specific for CD3 (2C11, hamster IgG). CD3⁺ foci were counted using $\times 20$ microscope visual fields.

In vivo cytotoxicity assay. Spleen cells from C57BL/6 mice were pulsed with 10 µg/mL of either SV40 TAg 560 568 SEFLLEKRI or a control peptide HSV gB498 505 SSIEFARL in the presence of either 0.5 or 5 mmol/L CFSE, respectively. After mixing at a 1:1 ratio, the labeled cells were injected intravenously into recipients and spleen cells were harvested 20 h later and analyzed by flow cytometry for the relative abundance of CFSE^{low} (SV40 TAg peptide) and CFSE^{hi} (HSV peptide) populations.

Detection of anti double stranded DNA. Anti DNA antibodies were measured by ELISA according to the published procedure (35).

MRI of prostate. The progression of prostate cancer in the TRAMP model was measured by MRI as described (36). Briefly, MRI experiments was done on a Varian system equipped with a 7.0 Tesla, 18.3 cm horizontal bore magnet (300 MHz proton frequency). For MRI examination, the mice will be anesthetized with sodium pentobarbital (70 mg/kg intraperitoneally) and maintained at 37°C inside the magnet using a heated circulation water blanket, with pelvis motion (due to respiration) minimized by a small plastic support placed before

insertion into a 3 cm diameter quadrature birdcage coil (USA Instruments). Multislice images was acquired using a T_1 weighted spin echo sequence (TR/TE = 880/13, field of view = 30×30 mm using a 128×128 matrix, slice thickness = 1.5 mm, and slice separation = 1.0–1.6 mm). Each set contained 9 to 25 slices and enough sets were obtained to provide contiguous image data of the prostate tumor. Prostate volume will be measured using the formula: $V = 4 / 3[(D_1 + D_2) / 4]^3 \pi$, where D_1 and D_2 correspond to the longest and shortest (transverse and sagittal) diameters measured from the MRI image. The accuracy of this measurement was confirmed by comparing pre necropsy MRI volumes with postnecropsy actual prostate volumes in select cases.

Results

Anti-B7-1/B7-2 antibody treatment of young TRAMP mice reduced Treg cells in both the thymus and the periphery and delay development of prostate cancer. We and others have reported that targeted mutation of CD28 and B7 1/B7 2 abrogated generation of Treg cells (23). To test whether this pathway can be targeted for transient reduction of Treg, we treated C57BL/6 mice with either anti B7 1/B7 2 mAbs or control IgG five times every other day. Thymi and spleens were harvested 8 days after the last injection. Cells were stained for flow cytometry analysis. This treatment did not affect either the total cellularity or the numbers of CD4 and CD8 T cells (Fig. 1A). However, the numbers of CD4⁺FoxP3⁺CD25⁺ cells were reduced by 50% in thymus and by 4 fold in the spleen (Fig. 1B). When gated on lymphocyte gate, all CD4⁺ T cells are CD3⁺ (Supplementary Fig. S1). Therefore, all FoxP3⁺CD25⁺ cells analyzed in this study are Treg. These data indicate that Treg cells can be significantly reduced in both the thymus and the spleen by anti B7 1/B7 2 antibodies.

To investigate whether anti B7 1/B7 2 antibody treatment delay the development of prostate cancer, 4 week old male TRAMP mice were treated with either control IgG or anti B7 1/B7 2 antibodies and the incidence of cancer development was followed by physical examination. Using 50% of mice with palpable prostate cancer as a reference point, we observed that anti B7 delayed the tumor development by >14 weeks (Fig. 1C). Therefore, anti B7 treatment may be valuable for prevention of prostate cancer development.

Enhanced tumor specific cytotoxicity after anti-B7-1/B7-2 antibody treatment. To test tumor antigen specific immunity following anti B7 1/B7 2 treatment, we further investigated the tumor specific cytotoxicity by an *in vivo* killing assay. Six week old male TRAMP mice were injected intraperitoneally with anti B7 1/B7 2 mAbs or control IgG five times every other day. Two weeks after the first injection, they received an intravenous injection of a 1:1 mixture of SV40 TAg peptide pulsed (CFSE^{lo}) and control HSV gB peptide pulsed (CFSE^{hi}) spleen cells. The spleens were harvested 20 h later and analyzed by flow cytometry. As shown in Fig. 2A, in mice treated with anti B7 antibodies, the SV40 TAg pulsed targets were preferentially eliminated, whereas the CFSE^{lo} and CFSE^{hi} cells remained at the 1:1 ratio in control immunoglobulin treated mice. These data showed that anti B7 treatment enhanced CTL response against the SV40 large TAg without intentional immunization.

Anti-B7 antibodies rescued SV40 large T-specific T cells from clonal deletion in the TRAMP mice. Our previous studies have shown that SV40 large TAg is expressed in the thymic peripheral

antigen expressing cells in the TRAMP mice and that such expression caused nearly complete deletion of transgenic T cells expressing a TCR specific for a SV40 large TAg peptide presented by H 2K^k (7). Moreover, we reported that perinatal blockade of B7 1 and B7 2 reduced clonal deletion of autoreactive T cells (26). To test whether the anti B7 treatment rescues SV40 TAg specific T cells from clonal deletion in the TRAMP mice, we produced TRAMP mice expressing the SV40 TAg specific TGB TCR and divided the double transgenic mice with either anti B7 mAbs or control IgG treatment groups.

As the mice recovered from irradiation, a new wave of bone marrow derived cells will differentiate into mature T cells in the thymus. This *de novo* process increases sensitivity of blocking studies (37). To study the effect of anti B7 treatment on newly formed T cells undergone thymic development and clonal deletion, we gave sublethal irradiation (500 rad) to TGB single transgenic and TRAMP/TGB double transgenic mice. At 1 week after six treatments, the thymic cellularity and mature CD8 T cells were measured by flow cytometry. As shown in Fig. 2B, due to clonal deletion, the numbers of reconstituted thymocytes were extremely low in the double transgenic TGB TRAMP mice compared with single transgenic TGB. Importantly, anti B7 treatment increased thymic cellularity by ~10 fold (Fig. 2B). A corresponding increase in the CD8 T cells expressing high levels of V β 8⁺ transgenic TCR was observed in both spleen and thymus (Fig. 2C, left). When the spleen cells were analyzed for CD4/CD8 T cell ratios, it was clear that, perhaps due to clonal deletion, T cells in the control immunoglobulin treated mice have lost the predominance of CD8 subset due to expression of MHC class I restricted TCR. This is corrected to a large extent by anti B7 treatment (Fig. 2C, right). Thus, anti B7 treatment greatly reduced efficiency of clonal deletion. However, the numbers of transgenic T cells in the anti B7 treated TGB TRAMP mice were still much reduced in comparison with TGB mice, which showed that the rescue is only partial.

To test the whether the T cells rescued by anti B7 treatment were responsive to tumor antigen, we stimulated spleen cells from control immunoglobulin or anti B7 treated mice with different concentration of the SV40 TAg peptide or control peptide from HSV peptide. As shown in Fig. 2D, anti B7 treated spleen cells underwent a significant proliferation to SV40 TAg peptide. Based on the dose response, the anti B7 treated spleen cells were at least 100 fold more responsive than the control immunoglobulin treated spleen cells, which corresponded to increased number of antigen specific T cells. Therefore, the anti B7 rescued T cells are functional. However, after *in vitro* stimulation, the rescued T cells showed poor cytotoxicity (data not shown), which suggests that the rescued T cells may be functionally impaired to some extent.

Anti-B7-1/B7-2 antibody treatment cause significant albeit transient reduction of Treg in mice with established prostate cancer. One of the most difficult challenges in cancer immunotherapy is the treatment of established solid tumors. It has been shown that microscopic lesion of prostate cancer can be observed in the TRAMP mice between ages 18 and 24 weeks (29). To confirm the development of tumor in the 25 week old TRAMP mice in our colony, we used the MRI to compare the size of the prostate at 25 weeks. As shown in Fig. 3A, all of the 12 TRAMP mice tested had considerably larger

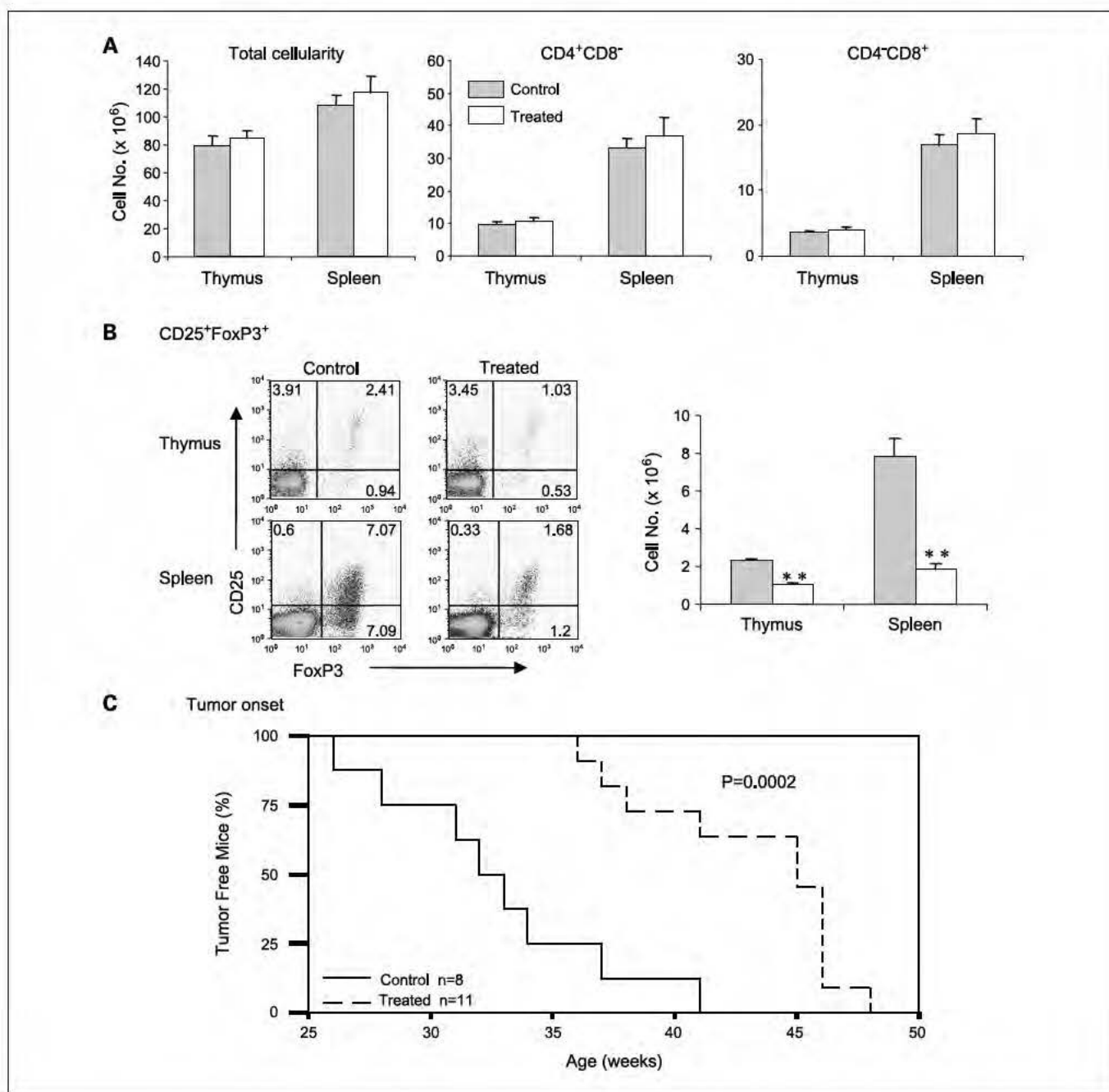


Fig. 1. Anti-B7-1/B7-2 antibody treatment reduced Treg in both the thymus and the periphery of normal mice and delayed the development of palpable tumors in TRAMP mice. *A* and *B*. C57BL/6 mice were injected intraperitoneally with either anti-B7-1/B7-2 mAbs (1:1 mixture of 100 μ g 3A12 and 100 μ g GL-1) or control IgG (1:1 mixture of 100 μ g hamster and 100 μ g rat IgG) at 6 wk old five times every other day. The mice were sacrificed 8 d after the last injection. Thymocytes and splenocytes were harvested and analyzed by flow cytometry. *A*, anti-B7-1/B7-2 antibody treatment did not alter the number of thymocytes, spleen cells, and CD4 and CD8 subsets. *B*, anti-B7-1/B7-2 antibody treatment reduced CD25⁺Foxp3⁺ cells in both thymus and spleen. Plots are from CD4⁺ cells among the lymphocyte gates. *, $P < 0.05$; **, $P < 0.01$, Student's *t* test. *C*, Kaplan-Meier analysis of tumor incidence. The experimental endpoint is 2 cm in tumor diameter as determined by palpation. Data have been repeated three times.

prostate organ sizes compared with non TRAMP littermate. Thus, essentially all of the 25 week old TRAMP mice developed cancer in the prostate.

To determine the effect of anti B7 antibodies for B7 1 and B7 2, we injected either control or anti B7 mAbs every other day for five times. The blood samples were collected at 0, 1, 2, or 6 weeks after antibody treatment and stained for either anti CD25 or anti Foxp3 in conjunction with anti CD4. As shown

in Fig. 3B, in comparison with control immunoglobulin treated mice, significant reduction of Treg can be observed in the peripheral blood at 1 and 2 weeks after completion of the treatment. Interestingly, the number of Treg is restored to normal levels at 6 weeks after completion of the treatments. Thus, in mice bearing established prostate cancer, anti B7 1 and anti B7 2 antibodies caused a significant albeit transient reduction of Treg in tumor bearing mice.

Anti-B7 antibodies delayed growth of established prostate cancer without autoimmune side effects. To determine whether anti B7 antibodies can confer therapeutic effect in mice with established prostate cancer, we randomly divided 25 week old TRAMP mice into two groups and measured their tumor size before the treatment with either control immunoglobulin or anti B7 antibodies, starting at 25 weeks. After five injections, the mice were followed for the tumor progression by either palpation or MRI. As shown in Fig. 3C, at age 33 weeks (8 weeks after first treatment), in the control IgG treated group, the volume of prostate expanded by 2.5 to 9 fold with an average of >4.5 fold. In contrast, all but one anti B7 treated mice show <2 fold expansion of the prostate volume. Mann Whitney test indicate that the difference was statistically significant ($P = 0.04$). Because the tumors are not palpable at the beginning of the treatment, we also used the time when the mice developed palpable tumors as a second endpoint with

larger sample size (12 mice for each group). As shown in Fig. 3D, even treated as late as age 25 weeks, the anti B7 antibodies delayed tumor development by ~ 7 weeks.

In the TRAMP model, lymph node metastasis has occurred at 25 weeks (29); we therefore tested the effect of anti B7 treatment on metastatic lesions in other organs, including lung, kidney, and liver. As shown in Fig. 4A, 3 of 6 mice in the control immunoglobulin treated group have substantially higher number of metastatic lesions in lung. In addition, massive metastatic lesions were found in kidney (1 of 6) and liver (2 of 6) (data not shown). Only one case of metastasis was observed in the anti B7 treated group, and the metastasis is limited to the lung. In addition, the metastatic lesions in the anti B7 treated group were substantially smaller than those found in the control immunoglobulin treated group (Fig. 4A).

Corresponding to reduced tumor growth, we have observed increased T cell infiltrating into tumors. Immunohistochemistry

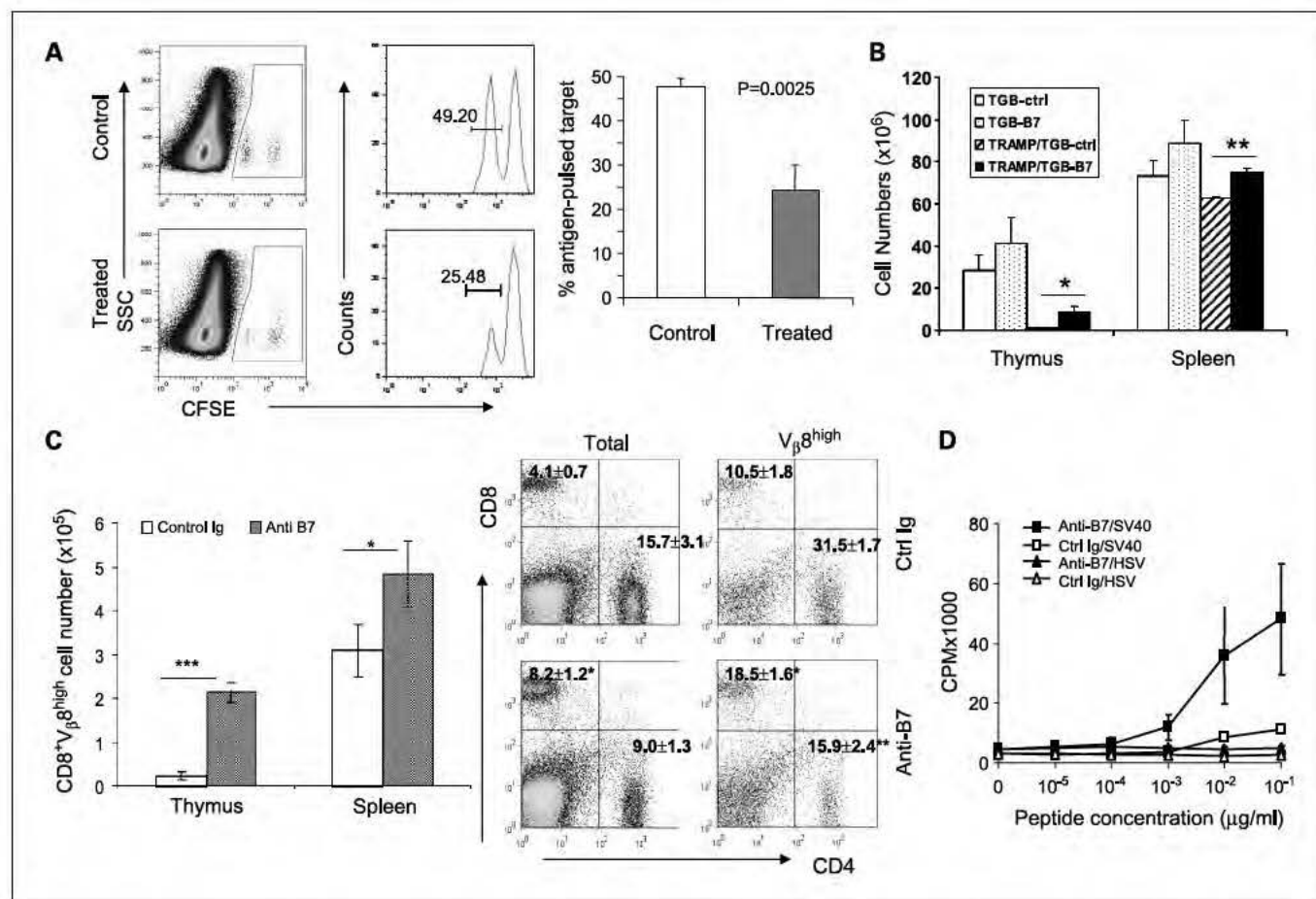


Fig. 2. Anti-B7-1/B7-2 antibody treatment enhanced TAG-specific CTL and partially rescued clonal deleted TAG-specific T cells in the TRAMP mice. **A**, 6-week-old male TRAMP mice were treated intraperitoneally with either anti-B7-1/B7-2 mAbs (1:1 mixture of 100 μ g 3A12 and 100 μ g GL-1) or control IgG (1:1 mixture of 100 μ g hamster and 100 μ g rat IgG) five times every other day. Two weeks after the first injection, mice received an intravenous injection of a 1:1 mixture of TAG peptide-pulsed (CFSE^{hi}) and control HSV peptide-pulsed (CFSE^{lo}) spleen cells (5×10^6 each). Twenty hours later, the spleens were harvested and analyzed by flow cytometry. *Left*, representative profiles; *right*, summary of two experiments involving a total of 6 mice per group. CFSE^{hi} and CFSE^{lo} cells are gated as indicated. The number shown in the gates are the percentage of gated cells. **B** to **D**, anti-B7 treatment rescued tumor-reactive T cells from clonal deletion. TRAMP/TGB double transgenic or TGB single transgenic mice that received sublethal irradiation (500 rad) were treated with either control immunoglobulin or anti-B7 mAbs five times every other days. The thymocytes and splenocytes were harvested on day 7 after final treatment and analyzed by flow cytometry. **B**, thymocyte and splenocyte cellularities in TGB single transgenic and TRAMP/TGB double transgenic mice treated with control immunoglobulin or anti-B7 antibodies. **C**, increase of CD8⁺V β 8^{high} T cells in thymus and spleen. *Left*, summary of CD8⁺V β 8^{high} cell number change in thymus and spleen from TRAMP/TGB double transgenic mice; *right*, representative profiles of CD4 and CD8 T cells in the spleens of control immunoglobulin or anti-B7-treated mice. The left flow cytometry shows those for total spleen cells, whereas the right flow cytometry shows those for gated V β 8^{high} cells. **D**, antigen reactivity of T cells rescued by anti-B7. The splenocytes from TRAMP/TGB double transgenic mice were stimulated with either SV40 TAG peptide or control HSV peptide for 72 h and pulsed with [³H] thymidine to determine the rate of T cell proliferation. **B** to **D**, mean \pm SE ($n = 3$). The conclusions have been confirmed with another independent experiment.

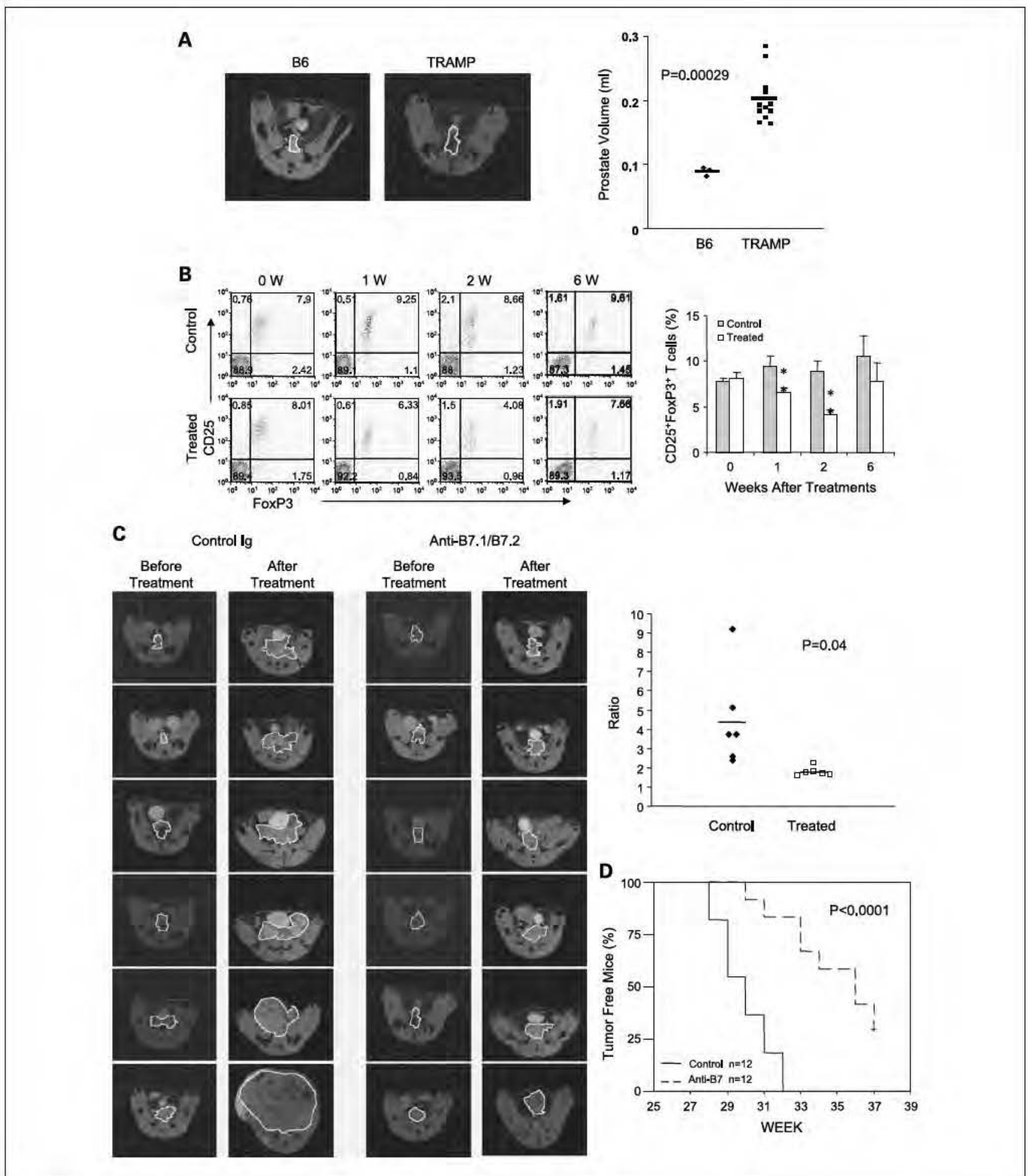


Fig. 3. Anti-B7-1/B7-2 mAb treatments of mice with established prostate cancer inhibited cancer progression. **A**, MRI measurement of prostate volumes of 25-week-old normal and TRAMP mice. *Left*, representative local images of male B6 and TRAMP mice. The prostate was identified with thick white outlines. *Right*, prostates sizes of 3 B6 and 12 TRAMP mice, all at age 25 wk. **B** and **C**, anti-B7 treatment initiated at 25-week-old TRAMP mice transiently depleted Treg. Male TRAMP mice were administered intraperitoneally with either anti-B7-1/B7-2 mAbs (1:1 mixture of 100 μ g 3A12 and 100 μ g GL-1) or control IgG (1:1 mixture of 100 μ g hamster and 100 μ g rat IgG) five times every other day. Peripheral blood was taken at 0, 1, 2, and 6 wk; 0 wk is the day before injection. Cells were stained for flow cytometry. Plots are gated on CD4⁺ cells. **B**, CD25⁺FoxP3⁺ cell number started to reduce following the first week of treatment and almost recovered to normal levels 1 mo after the treatment was stopped. Data have been repeated two times, involving a total of 12 mice per group. **D**, MRI image of TRAMP mice at 25 and 33 wk (8 wk after starting treatments with either control immunoglobulin or anti-B7 mAbs). Summary data are ratio of prostate volumes at 33 versus 25 wk when the treatments started. **D**, Kaplan-Meier analysis for incidence of palpable tumors in TRAMP mice treated with either control immunoglobulin or anti-B7 antibodies at age 25 wk.

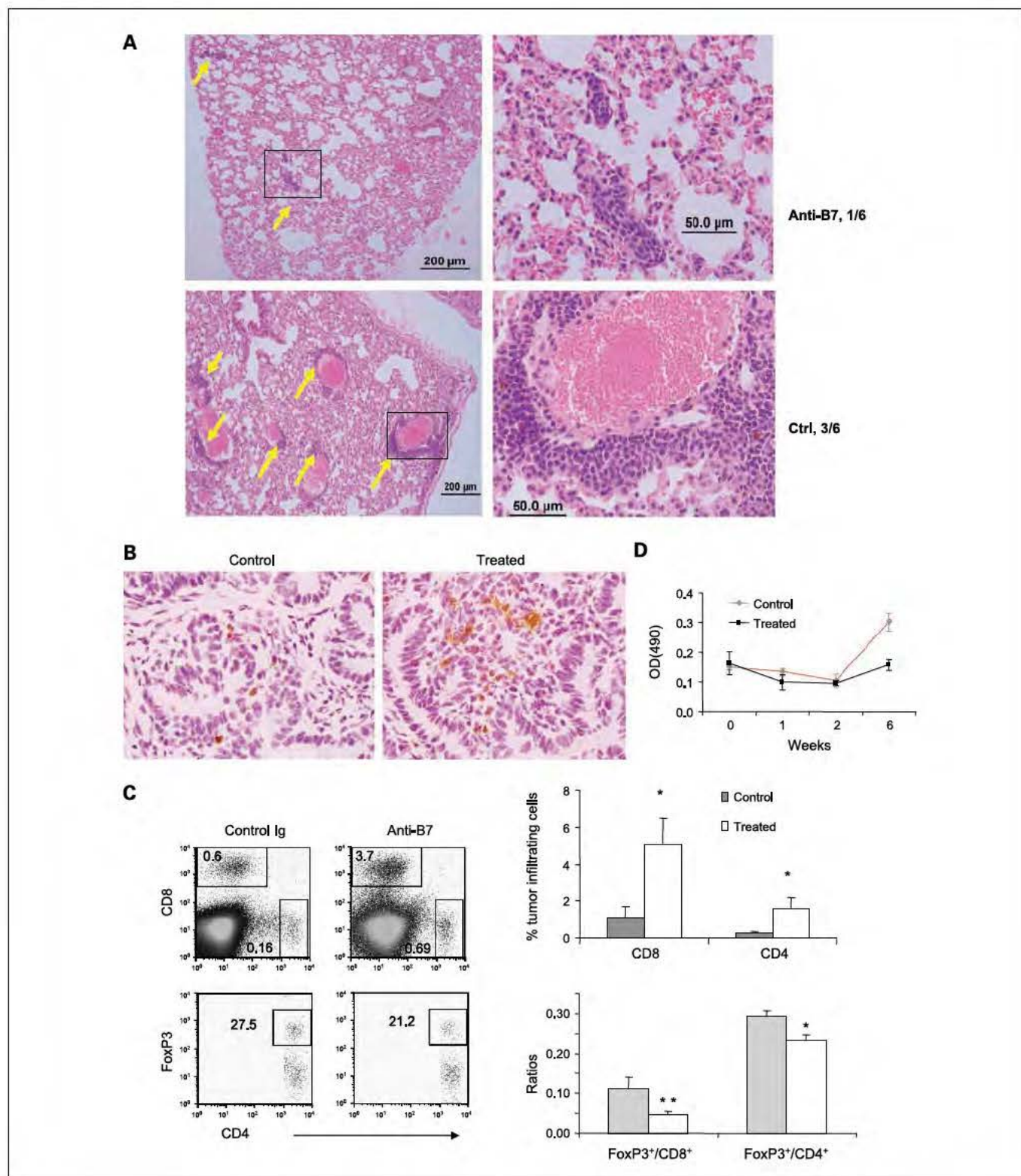


Fig. 4. Anti-B7 blockade in tumor-bearing mice reduces the number and size of metastatic lesions in the TRAMP mice and increases infiltration of T cells into tumors but does not cause autoimmunity. **A**, internal organs of mice from Fig. 3C were analyzed for metastatic lesions. Three sections of liver, lung, kidney, intestine, and heart, 30 μ m apart, were examined double blind by a pathologist. A representative field of lung sections of control immunoglobulin-treated mice (3 of 6 mice analyzed have metastasis) and the only metastatic lesion in anti-B7 treated group are shown. *Yellow arrows*, metastatic lesions. In the control immunoglobulin-treated group, massive metastases were also observed in the liver (2 of 6) and kidney (1 of 6). **B** to **D**, mice from Fig. 3C were analyzed for infiltrating lymphocytes and autoimmune reactions. **B**, representative tumor sections stained with anti-CD3 mAb. **C**, fluorescence-activated cell sorting profiles showing representation of CD4 and CD8 T cells and the CD4⁺CD25⁺Foxp3⁺ T cells. *Top left*, profiles of mononuclear cells isolated from the tumor; *bottom left*, profiles from the gated CD4⁺ T cells. Data are from pooled cells from 6 mice per group. *Top right*, frequencies of CD4 and CD8 T cells among mononuclear cells isolated from the prostate cancer; *bottom right*, ratio of Treg over CD4 or CD8 T cells. Mean \pm SE ($n = 6$). **D**, serum anti-double-stranded DNA antibodies. Data are A_{490} from an ELISA using 1:50 dilution of sera. Mean \pm SE ($n = 6$).

staining revealed an increased numbers of T cell infiltration (Fig. 4B). Quantitative analysis by flow cytometry indicated that the frequency of T cells among the mononuclear cells from the collagenase treated prostate cancer tissue increased by 4.5 fold, with the majority of the T cells are of CD8 subsets (Fig. 4C). In both groups, higher percentage of CD4⁺ T cells expressed Foxp3 than what was found in the lymphoid organ (Fig. 4C, bottom left), similar to observations made by others (33). Nevertheless, the percentage of Treg is significantly lower in the anti B7 treated group. Moreover, the ratio of Treg over effector CD4 and CD8 T cells significantly decreased in anti B7 treated group (Fig. 4C, bottom right). Therefore, anti B7 treatment alters the ratio of Treg over effector T cells in the tumor, presumably in favor of local immune response.

A general concern for immunotherapy of cancer is autoimmune side effect. To determine whether autoantibodies were induced in tumor bearing TRAMP mice, the sera were collected at 1, 2, and 6 weeks after the start of anti B7 1/B7 2 antibody treatments. The anti double stranded DNA antibodies were detected by ELISA. As shown in Fig. 4D, although an increase in anti DNA antibodies was detected at 6 weeks after control immunoglobulin treatment, presumably due to tumor growth, such increase was not observed in the anti B7 treated mice. Histologic analysis showed no inflammation of internal organs in either group (data not shown). Therefore, anti B7 antibodies can induce significant protection against established tumor without eliciting autoimmune side effect.

Anti-B7 antibodies inhibit MC38 colon carcinoma cell growth. To confirm the general antitumor effect of anti B7 treatment, we tested it with MC38 colon carcinoma tumor model. Male C57BL/6 mice were injected 5×10^6 MC38 tumor cells subcutaneously. Ten days after injection, mice developed palpable tumors and were divided evenly into two groups based on the tumor sizes. MC38 tumor bearing mice were administered intraperitoneally with either anti B7 1/B7 2 mAbs (1:1 mixture of 100 μ g 3A12 and 100 μ g GL1) or control IgG three times every other day. Peripheral blood samples were taken at 0 and 6 days, and spleens were collected at 14 days after completion of antibody treatments. As shown in Fig. 5A, at 6 and 14 days after anti B7 antibody treatment, the CD4⁺CD25⁺ Foxp3⁺ Treg cells were significantly reduced. Correspondingly, anti B7 treatment conferred a significant reduction in the growth rate of MC38 colon carcinoma ($P = 0.035$; Fig. 5B).

Transient depletion of Treg by anti-CD25 antibody delays established prostate cancer growth in TRAMP mice. To test whether transient depletion of Treg alone inhibits tumor growth, we treated 25 week old TRAMP mice with anti CD25 antibody to deplete CD4⁺CD25⁺ cells. Male 25 week old TRAMP mice were examined by MRI to measure prostate size and divided into two groups. The mice were treated intraperitoneally with either 1 mg anti CD25 mAbs (PC61) or 1 mg control rat immunoglobulin. Peripheral blood samples were taken at 0 and 3 days, and spleen were collected on day 35; 0 day is the day before injection. As shown in Fig. 6A, 99% of Foxp3⁺CD25⁺ cells were depleted in 3 days after anti CD25 treatment; however, the Foxp3⁺CD25⁺ cells were fully recovered to normal levels at 5 weeks after the treatment. Five weeks after anti CD25 treatment when mice reached age 30 weeks, two groups of TRAMP mice were reexamined by MRI. As shown in Fig. 6B, the prostate sizes were enlarged by 3 to 5 fold

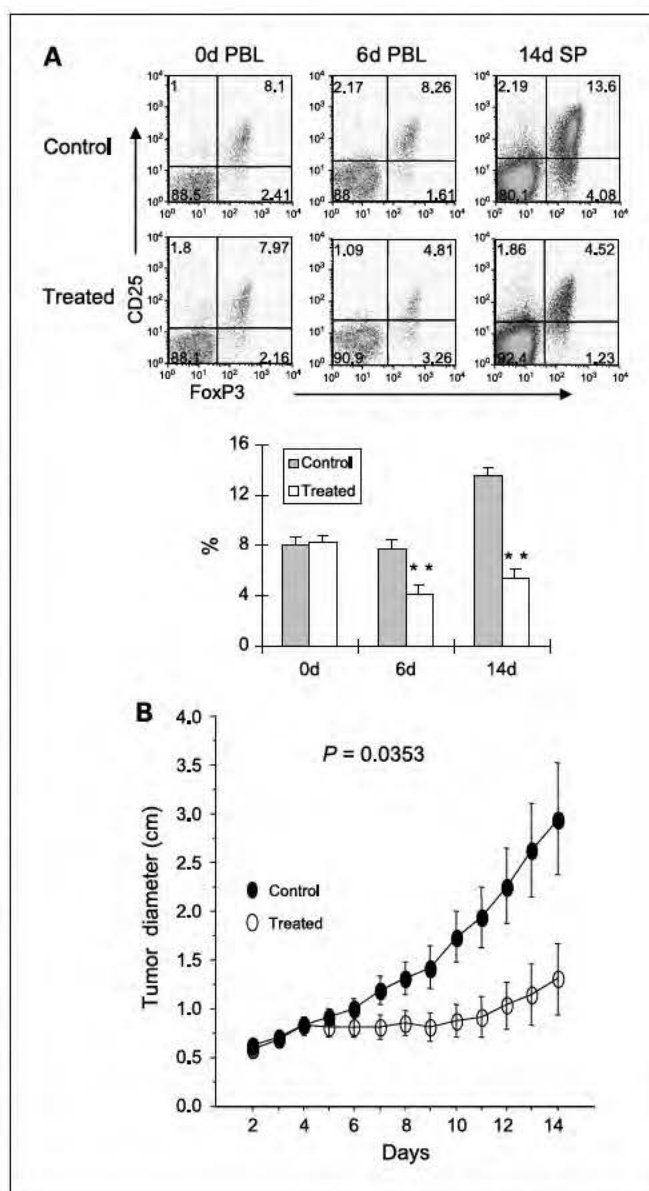


Fig. 5. Anti-B7-1/B7-2 mAb treatments of mice bearing MC38 colon carcinoma. Eight-week-old male C57BL/6 mice were injected subcutaneously with 5×10^5 MC38 tumor cells. Ten days after injection, mice were divided evenly into two groups based on the tumor sizes. The mice were administered intraperitoneally with either anti-B7-1/B7-2 mAbs (1:1 mixture of 100 μ g 3A12 and 100 μ g GL-1) or control IgG (1:1 mixture of 100 μ g hamster and 100 μ g rat IgG) three times every other day. Peripheral blood was taken at 0 and 6 d, and spleen was collected at 14 d; 0 day is the day before the administration of antibodies. Cells were stained for flow cytometry. Plots of gated CD4⁺ cells are presented. *A*, CD4⁺FoxP3⁺CD25⁺ cell number started to reduce following the first week of treatment. *Top*, representative profiles; *bottom*, summary data. *B*, anti-B7 treatment delayed growth of MC38 tumor (6 mice per group). Mean \pm SE of tumor diameters at different time points. Day 1 is defined as the day of first injection of antibody. The statistical significance is determined by Plois Fisher's test.

during the 5 week period due to the aggressive prostate cancer growth. Compared with the control group, the prostate sizes were increased by 2 to 3 fold in anti CD25 treated group (Fig. 6C). The significant difference revealed an effect of Treg depletion on tumor growth. However, this treatment is substantially less effective than transient B7 blockade (the average after/before treatment prostate size ratio in anti CD25

treatment group is 2.55 after 5 weeks compared with anti B7 treatment average ratio is 1.72 after 8 weeks; Fig. 3).

Discussion

Traditionally, blockade of costimulatory molecules B7 1 and B7 2 has been explored for treatment of autoimmune diseases and transplant rejection (38). Recent studies that reveal a

critical role for B7 1/B7 2 in the production and maintenance of Treg (23–25) and in clonal deletion of self reactive (26) as well as cancer reactive T cells (7) suggest that this pathway may be targeted for overcoming the barrier of immune tolerance in cancer setting. The data described herein showed unexpected efficacy of this new approach.

We have chosen the TRAMP mice, which developed malignant transformation of prostate epithelial cells as early

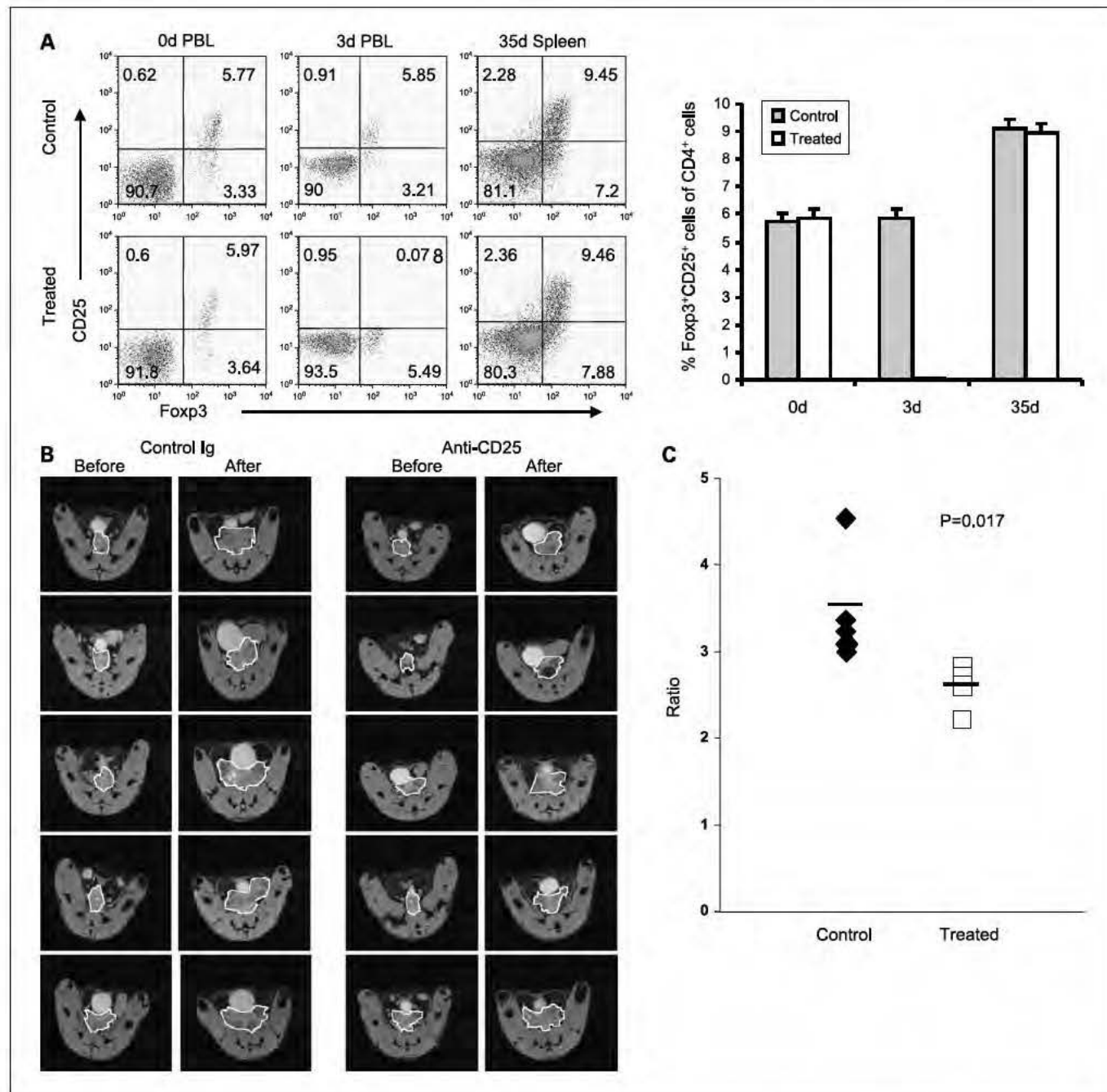


Fig. 6. Anti-CD25 treatments of mice with established prostate cancer inhibited cancer progression. **A**, anti-CD25 (clone PC61) treatment initiated at 25-week-old TRAMP mice transiently depleted Treg. Male TRAMP mice were administered intraperitoneally with one dose of anti-CD25 (1 mg/mouse) or control rat IgG (1 mg). Peripheral blood was taken at 0, 1, 2, and 6 wk; 0 wk is the day before injection. Cells were stained for flow cytometry. Plots of gated CD4⁺ cells are shown. The conjugated anti-CD25 from a different clone 7D4 was used to avoid blocking by the depleting antibody. CD4⁺CD25⁺Foxp3⁺ cells were reduced at 6 d after anti-CD25 treatment but fully recovered at 35 d. **B**, MRI image of TRAMP mice at 25 and 30 wk (5 wk after the treatments with either control immunoglobulin or anti-CD25 antibody, 5 mice per group). **C**, summary data are ratio of prostate volumes at 30 wk versus 25 wk when the treatments started. The difference was compared by a Student's *t* test.

as 12 weeks to test this notion. Our data showed that a short term anti B7 blockade before the development of pathologic lesions delays the development of palpable tumor for ~14 weeks. These data show that a short term anti B7 treatment may prevent the development of prostate cancer among individuals with predisposition of prostate cancer.

It is generally agreed that immunotherapy is very inefficient for treatment of established tumors (39). This can be more challenging in transgenic tumor models where malignant tumor cells continue to arise due to transgenic expression of oncogenes. Our data showed that, even when administered at a time when the TRAMP mice show >3 fold enlargement of prostate size, transient blockade of B7 1 and B7 2 dramatically reduced the rate of tumor growth. Thus, at 8 weeks after initiation of the treatment, the prostate of the control immunoglobulin treated expanded by 5 fold in volume. In contrast, those from anti B7 treated mice expanded by <2 fold during the same period. When the palpable tumors were used as endpoint, the anti B7 treatment at 25 weeks reduced tumor development by 7 weeks. Nevertheless, perhaps because of the continuous production of new cancer cells from the germ line insertion of SV40 large TAg and waning of antibodies, short term treatment did not completely eradicate the tumors. Because the majority of tumors that developed in human have clonal origin, the malignant transformation is likely less frequent than what is observed in transgenic model of spontaneous tumors. Therefore, the relatively simple treatment may show greater efficacy. Given the broad function of B7 1 and B7 2 in host immune system, including T cell costimulation at both priming and effector phases, Treg generation and maintenance, and clonal deletion, it is unlikely that a single mechanism is responsible for the therapeutic efficacy reported herein.

First, we have shown significant albeit transient reduction of Treg in both thymus and the peripheral blood. Because the treatment with anti CD25 antibody also showed some efficacy in slowing prostate tumor growth in TRAMP mice, Treg depletion alone is sufficient to convey significant, although less marked, protection. It is worth noting that anti CD25 antibody depletes almost 95% of CD4⁺CD25⁺ cells in 6 days; however, 60% of CD4⁺Foxp3⁺ cells still remained in peripheral blood at the same time. Because the treated mice had more CD25⁺Foxp3⁺ cells than the untreated cells, anti CD25 ablated part of CD25⁺Foxp3⁺ cells and down regulation of CD25 on others. On the other hand, anti B7 treatment caused similar extent of reduction in the CD4⁺Foxp3⁺ cells regardless of their CD25 phenotype. It is unclear whether the different depletion profile contributed to different efficacy.

Interestingly, the number of Treg returns to normal levels at 6 weeks after reconstitution. It is therefore of interest why the antitumor effect appears to have lasted long after the frequency of Treg is restored. In this regard, it should be emphasized that *in vivo* Treg reconstitution is almost universal for all methods of

Treg depletion, including antibody elimination and treatment of toxin targeting Treg that express the specific receptor for the toxin (40–42). In all cases, however, restoration of Treg did not prevent the immune response against antigen or pathogen. These studies suggested that numerical restoration of Treg is usually not accompanied by immune suppression of ongoing immune response and therefore made it plausible that temporary reduction of Treg can promote cancer immunity.

Second, in line of the function of B7 in clonal deletion of autoreactive T cells, including some tumor reactive T cells, it is possible that anti B7 treatment also rescues some tumor reactive T cells that are otherwise deleted. In this regard, we showed that transient blockade of B7 1 and B7 2 reduced the clonal deletion of SV40 T reactive CTL. Therefore, it is likely that anti B7 blockade may also increase the frequency of tumor reactive T cells. Taken together, by reducing the burden of Treg and increasing the frequency of cancer reactive T cells, B7 blockade resets the balance between regulatory burden and effector function. These two factors provide plausible explanation for the prevention described herein. Because the TGB mice do not survive long enough for us to study clonal deletion at 25 weeks, due to insertional mutation by TCR transgene (43), the effect of rescue of tumor reactive T cells in the therapy setting remains to be shown.

It is possible to argue that because the majority of cancer patients developed cancer late in their life when the thymic function has deteriorated, the rescue of TCR repertoire may be less relevant for cancer immunotherapy in humans. Nevertheless, we would like to point out that continuous production of T cells has been shown throughout the lifespan (44). Moreover, it is worth pointing out that hormone ablation is part of the standard therapy for prostate cancer. An unexpected benefit of this therapy is reinvigoration of thymic function (45). Therefore, it may be valuable to combine anti B7 blockade with hormone ablation in human prostate cancer treatment.

Finally, it is worth pointing out that blockade of B7 1 and B7 2 with their soluble receptor CTLA4Ig has been approved for therapy of autoimmune disease with little side effect (38). In this study, we showed that, despite the modulation of Treg and rescue of potentially self reactive T cells, anti B7 blockade does not trigger autoimmune side effect. The availability of a safe drug makes blockade of B7 1 and B7 2 an attractive approach for the cancer immunotherapy.

Disclosure of Potential Conflicts of Interest

No potential conflicts of interest were disclosed.

Acknowledgments

We thank the University of Michigan Cancer Center Imaging Core for the MRI analysis of prostate cancer. Part of the study was done when the laboratories were at the Ohio State University.

References

- Boel P, Wildmann C, Sensi ML, et al. BAGE: a new gene encoding an antigen recognized on human melanomas by cytolytic T lymphocytes. *Immunity* 1995;2:167–75.
- Brichard V, Van Pel A, Wolfel T, et al. The tyrosinase gene codes for an antigen recognized by autologous cytolytic T lymphocytes on HLA-A2 melanomas. *J Exp Med* 1993;178:489–95.
- Gaugler B, Van den Eynde B, van der Bruggen P, et al. Human gene MAGE-3 codes for an antigen recognized on a melanoma by autologous cytolytic T lymphocytes. *J Exp Med* 1994;179:921–30.
- van der Bruggen P, Traversari C, Chomez P, et al. A gene encoding an antigen recognized by cytolytic T lymphocytes on a human melanoma. *Science* 1991;254:1643–7.
- Kisielow P, Bluthmann H, Staerz UD, Steinmetz M, von Boehmer H. Tolerance in T-cell-receptor transgenic mice involves deletion of nonmature CD4⁺8⁺ thymocytes. *Nature* 1988;333:742–6.
- Sha WC, Nelson CA, Newberry RD, Kranz DM, Russell JH, Loh DY. Positive and negative selection of an antigen receptor on T cells in transgenic mice. *Nature* 1988;336:73–6.

7. Zheng X, Gao JX, Zhang H, Geiger TL, Liu Y, Zheng P. Clonal deletion of simian virus 40 large T antigen-specific T cells in the transgenic adenocarcinoma of mouse prostate mice: an important role for clonal deletion in shaping the repertoire of T cells specific for antigens overexpressed in solid tumors. *J Immunol* 2002;169:4761-9.
8. Sakaguchi S, Takahashi T, Nishizuka Y. Study on cellular events in postthymectomy autoimmune oophoritis in mice. I. Requirement of Lyt-1 effector cells for oocytes damage after adoptive transfer. *J Exp Med* 1982;156:1565-76.
9. Sakaguchi S, Sakaguchi N, Shimizu J, et al. Immunologic tolerance maintained by CD25⁺CD4⁺ regulatory T cells: their common role in controlling autoimmunity, tumor immunity, and transplantation tolerance. *Immunological reviews* 2001;182:18-32.
10. Sakaguchi S. Naturally arising CD4⁺ regulatory T cells for immunologic self-tolerance and negative control of immune responses. *Annu Rev Immunol* 2004;22:531-62.
11. Randolph DA, Fathman CG. CD4⁺CD25⁺ regulatory T cells and their therapeutic potential. *Ann Rev Med* 2006;57:381-402.
12. Moller G. Do suppressor T cells exist? *Scand J Immunol* 1988;27:247-50.
13. Woo EY, Yeh H, Chu CS, et al. Cutting edge: regulatory T cells from lung cancer patients directly inhibit autologous T cell proliferation. *J Immunol* 2002;168:4272-6.
14. Woo EY, Chu CS, Goletz TJ, et al. Regulatory CD4(+)CD25(+) T cells in tumors from patients with early-stage non-small cell lung cancer and late-stage ovarian cancer. *Cancer Res* 2001;61:4766-72.
15. Liyanage UK, Moore TT, Joo HG, et al. Prevalence of regulatory T cells is increased in peripheral blood and tumor microenvironment of patients with pancreas or breast adenocarcinoma. *J Immunol* 2002;169:2756-61.
16. Turk MJ, Guevara-Patino JA, Rizzuto GA, Engelhorn ME, Sakaguchi S, Houghton AN. Concomitant tumor immunity to a poorly immunogenic melanoma is prevented by regulatory T cells. *J Exp Med* 2004;200:771-82.
17. North RJ. Cyclophosphamide-facilitated adoptive immunotherapy of an established tumor depends on elimination of tumor-induced suppressor T cells. *J Exp Med* 1982;155:1063-74.
18. Barnett B, Kryczek I, Cheng P, Zou W, Curiel TJ. Regulatory T cells in ovarian cancer: biology and therapeutic potential. *Am J Reprod Immunol* 2005;54:369-77.
19. Wei S, Kryczek I, Zou L, et al. Plasmacytoid dendritic cells induce CD8⁺ regulatory T cells in human ovarian carcinoma. *Cancer Res* 2005;65:5020-6.
20. Curiel TJ, Coukos G, Zou L, et al. Specific recruitment of regulatory T cells in ovarian carcinoma fosters immune privilege and predicts reduced survival. *Nat Med* 2004;10:942-9.
21. Steitz J, Bruck J, Lenz J, Knop J, Tuting T. Depletion of CD25(+)CD4(+) T cells and treatment with tyrosinase-related protein 2-transduced dendritic cells enhance the interferon α -induced, CD8(+) T-cell-dependent immune defense of B16 melanoma. *Cancer Res* 2001;61:8643-6.
22. Tien AH, Xu L, Helgason CD. Altered immunity accompanies disease progression in a mouse model of prostate dysplasia. *Cancer Res* 2005;65:2947-55.
23. May KF, Chang X, Zhang H, et al. B7-deficient autoreactive T cells are highly susceptible to suppression by CD4⁺CD25⁺ regulatory T cells. *J Immunol* 2007;178:1542-52.
24. Salomon B, Lenschow DJ, Rhee L, et al. B7/CD28 costimulation is essential for the homeostasis of the CD4⁺CD25⁺ immunoregulatory T cells that control autoimmune diabetes. *Immunity* 2000;12:431-40.
25. Tang Q, Henriksen KJ, Boden EK, et al. Cutting edge: CD28 controls peripheral homeostasis of CD4⁺CD25⁺ regulatory T cells. *J Immunol* 2003;171:3348-52.
26. Gao J-X, Zhang H, Bai XF, et al. Perinatal blockade of B7-1 and B7-2 inhibits clonal deletion of highly pathogenic autoreactive T cells. *J Exp Med* 2002;195:959-71.
27. Noel PJ, Alegre ML, Reiner SL, Thompson CB. Impaired negative selection in CD28-deficient mice. *Cell Immunol* 1998;187:131-8.
28. Greenberg NM, DeMayo F, Finegold MJ, et al. Prostate cancer in a transgenic mouse. *Proc Natl Acad Sci U S A* 1995;92:3439-43.
29. Gingrich JR, Barrios RJ, Morton RA, et al. Metastatic prostate cancer in a transgenic mouse. *Cancer Res* 1996;56:4096-102.
30. Geiger T, Gooding LR, Flavell RA. T-cell responsiveness to an oncogenic peripheral protein and spontaneous autoimmunity in transgenic mice. *Proc Natl Acad Sci U S A* 1992;89:2985-9.
31. Wu Y, Guo Y, Liu Y. A major costimulatory molecule on antigen-presenting cells, CTLA4 ligand A, is distinct from B7. *J Exp Med* 1993;178:1789-93.
32. Freeman GJ, Borriello F, Hodes RJ, et al. Murine B7-2, an alternative CTLA4 counter-receptor that costimulates T cell proliferation and interleukin 2 production. *J Exp Med* 1993;178:2185-92.
33. Degl'Innocenti E, Grioni M, Capuano G, et al. Peripheral T-cell tolerance associated with prostate cancer is independent from CD4⁺CD25⁺ regulatory T cells. *Cancer Res* 2008;68:292-300.
34. Bonneau RH, Salvucci LA, Johnson DC, Tevethia SS. Epitope specificity of H-2Kb-restricted, HSV-1-, and HSV-2-cross-reactive cytotoxic T lymphocyte clones. *Virology* 1993;195:62-70.
35. Sun Y, Chen HM, Subudhi SK, et al. Costimulatory molecule-targeted antibody therapy of a spontaneous autoimmune disease. *Nat Med* 2002;8:1405-13.
36. Eng MH, Charles LG, Ross BD, et al. Early castration reduces prostatic carcinogenesis in transgenic mice. *Urology* 1999;54:1112-9.
37. Wang J, Fu YX. LIGHT (a cellular ligand for herpes virus entry mediator and lymphotxin receptor)-mediated thymocyte deletion is dependent on the interaction between TCR and MHC/self-peptide. *J Immunol* 2003;170:3986-93.
38. Bluestone JA, St Clair EW, Turka LA. CTLA4lg: bridging the basic immunology with clinical application. *Immunity* 2006;24:233-8.
39. Yu P, Rowley DA, Fu YX, Schreiber H. The role of stroma in immune recognition and destruction of well-established solid tumors. *Curr Opin Immunol* 2006;18:226-31.
40. Kim JM, Rasmussen JP, Rudensky AY. Regulatory T cells prevent catastrophic autoimmunity throughout the lifespan of mice. *Nat Immunol* 2007;8:191-7.
41. Lahl K, Loddenkemper C, Drouin C, et al. Selective depletion of Foxp3⁺ regulatory T cells induces a scurfy-like disease. *J Exp Med* 2007;204:57-63.
42. Scott-Browne JP, Shafiani S, Tucker-Heard G, et al. Expansion and function of Foxp3-expressing T regulatory cells during tuberculosis. *J Exp Med* 2007;204:2159-69.
43. Wang Y, Liu Y, Wu C, et al. Epm2a suppresses tumor growth in an immunocompromised host by inhibiting Wnt signaling. *Cancer Cell* 2006;10:179-90.
44. Douek DC, McFarland RD, Keiser PH, et al. Changes in thymic function with age and during the treatment of HIV infection. *Nature* 1998;396:690-5.
45. Sutherland JS, Goldberg GL, Hammett MV, et al. Activation of thymic regeneration in mice and humans following androgen blockade. *J Immunol* 2005;175:2741-53.

Dendritic cells in the thymus contribute to T-regulatory cell induction

Anna I. Proietto^{a,b,1}, Serani van Dommelen^a, Penghui Zhou^c, Alexandra Rizzitelli^{a,2}, Angela D'Amico^a, Raymond J. Steptoe^d, Shalin H. Naik^{a,3}, Mireille H. Lahoud^a, Yang Liu^c, Pan Zheng^c, Ken Shortman^a, and Li Wu^{a,1}

^aThe Walter and Eliza Hall Institute of Medical Research, Parkville, Victoria 3050, Australia; ^bDepartment of Medical Biology, The University of Melbourne, Parkville, Victoria 3010, Australia; ^cDivision of Immunotherapy, Section of General Surgery, Department of Surgery, University of Michigan, Ann Arbor, MI 49109; and ^dDiamantina Institute for Cancer, Immunology, and Metabolic Medicine, The University of Queensland, Brisbane 4102, Australia

Communicated by Jacques F. A. P. Miller, The Walter and Eliza Hall Institute of Medical Research, Parkville, VIC, Australia, October 13, 2008 (received for review September 19, 2008)

Central tolerance is established through negative selection of self-reactive thymocytes and the induction of T-regulatory cells (T_{RS}). The role of thymic dendritic cells (TDCs) in these processes has not been clearly determined. In this study, we demonstrate that *in vivo*, TDCs not only play a role in negative selection but in the induction of T_{RS}. TDCs include two conventional dendritic cell (DC) subtypes, CD8^{lo}Sirpα^{hi/+} (CD8^{lo}Sirpα⁺) and CD8^{hi}Sirpα^{lo/-} (CD8^{hi}Sirpα⁻), which have different origins. We found that the CD8^{hi}Sirpα⁺ DCs represent a conventional DC subset that originates from the blood and migrates into the thymus. Moreover, we show that the CD8^{lo}Sirpα⁺ DCs demonstrate a superior capacity to induce T_{RS} *in vitro*. Finally, using a thymic transplantation system, we demonstrate that the DCs in the periphery can migrate into the thymus, where they efficiently induce T_R generation and negative selection.

thymic selection | migratory dendritic cells | tolerance

Tolerance to self-antigens is established in the thymus. Developing thymocytes undergo stringent selection to eliminate self-reactivity (1). Developing T cells that recognize self-peptide with a sufficiently high affinity can encounter two fates: (i) deletion through negative selection or (ii) differentiation into T-regulatory cells (T_{RS}). T_{RS} express the transcription factor Foxp3 (2–4) and can suppress self-reactive T cells that have escaped negative selection (5, 6). During mouse ontogeny, T_{RS} appear in the thymus 3 days after birth (7). Deficiency in T_R development or function results in multiorgan autoimmunity (6).

A role for thymic dendritic cells (TDCs) in negative selection (8–12) and for thymic epithelial cells (TECs) in negative selection and T_R induction has been demonstrated (9, 13–16). The role of dendritic cells (DCs) in T_R generation in the thymus is unclear, however. Given the importance of DCs in the generation of peripherally induced T_{RS} (17, 18), and in light of a recent study demonstrating the potential of human TDCs to induce T_{RS} *in vitro* (19), the possible role of TDCs in T_R induction *in vivo* needs careful dissection using mouse models.

In mouse thymus, three subsets of DCs have been identified. The plasmacytoid dendritic cell (pDC) and two conventional dendritic cell (cDC) subsets defined based on CD8α and Sirpα expression: the CD8^{lo}Sirpα^{hi/+} cDCs (≈30% of cDCs, Sirpα⁺ TcDCs hereafter) and the CD8^{hi}Sirpα^{lo/-} cDCs (≈70% of cDCs, Sirpα⁻ TcDCs hereafter) (20, 21). Sirpα⁻ TcDCs develop from intrathymic lymphoid precursors (22, 23). The origin of Sirpα⁺ TcDCs is less clear, although one study demonstrated that the CD8^{lo}CD11b⁺ cDCs (equivalent to Sirpα⁺ cDCs) migrate into the thymus from the periphery (24). The role of the individual TDC subsets in T-cell selection is yet to be determined.

In addition to the contribution of medullary thymic epithelial cells (mTECs) to T_R generation (16), in this study, we demonstrate that TDCs make a significant contribution to T_R induction as well as to negative selection. This was established *in vivo* using two bone marrow (BM) chimeric mouse models in which the hemopoietic-

derived compartment was impaired in antigen presentation (MHC class II [MHCII]^{-/-}) or T-cell activation (B7^{-/-}). Using an *in vitro* culture system, we established that the Sirpα⁺ TcDCs played the major role in T_R induction when compared with other DC subtypes. This functional capacity of the Sirpα⁺ TcDCs correlates with a unique set of properties, particularly their maturity, their chemokine production, and their migratory origin. These findings suggest that a subset of TDCs migrating from the periphery makes a specialized contribution to T_R induction in the thymus.

Results

TDCs Contribute to T_R Induction and Negative Selection *In Vivo*. To dissect the contribution of DCs from that of mTECs in the induction of T_{RS}, two different *in vivo* systems were used. In the first, irradiated C57BL/6 (B6) WT CD45.1 recipients were reconstituted with BM from MHCII^{-/-} or B6 WT (CD45.2) mice. In MHCII^{-/-} BM chimeras, the host epithelial cells can still present antigen via MHCII, whereas the BM-derived cells, including TDCs, cannot. In the second system, irradiated CD45.1 recipients were reconstituted with B7^{-/-} BM (lacking CD80 and CD86) or WT BM for controls. Because expression of MHCII and costimulatory molecules CD80 and CD86 is essential for the induction of thymic-derived T_{RS} (5, 14, 15, 19, 25, 26), these systems enabled us to discern the contribution of DCs to T_R induction.

Because some DCs are radioresistant, it was important to establish whether TDCs in the chimeras were all of donor origin (27, 28). Staining the TDC-enriched light density cell fraction for donor-derived DCs 6 weeks after BM reconstitution demonstrated that >98% of DCs were of donor origin (MHCII⁻), indicating effective elimination of host DCs (Fig. 1A). The TDCs from the MHCII^{-/-} BM chimeras did not express MHCII (Fig. 1B). Furthermore, both cDC subsets were observed in similar proportions and number in WT and MHCII^{-/-} chimeras (data not shown).

To assess the effect on thymocyte development in mice lacking MHCII on DCs, the proportion and total numbers of the individual donor-derived thymocyte populations were determined (Fig. 1C–E). Total thymic cellularity was comparable between the MHCII^{-/-} and WT BM chimeras [supporting information (SI) Table S1], and the numbers of CD4⁻CD8⁻ double-negative, CD4⁺CD8⁺ double-positive, and CD8⁺CD4⁻ (CD8⁺ hereafter) T-cell popula-

Author contributions: A.I.P., Y.L., P. Zheng, and L.W. designed research; A.I.P., S.v.D., P. Zhou, A.R., and A.D. performed research; R.J.S. contributed new reagents/analytic tools; A.I.P., S.v.D., P. Zhou, Y.L., P. Zheng, K.S., and L.W. analyzed data; and A.I.P. and L.W. wrote the paper.

The authors declare no conflict of interest.

¹To whom correspondence should be addressed. E-mail: proietto@wehi.edu.au or wu@wehi.edu.au.

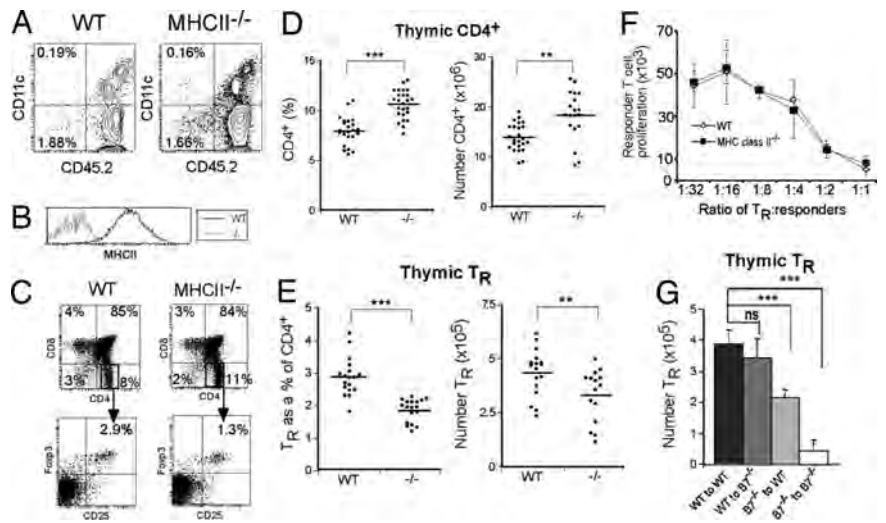
²Present address: The Netherlands Cancer Institute, 1066 Amsterdam, The Netherlands.

³Present address: Biochemistry Department, Monash University, Melbourne, Clayton Victoria 3800, Australia.

This article contains supporting information online at www.pnas.org/cgi/content/full/0810268105/DCSupplemental.

© 2008 by The National Academy of Sciences of the USA

Fig. 1. MHCII⁺ DCs contribute to negative selection and T_R induction. (A) The light density fraction of cells from the thymus of WT and MHCII^{-/-} BM chimeras was analyzed to determine the % of donor-derived DCs. More than 98% of CD11c⁺ cells were CD45.2⁺ donor-derived DCs in both BM chimera groups. (B) MHCII expression on CD11c⁺ TDCs in WT (black line) and MHCII^{-/-} (gray line) chimeras. (C) The % of double-negative, double-positive, CD4⁺, and CD8⁺ thymocytes (Upper) and CD4⁺CD25⁺Foxp3⁺ T_Rs (Lower). (D) The % and total number of CD4⁺ thymocytes in WT and MHCII^{-/-} BM chimeras. (E) The % and total number of T_Rs in WT and MHCII^{-/-} BM chimeras ($n = 20$ – 24 per group for D and E). (F) Suppressive activity of CD4⁺CD25⁺ thymocytes from MHCII^{-/-} or WT chimeras. Data are the mean (error bars, \pm SD) of triplicate cultures from one of two experiments. (G) The number of T_Rs (CD4⁺Foxp3⁺) in the thymus of B6 to B6, B6 to B7^{-/-}, B7^{-/-} to B6, and B7^{-/-} to B7^{-/-} BM chimeras was analyzed by flow cytometry. Data are the mean of three independent experiments (error bars, \pm SD) ($n = 68$ for G). *, $P < 0.05$; **, $P < 0.001$; ***, $P < 0.0001$.



tions were not significantly different between the two groups (Table S1). There was a 20% increase in the number of CD4⁺CD8⁻ (CD4⁺ hereafter) thymocytes in the MHCII^{-/-} BM chimeras, however, suggesting that there was incomplete negative selection (Fig. 1D). Syngeneic mixed leukocyte reaction assays confirmed that the CD4⁺ thymocytes contained auto-reactive T cells (data not shown). Concomitant with this increase was a statistically significant 30% decrease in the number of CD4⁺CD25⁺Foxp3⁺ T_Rs ($P = 0.008$) (Fig. 1E).

To test the function of the T_Rs in the WT and MHCII^{-/-} chimeras, they were sorted and used in an *in vitro* T_R suppression assay. The T_Rs from both groups were functional (Fig. 1F).

In the second BM chimeric system, B7^{-/-} mice were used. Initially, it was established that B7^{-/-} mice have a deficiency in the proportion of T_Rs that equated to a 94% decrease (Fig. S1A). To establish if this was attributable to cells in the hemopoietic or epithelial cell compartment, four cohorts of chimeras were set up. CD45.1 WT or CD45.1 B7^{-/-} mice were reconstituted with CD45.2 WT or B7^{-/-} BM and analyzed for T_R development 8 weeks after reconstitution. Total thymic cellularity did not differ between the four cohorts (data not shown). There was a 50% decrease in the number of thymic T_Rs in the B7^{-/-} to WT chimeric mice, however (Fig. 1G; Fig. S1B).

Overall, these results suggest a nonredundant role for TDCs in the induction of thymic T_Rs and in the negative selection of self-reactive CD4⁺ thymocytes.

DCs Induce Antigen-Specific T_Rs and Negative Selection *In Vivo*. T_R induction and negative selection of self-reactive thymocytes

require self-peptide presentation on MHCII via an antigen-presenting cell (14, 15). To address T_R induction by DCs in an antigen-specific system, Rag2^{-/-} OTII T-cell receptor (TCR) transgenic (tg) mice (which lack OVA-specific T_Rs because of the absence of the OVA antigen) were crossed with CD11cOVA tg mice (membrane-bound OVA expressed under the CD11c promoter). In these Rag2^{-/-}OTII/CD11cOVA (Rag2^{-/-}O/OVA) double-tg mice, OVA is expressed on CD11c⁺ TDCs and can influence the development of CD4⁺ T cells that express the OVA-specific TCR (29). To follow development of newly formed thymocytes from the double-tg BM cells, irradiated WT CD45.1 recipients were reconstituted with the BM of CD45.2 Rag2^{-/-}O/OVA mice or Rag2^{-/-}OTII mice for controls. Thymocytes were analyzed by flow cytometry 6 weeks later. Total cellularity of the Rag2^{-/-}O/OVA BM chimeric thymuses was reduced compared with controls (Fig. 2A). The presentation of OVA by DCs in Rag2^{-/-}O/OVA BM chimeric mice led to the deletion of the majority of OTII⁺CD4⁺ cells, as seen by a >90% reduction in the total number of CD45.2⁺CD4⁺Vα2⁺ OTII thymocytes compared with controls (Fig. 2B and C). Furthermore, there was a clear induction of OTII T_Rs in the thymus of Rag2^{-/-}O/OVA BM chimeras (mean 15 \pm 2% of OTII⁺CD4⁺ cells) compared with the controls (0.1% of OTII⁺CD4⁺ thymocytes). This represented a greater than 150-fold increase in T_R numbers in the thymus of Rag2^{-/-}O/OVA BM chimeras compared with controls (Fig. 2B and D).

Overall, these results demonstrate that DCs are capable of T_R induction and negative selection in an antigen-specific manner.

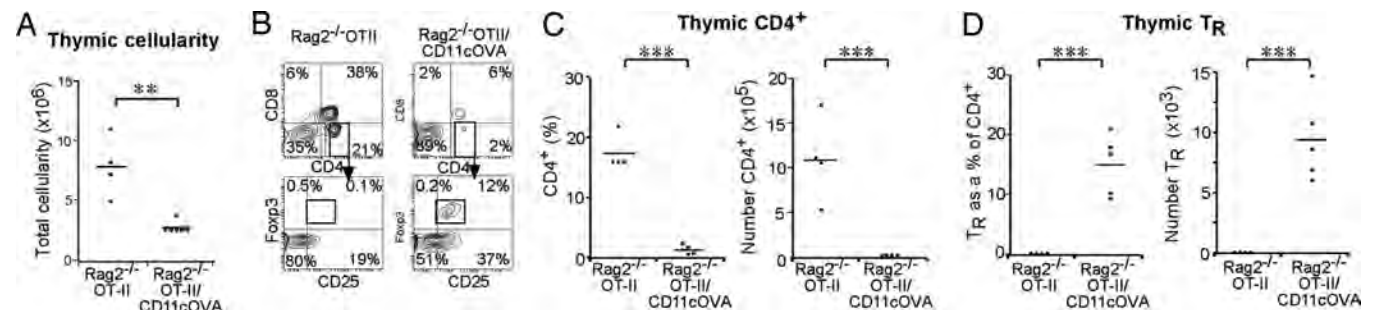


Fig. 2. OVA expressing DCs induce OTII T_Rs and deletion of OTII CD4⁺ T cells. Irradiated WT CD45.1 mice were reconstituted with double-tg Rag2^{-/-}OTII/CD11cOVA (Rag2^{-/-}O/OVA) BM or Rag2^{-/-}OTII BM as a control ($n = 4$ – 5 per group). (A) Total thymic cellularity of Rag2^{-/-}O/OVA and control BM chimeras. (B) CD45.2⁺Vα2⁺ thymocytes were gated, and the % of CD4⁺ and CD8⁺ thymocytes was determined. To assess T_R induction, CD4⁺ OTII⁺ thymocytes were gated for and expression of CD25 and Foxp3 was determined. The % and number of OTII⁺ CD4⁺ thymocytes (C) and the % and number of T_Rs (D) in Rag2^{-/-}O/OVA and control BM chimeras.

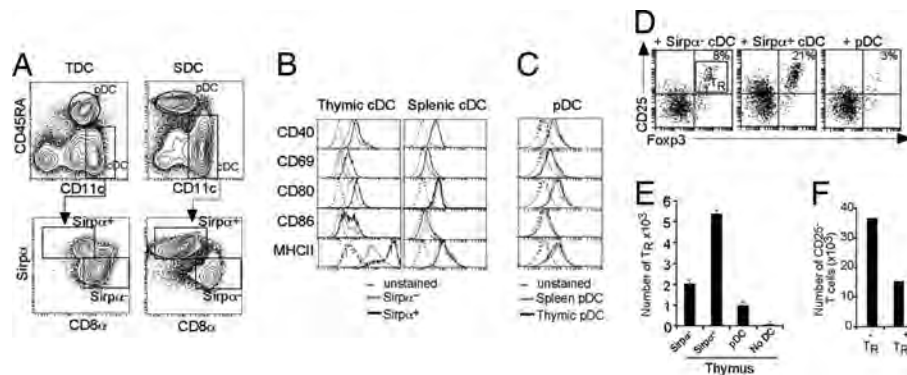


Fig. 3. $\text{Sirp}\alpha^+$ TcDCs are more mature and efficiently induce T_R *in vitro*. (A) Enriched TDCs and SDCs were segregated into pDCs ($\text{CD}11\text{c}^{\text{int}}\text{CD}45\text{RA}^+$) and cDCs ($\text{CD}11\text{c}^+$ $\text{CD}45\text{RA}^-$) and further segregated into $\text{CD}8^{\text{lo}}\text{Sirp}\alpha^+$ and $\text{CD}8^{\text{hi}}\text{Sirp}^-$ cDCs. Thymic and splenic $\text{Sirp}\alpha^+$ and $\text{Sirp}\alpha^-$ cDCs (B) and thymic and splenic pDCs (C) were analyzed for the expression of costimulatory molecules, CD69, and MHCII. (D) T_R ($\text{CD}4^+\text{CD}25^+\text{Foxp}3^+$) induction by TDC subsets in the cocultures of TDCs and $\text{CD}4^+\text{CD}25^-$ thymocytes for 5 days. Data shown are representative of six experiments. (E) The number of T_R s induced was determined by flow cytometric analysis of the cultured cells of D using calibration beads ($n = 6$) (error bars, \pm SD). (F) Suppressive capacity of T_R s induced in cultures by $\text{Sirp}\alpha^+$ TcDCs. *In vitro*-derived T_R s were sorted as $\text{CD}4^+\text{CD}25^+\text{CD}62\text{L}^+$ and subject to a suppression assay as per Fig. 1F. The number of proliferating CFSE-labeled $\text{CD}4^+\text{CD}25^-$ T cells was determined 3 days later ($n = 2$).

$\text{Sirp}\alpha^+$ TcDCs Are More Mature in Surface Phenotype Than the $\text{Sirp}\alpha^-$ TcDCs. Because TDCs were involved in T_R generation and negative selection, we investigated the contribution of the TDC subtypes to these processes. We compared TDCs for expression of MHCII and costimulatory molecules, because these are important in T_R induction and negative selection (19, 30–34). We then compared the TDCs with their splenic DC (SDC) equivalents. TDCs and SDCs were segregated into pDCs and cDCs, which could be further segregated as $\text{Sirp}\alpha^+\text{CD}8^{\text{lo}}$ and $\text{Sirp}\alpha^-\text{CD}8^+$ cDCs (21) (Fig. 3A). Strikingly, the $\text{Sirp}\alpha^+$ TcDCs expressed higher levels of MHCII and CD86 and slightly increased levels of the activation marker CD69 and the costimulatory molecules CD40 and CD80 compared with $\text{Sirp}\alpha^-$ TcDCs (Fig. 3B). This difference was not observed between the DC subsets in the spleen, where both cDC subsets expressed comparable levels of these markers (refs. 35, 36; Fig. 3B). Nor was there a difference in expression of these molecules in thymic versus splenic pDCs (Fig. 3C). Thus, in the steady state, $\text{Sirp}\alpha^+$ TcDCs are phenotypically more “mature” than other TDC subtypes.

$\text{Sirp}\alpha^+$ TcDCs Are More Efficient at Inducing Functional T_R s *In Vitro*. To compare the capacity of each TcDC subset to induce T_R s, sorted TDC subsets were cocultured with syngeneic $\text{CD}4^+\text{CD}8^- \text{CD}25^-$ thymocytes (which contain T_R precursors) for 5 days. To maintain T_R survival, an optimal level of IL-7 was added (37). The number of T_R s that developed in these cultures was enumerated. The $\text{Sirp}\alpha^+$ TcDCs were the most efficient at inducing T_R s, as shown by the higher number of $\text{CD}4^+\text{CD}25^+\text{Foxp}3^+$ cells in the cultures (Fig. 3D and E). In the cultures containing $\text{Sirp}\alpha^+$ TcDCs, there was also some level of T-cell activation, as evidenced by a population of $\text{CD}4^+\text{CD}25^{\text{int}}\text{Foxp}3^-$ (Fig. 3D and data not shown). This T-cell activation was accompanied by T-cell proliferation and a higher total number of T cells within the cultures (Fig. S2A). Given that the proportion of T_R s induced in $\text{Sirp}\alpha^+$ TcDC cocultures ($14 \pm 5\%$) was also significantly higher compared with $\text{Sirp}\alpha^-$ TcDC cocultures ($9 \pm 1\%$) (Fig. 3D), it was clear that the increased number of T_R s could not be attributable solely to a higher absolute number of T cells generated. Furthermore, we determined that the T_R induction observed was attributable to *de novo* generation and not to proliferation of preexisting $\text{CD}4^+\text{CD}25^- \text{Foxp}3^+$ cells within the starting population of thymocytes by using Foxp3-GFP mice to gate out $\text{CD}4^+\text{CD}25^- \text{Foxp}3^+$ cells (Fig. S2B).

T_R generation *in vitro* was thymus specific. When TDCs were cultured with splenic $\text{CD}4^+\text{CD}25^-$ naive T cells rather than thymic $\text{CD}4^+\text{CD}25^-$ T cells, no T_R induction was observed (Fig. S2C), even in the presence of T-cell activation and proliferation (Fig.

S2D). Conversely, when SDCs were cocultured with thymic $\text{CD}4^+\text{CD}25^-$ T cells, few T_R s were generated (data not shown).

To test the function of *in vitro*-derived T_R s, T_R s were sorted as $\text{CD}4^+\text{CD}25^+\text{CD}62\text{L}^+$ cells and used in a T_R suppression assay. $\text{CD}62\text{L}$ was included as a marker to exclude activated T cells. *In vitro* derived T_R s were able to suppress T-cell proliferation (Fig. 3F).

BM-derived cells that express MHCII within the thymus include B cells and macrophages. To exclude the possibility of T_R induction by those cells, the same coculture method was used. We demonstrated that the T_R induction capacities of both of these cell types were negligible (Fig. S2E).

$\text{Sirp}\alpha^+$ TcDCs Produce Chemokines and Attract $\text{CD}4^+$ Thymocytes. The chemokine-mediated migration of developing thymocytes through the thymus ensures their interaction with the appropriate thymic stromal cells. We examined chemokine production as a factor that may explain the effectiveness of the $\text{Sirp}\alpha^+$ TcDCs in inducing T_R s. The expression of the genes encoding six chemokines known to be involved in thymocyte differentiation was examined by real-time (RT) PCR, comparing the TDC and SDC subsets, macrophages, and thymic mTECs.

The mTECs expressed significantly higher levels of *CCL19*, *CCL21*, and *CCL25*, higher than the DC subsets (Fig. S3A). In contrast, *CCL17* and *CCL22* were expressed at very high levels only by the $\text{Sirp}\alpha^+$ TcDCs (Fig. S3A). The expression of *CCL22* by the $\text{Sirp}\alpha^+$ TcDCs was confirmed at the protein level by intracellular chemokine staining (Fig. S3B).

CCL17 and *CCL22* both bind to CCR4. Using RT-PCR, we found that the $\text{CD}4^+$ thymocytes expressed the highest levels of *CCR4* (Fig. S3C), a finding consistent with other studies (38). To test whether the DC-expressed chemokines were chemotactic for $\text{CD}4^+$ thymocytes, migration assays were performed. Sorted TDC and SDC subsets were cultured alone for 3 h. The supernatants were then used as a source of chemotactins for $\text{CD}4^+$ thymocytes, seeded in transwells, and incubated for 2 h. The supernatants from the $\text{Sirp}\alpha^+$ TcDC cultures showed the greatest capacity to attract $\text{CD}4^+$ thymocytes (Fig. S3D). Thus, the $\text{Sirp}\alpha^+$ TcDCs, through their chemokine production, have a special capacity to attract newly formed $\text{CD}4^+$ T cells.

$\text{CD}11\text{c}^+\text{Sirp}\alpha^+\text{CD}11\text{b}^+$ cDCs Are Found in Blood and Migrate into the Thymus. A number of observations have led to the suggestion that the TDC subsets have different developmental origins, with a major proportion of the TcDCs being derived from an early intrathymic precursor (24, 39). To test the origin of each TcDC, the earliest intrathymic precursors (Lineage⁻Thy-1^{lo}c-kit⁺) that have DC po-

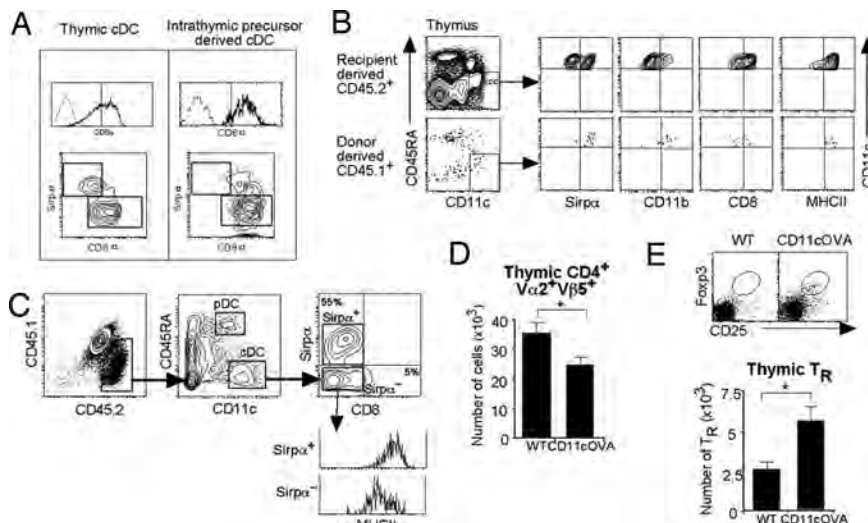


Fig. 4. $\text{Sirp}\alpha^+$ TcDCs originate from peripheral blood and can migrate into the thymus. (A) DC generation from purified Lineage⁻Thy-1^{lo}c-kit⁺ intrathymic precursors (CD45.2) was analyzed 2 weeks after precursor transfer. The intrathymic precursor-derived cDCs were mainly CD8⁺ $\text{Sirp}\alpha^-$ (Right). A representative contour plot of the normal TcDC subsets is shown (Left) for comparison. (B) White blood cells (20×10^6) from CD45.1 mice were transferred i.v. into nonirradiated CD45.2 recipients. The phenotype of donor-derived cells in the thymus of recipients was determined 3 days later by gating for CD45.1⁺CD11c⁺CD45RA^{lo} cDCs. Expression of $\text{Sirp}\alpha$, CD11b, CD8, and MHCII was determined on this population. (C–E) Thymic lobes from OTII tg CD45.2⁺ mice crossed to CD45.1⁺ WT mice were grafted under the kidney capsule of CD45.2⁺ CD11cOVA tg or WT recipients. (C) The phenotype of recipient-derived CD45.2⁺CD45.1⁻ cDCs in the grafted thymic lobes from WT and CD11cOVA tg mice was determined. The recipient CD45.2⁺CD45.1⁻CD11c⁺CD45RA⁻ cDCs were gated for, and the expression of CD8 and $\text{Sirp}\alpha$ was determined. The level of expression of MHCII was determined on $\text{Sirp}\alpha^-$ and $\text{Sirp}\alpha^+$ cDCs. (D) The total number of CD45.1⁺CD4⁺V α 2⁺V β 5⁺ cells (OTII) was calculated in OTII lobes grafted into WT or CD11cOVA tg recipients. Data are the mean of three independent experiments (error bars, \pm SD) ($n = 11$ –21). *, $P < 0.05$. (E) CD45.1⁺CD4⁺V α 2⁺V β 5⁺ cells in the OTII lobes from WT and CD11cOVA tg recipients (as in D) were further analyzed for CD25 and Foxp3 expression. The total number of CD45.1⁺CD4⁺V α 2⁺V β 5⁺CD25⁺Foxp3⁺ T_RS was calculated. Data are the mean of three independent experiments (error bars, \pm SD) ($n = 11$ –21). *, $P < 0.05$.

tential were transferred intrathymically into sublethally irradiated CD45.1 recipient mice. DC generation was analyzed 2 weeks after transfer. The cDCs that developed from the intrathymic precursors were mainly CD8⁺ $\text{Sirp}\alpha^-$ (Fig. 4A).

In contrast, the CD8⁻CD11b⁺ TDC subset has been shown to migrate in parabiotic mice from the circulation into the thymus of the conjoined mouse (24). To determine whether the $\text{Sirp}\alpha^+$ TcDCs correspond to this population, the CD11c⁺ DCs within mouse blood were characterized. Total peripheral blood mononuclear cells were enriched for DCs. The preparation was then stained for DC markers. Gating on CD11c⁺ cells revealed that more than 70% of the blood DCs were $\text{Sirp}\alpha^+$ CD11b⁺ (Fig. S4). Among the blood DCs, 25% expressed high levels of MHCII, indicating that immature and mature DCs were present in mouse blood.

To determine whether these blood DCs migrate to the thymus, white blood cells from CD45.1 mice were transferred i.v. into nonirradiated CD45.2 recipients and the phenotype of donor-derived cells in the recipient thymus was determined 3 days later. Donor-derived cells made up 0.1% of total cells in the recipient thymus, and of these, 10% were CD11c⁺CD45RA⁻ cDCs. These cDCs were all $\text{Sirp}\alpha^+$ CD11b⁺CD8^{lo}MHCII^{hi} (Fig. 4B), correlating with DCs found circulating in the blood.

Impact of Migrating DCs on T-Cell Development. To determine the impact of circulating DCs on thymic T-cell selection, day 1 neonatal thymic lobes from CD45.1/OTII tg mice were grafted under the kidney capsule of recipient CD45.2 WT or CD45.2 CD11cOVA tg mice. This system allows recipient DCs to migrate into the grafted thymic lobes via the blood. Therefore, the effects of peripherally derived CD45.2 CD11cOVA migrating DCs on OTII T-cell development in the grafted lobes could be assessed. The kinetics of DC migration were determined. At day 7, before the recipient BM progenitors had contributed to the TDC population, the DCs entering the thymic lobes were predominantly the $\text{Sirp}\alpha^+$ cDCs ($80 \pm 5\%$; data not shown). We therefore waited a further 3–5 days

to see the effects of these incoming DCs on T-cell development. Thymic lobes were removed 10–12 days after transplantation, and the phenotype of the incoming CD45.2⁺ DCs and the resident CD45.1⁺ OTII T cells was studied.

At day 10, DCs in the grafted thymic lobes were analyzed for DC markers to assess the phenotype of the host-derived CD45.2⁺ migrating DCs. Of these CD11c⁺ cells, $54 \pm 6\%$ were mature MHCII^{hi}CD8⁻ $\text{Sirp}\alpha^+$ cDCs, $4 \pm 1\%$ were mature CD8⁺ $\text{Sirp}\alpha^-$ cDCs, and the remaining were MHCII^{lo/int}CD8⁻ $\text{Sirp}\alpha^-$, the precursors of CD8⁺ $\text{Sirp}\alpha^-$ cDCs (Fig. 4C). The latter two populations represented newly formed cells derived from recipient BM progenitors that had seeded the thymic grafts.

Thymocyte populations were analyzed by flow cytometry. The number of CD45.1⁺OTII⁺CD4⁺V α 2⁺V β 5⁺ T cells was reduced in lobes grafted into CD11cOVA tg mice compared with controls (Fig. 4D), whereas the number of CD45.1⁺V α 2⁻V β 5⁻CD4⁺ was similar in both groups (data not shown), suggesting that antigen-specific negative selection of OTII⁺ T cells was occurring. In addition, a more than twofold increase in the number of OTII⁺Foxp3⁺ T_RS was seen in the lobes grafted into CD11cOVA tg mice compared with controls (Fig. 4E). Together, these results indicate that DCs migrating into the thymus from the periphery can induce negative selection and antigen-specific T_R development.

Discussion

The present study demonstrates a role for mouse TDCs in T_R differentiation as well as negative selection. In the absence of a MHCII-expressing hemopoietic compartment, we found a 30% reduction in the total number of polyclonal T_RS and an increase in the number of self-reactive CD4 T cells in the thymus. This demonstrates that in addition to mTECs (16, 40), BM-derived cells make a significant contribution to T_R generation and negative selection of CD4 T cells in a steady-state mouse. In addition, a 50% reduction in T_R numbers was observed when the hemopoietic compartment lacked expression of CD80 and CD86. Although

these BM chimeras indicated that a BM-derived cell was important for T_R induction, the *in vitro* coculture system indicated that only TDCs, and not B cells and macrophages, were efficient in inducing T_{RS} . Thus, taken together, it appears that TDCs are the major hemopoietic cells that contribute significantly to T_R generation and negative selection of $CD4^+$ T cells *in vivo*. Previous studies have discounted a nonredundant role for DCs in T_R induction (41, 42). The irradiation protocol used (850–900 rad), which may not be sufficient to completely ablate host-derived cells, coupled with the later time point for analysis (8–10 weeks), may have contributed to these results, however. Mice with reduced thymic cellularity and a profound increase in $CD4^+$ thymocyte cell numbers were observed in previous reports (41). We also see similar results in $MHCII^{-/-}$ BM chimeras at later time points. These mice have reduced thymic cellularity and show immune cell infiltration into organs—an initial sign of autoimmunity (data not shown). At this stage, the massive accumulation of autoreactive $CD4^+$ T cells in the thymus has masked the changes in T_R numbers.

Apart from the issue of their quantitative contribution to the total T_R population, our results now demonstrate that TDCs can induce Ag-specific T_R .

Three types of DCs are found in the mouse thymus (pDCs, $Sirp\alpha^+ CD8^+$ TcDCs, and $Sirp\alpha^+ CD8^-$ TcDCs), and these have counterparts in the human thymus (43). We show that the minor $Sirp\alpha^+$ TcDC subset is much more efficient than the other DCs at polyclonal T_R induction *in vitro*.

Why would the $Sirp\alpha^+$ TcDCs be more efficient in T_R generation? First, the $Sirp\alpha^+$ TcDCs are more mature, in terms of expression of MHCII and costimulatory molecule, than the other TDCs, consistent with the phenotype of migratory DCs. This may enable them to interact more efficiently with the $CD4^+$ thymocytes. Second, the $Sirp\alpha^+$ cDCs are more efficient at presentation of antigens on MHCII than the $CD8^+$ cDCs (44–46). Finally, we found that the $Sirp\alpha^+$ TcDCs express high levels of *CCL17* and *CCL22*, and this may facilitate an interaction with the $CD4^+$ thymocytes expressing high levels of *CCR4*. In a cell migration assay, $CD4^+$ thymocytes preferentially migrated toward supernatants from the $Sirp\alpha^+$ TcDCs. This provides a mechanism by which rare antigen-specific thymocytes can encounter their cognate antigen with a higher frequency.

Previous studies showed that migratory DC can induce negative selection of T cells specific for a peripherally expressed antigen (10). We now add to this picture by demonstrating that $Sirp\alpha^+$ cDCs or their immediate precursors present in blood migrate into the thymus and induce both negative selection and T_R development.

Would this process be detrimental to the host during a viral infection? Viral antigens in the periphery ferried to the thymus may induce T_{RS} , which could induce tolerance to the virus and potentially jeopardize a memory response. It is possible that thymic homing receptors or lymphoid egress receptors are down-regulated in DCs that have been activated by virus infection. Indeed, activated T cells down-regulate the egress receptor sphingosine 1-phosphate receptor-1, leading to retention of T cells in the lymphoid tissues (47). Whether this also occurs in activated DCs would be an interesting question to address in future studies.

In summary, we demonstrate that thymic DCs contribute to T_R induction *in vivo*. More significantly, we show that peripheral DCs can migrate into the thymus, where they induce the development of T_{RS} and the deletion of self-reactive $CD4^+$ thymocytes. Based on these observations, we propose a mechanism by which central tolerance to peripherally expressed antigens is induced by migrating DCs, a mechanism additional to the ectopic expression of peripheral antigens by mTECs.

Materials and Methods

Mice. All mice were bred under specific pathogen-free conditions. $B7^{-/-}$ mice were purchased from The Jackson Laboratory and maintained in the University Laboratory Animal Research Facility at the University of Michigan. All other mice

were obtained from The Walter and Eliza Hall Institute animal breeding facility. C57BL/6 (B6) mice 6–8 weeks of age were used for isolation of DCs and thymocytes. B6 $CD45.1$ mice 10 weeks of age were used as BM recipients. The mouse strains used included OTII tg ($CD4^+$ T cells expressing the TCR specific for MHCII-restricted Ova peptide) (48) on a B6, $CD45.1$, or $Rag2^{-/-}$ background; $IA/IA^{-/-}$ ($MHCII^{-/-}$) (49); $B7^{-/-}$ (50); and $CD11cOVA$ tg mice that express membrane-bound ovalbumin (amino acids 323–339) under control of the $CD11c$ promoter (29, 51).

BM Chimeras. $CD45.1$ recipient mice were lethally irradiated with two doses of 5.5 Gy (3 h apart) and then received 5×10^6 $CD45.2$ donor BM cells i.v. from B6 or $MHCII^{-/-}$ mice or from $Rag2^{-/-}$ OTII/ $CD11cOVA$ double-tg mice. For $B7^{-/-}$ chimeras, $CD45.1$ recipient mice were lethally irradiated with 8.0 Gy of total body irradiation. A total of 5×10^6 T-cell depleted B6 WT or $B7^{-/-}$ donor BM cells were injected i.v. into the recipients the next day. Chimeras were analyzed by flow cytometry 6–8 weeks after reconstitution.

Antibodies. Details can be found in [SI Experimental Procedures](#).

Isolation of DCs. Details can be found in [SI Experimental Procedures](#).

Isolation of Thymocytes. Details can be found in [SI Experimental Procedures](#).

Carboxyfluorescein Succinimidyl Ester Labeling. Details can be found in [SI Experimental Procedures](#).

Isolation of Thymic B Cells, Macrophages, and mTECs. Details can be found in [SI Experimental Procedures](#).

T_R Suppression Assay. Details can be found in [Supplementary Experimental Procedures](#).

Generation of T_{RS} In Vitro. *In vitro* T_R induction assays were performed in triplicate in a round-bottom 96-well plate with 1×10^4 sorted thymic or splenic DC subsets from $CD45.2$ mice and 2×10^4 sorted $CD4^+ CD25^-$ thymocytes from $CD45.1$ mice, cultured together with an optimal concentration of IL-7 for 5 days. T_{RS} were assessed by staining for $CD45.1$ (A201.1), $CD4$, $CD25$, and $Foxp3$. When GFP- $Foxp3$ mice were used as the $CD4^+$ thymocyte source, thymocytes were sorted as $CD4^+ CD25^- Foxp3^-$ (excluding all $Foxp3^+$ cells). IL-7 used was from the culture supernatant of J558L cells transfected with the murine IL-7 cDNA in the BMG *neo* vector (55). To determine the optimal concentration of the IL-7 supernatant, the supernatant was titrated on IL-7-dependent pro-B cells (37).

Quantitative PCR. Quantitative PCR was performed for chemokine gene expression by DC subsets as previously described (56). Further details can be found in [Supplementary Experimental Procedures](#).

Cell Migration Assay. Sorted TDC and SDC subsets (5×10^5 in 600 μ l) were cultured in a 24-well plate for 3 h. The supernatant was removed and placed in the base of transwell chambers (5.0- μ M pore size; COSTAR). Sorted $CD4^+ CD25^-$ thymocytes (2×10^5) were placed in the top of the chamber and allowed to migrate for 2 h at 37 °C. The number of cells that had migrated was enumerated using fixed numbers of beads as a calibration standard.

In Vivo DC Migration Assay. Details can be found in [Supplementary Experimental Procedures](#).

Staining Blood DCs. Details can be found in [Supplementary Experimental Procedures](#).

Thymic Grafting. Thymic lobes from 1-day-old donor mice were grafted under the kidney capsule of anesthetized 8-week-old recipient mice using a procedure described elsewhere (57). At specified times postgrafting, grafted thymic lobes were recovered and processed individually. Thymic lobes were digested in collagenase/DNase and analyzed by flow cytometry.

Statistical Analysis. Statistical significance was assessed by the two-tailed unpaired Student's *t* test. Differences with *P* values less than 0.05 were considered significant.

ACKNOWLEDGMENTS. We thank T. Berketa and J. Carneli for animal husbandry; C. Young, C. Tarlington, V. Milovac, J. Garbe, T. McLeod-Dryden, and S. Fung for assistance with flow cytometric sorting and analysis; M. Bradtke and D. Vremec for technical assistance; and I.

Caminschi, J. Miller, J. Villadangos, and W. Heath for discussions. L. Wu and K. Shortman were supported by a grant from the Australian Stem Cell

Centre and a grant from the Australian National Health and Medical Research Council.

- Palmer E (2003) Negative selection—clearing out the bad apples from the T-cell repertoire. *Nat Rev Immunol* 3:383–391.
- Fontenot JD, Gavin MA, Rudensky AY (2003) Foxp3 programs the development and function of CD4+CD25+ regulatory T cells. *Nat Immunol* 4:330–336.
- Hori S, Nomura T, Sakaguchi S (2003) Control of regulatory T cell development by the transcription factor Foxp3. *Science (New York, NY)* 299:1057–1061.
- Khattari R, Cox T, Yasayko SA, Ramsdell F (2003) An essential role for Scurfin in CD4+CD25+ T regulatory cells. *Nat Immunol* 4:337–342.
- Jordan MS, et al. (2001) Thymic selection of CD4+CD25+ regulatory T cells induced by an agonist self-peptide. *Nat Immunol* 2:301–306.
- Sakaguchi S (2004) Naturally arising CD4+ regulatory T cells for immunologic self-tolerance and negative control of immune responses. *Annu Rev Immunol* 22:531–562.
- Fontenot JD, Dooley JL, Farr AG, Rudensky AY (2005) Developmental regulation of Foxp3 expression during ontogeny. *J Exp Med* 202:901–906.
- Gao EK, Lo D, Sprent J (1990) Strong T cell tolerance in parent—F1 bone marrow chimeras prepared with supralethal irradiation. Evidence for clonal deletion and anergy. *J Exp Med* 171:1101–1121.
- Gallegos AM, Bevan MJ (2004) Central tolerance to tissue-specific antigens mediated by direct and indirect antigen presentation. *J Exp Med* 200:1039–1049.
- Bonasio R, et al. (2006) Clonal deletion of thymocytes by circulating dendritic cells homing to the thymus. *Nat Immunol* 7:1092–1100.
- Brocker T (1997) Survival of mature CD4 T lymphocytes is dependent on major histocompatibility complex class II-expressing dendritic cells. *J Exp Med* 186:1223–1232.
- van Meerwijk JP, et al. (1997) Quantitative impact of thymic clonal deletion on the T cell repertoire. *J Exp Med* 185:377–383.
- Webb SR, Sprent J (1990) Tolerogenicity of thymic epithelium. *Eur J Immunol* 20:2525–2528.
- Bensinger SJ, Bandeira A, Jordan MS, Caton AJ, Laufer TM (2001) Major histocompatibility complex class II-positive cortical epithelium mediates the selection of CD4(+)25(+) immunoregulatory T cells. *J Exp Med* 194:427–438.
- Apostolou I, Sarukhan A, Klein L, von Boehmer H (2002) Origin of regulatory T cells with known specificity for antigen. *Nat Immunol* 3:756–763.
- Aschenbrenner K, et al. (2007) Selection of Foxp3+ regulatory T cells specific for self antigen expressed and presented by Aire+ medullary thymic epithelial cells. *Nat Immunol* 8:351–358.
- Coombs JL, et al. (2007) A functionally specialized population of mucosal CD103+ DCs induces Foxp3+ regulatory T cells via a TGF- β and retinoic acid dependent mechanism. *J Exp Med* 204:1757–1764.
- Mucida D, et al. (2007) Reciprocal TH17 and regulatory T cell differentiation mediated by retinoic acid. *Science (New York, NY)* 317:256–260.
- Watanabe N, et al. (2005) Hassall's corpuscles instruct dendritic cells to induce CD4+CD25+ regulatory T cells in human thymus. *Nature* 436:1181–1185.
- Vremec D, Pooley J, Hochrein H, Wu L, Shortman K (2000) CD4 and CD8 expression by dendritic cell subtypes in mouse thymus and spleen. *J Immunol* 164:2978–2986.
- Lahoud MH, et al. (2006) Signal regulatory protein molecules are differentially expressed by CD8-dendritic cells. *J Immunol* 177:372–382.
- Wu L, Li CL, Shortman K (1996) Thymic dendritic cell precursors: relationship to the T lymphocyte lineage and phenotype of the dendritic cell progeny. *J Exp Med* 184:903–911.
- Ardavin C, Wu L, Li CL, Shortman K (1993) Thymic dendritic cells and T cells develop simultaneously in the thymus from a common precursor population. *Nature* 362:761–763.
- Donskoy E, Goldschneider I (2003) Two developmentally distinct populations of dendritic cells inhabit the adult mouse thymus: demonstration by differential importation of hematogenous precursors under steady state conditions. *J Immunol* 170:3514–3521.
- Fontenot JD, et al. (2005) Regulatory T cell lineage specification by the forkhead transcription factor foxp3. *Immunity* 22:329–341.
- Bochtler P, Wahl C, Schirmbeck R, Reimann J (2006) Functional adaptive CD4 foxp3 T cells develop in MHC class II-deficient mice. *J Immunol* 177:8307–8314.
- Bogunovic M, et al. (2006) Identification of a radio-resistant and cycling dermal dendritic cell population in mice and men. *J Exp Med* 203:2627–2638.
- Merad M, et al. (2002) Langerhans cells renew in the skin throughout life under steady-state conditions. *Nat Immunol* 3:1135–1141.
- Stephote RJ, et al. (2007) Cognate CD4+ help elicited by resting dendritic cells does not impair the induction of peripheral tolerance in CD8+ T cells. *J Immunol* 178:2094–2103.
- Takeda I, et al. (2004) Distinct roles for the OX40-OX40 ligand interaction in regulatory and nonregulatory T cells. *J Immunol* 172:3580–3589.
- Salomon B, et al. (2000) B7/CD28 costimulation is essential for the homeostasis of the CD4+CD25+ immunoregulatory T cells that control autoimmune diabetes. *Immunity* 12:431–440.
- Takahashi T, et al. (2000) Immunologic self-tolerance maintained by CD25(+)CD4(+) regulatory T cells constitutively expressing cytotoxic T lymphocyte-associated antigen 4. *J Exp Med* 192:303–310.
- Tang Q, et al. (2003) Cutting edge: CD28 controls peripheral homeostasis of CD4+CD25+ regulatory T cells. *J Immunol* 171:3348–3352.
- Kumanogoh A, et al. (2001) Increased T cell autoreactivity in the absence of CD40-CD40 ligand interactions: A role of CD40 in regulatory T cell development. *J Immunol* 166:353–360.
- Wilson NS, et al. (2003) Most lymphoid organ dendritic cell types are phenotypically and functionally immature. *Blood* 102:2187–2194.
- Wilson NS, Villadangos JA (2004) Lymphoid organ dendritic cells: Beyond the Langerhans cells paradigm. *Immunol Cell Biol* 82:91–98.
- Nutt SL, Urbaneck P, Rolink A, Busslinger M (1997) Essential functions of Pax5 (BSAP) in pro-B cell development: Difference between fetal and adult B lymphopoiesis and reduced V-to-DJ recombination at the IgH locus. *Genes Dev* 11:476–491.
- Chantry D, et al. (1999) Macrophage-derived chemokine is localized to thymic medullary epithelial cells and is a chemoattractant for CD3(+), CD4(+), CD8(low) thymocytes. *Blood* 94:1890–1898.
- Wu L, et al. (1995) Mouse thymus dendritic cells: Kinetics of development and changes in surface markers during maturation. *Eur J Immunol* 25:418–425.
- Klein L, Roettinger B, Kyewski B (2001) Sampling of complementing self-antigen pools by thymic stromal cells maximizes the scope of central T cell tolerance. *Eur J Immunol* 31:2476–2486.
- Liston A, et al. (2008) Differentiation of regulatory Foxp3+ T cells in the thymic cortex. *PNAS* 105:11903–11908.
- Ribot J, Romagnoli P, van Meerwijk JP (2006) Agonist ligands expressed by thymic epithelium enhance positive selection of regulatory T lymphocytes from precursors with a normally diverse TCR repertoire. *J Immunol* 177:1101–1107.
- Vandenabeele S, Hochrein H, Mavaddat N, Winkel K, Shortman K (2001) Human thymus contains 2 distinct dendritic cell populations. *Blood* 97:1733–1741.
- Dudzick D, et al. (2007) Differential antigen processing by dendritic cell subsets in vivo. *Science (New York, NY)* 315:107–111.
- Pooley JL, Heath WR, Shortman K (2001) Cutting edge: Intravenous soluble antigen is presented to CD4 T cells by CD8- dendritic cells, but cross-presented to CD8 T cells by CD8+ dendritic cells. *J Immunol* 166:5327–5330.
- Schnorrer P, et al. (2006) The dominant role of CD8+ dendritic cells in cross-presentation is not dictated by antigen capture. *PNAS* 103:10729–10734.
- Shiow LR, et al. (2006) CD69 acts downstream of interferon- α /beta to inhibit S1P1 and lymphocyte egress from lymphoid organs. *Nature* 440:540–544.
- Barnden MJ, Allison J, Heath WR, Carbone FR (1998) Defective TCR expression in transgenic mice constructed using cDNA-based alpha- and beta-chain genes under the control of heterologous regulatory elements. *Immunol Cell Biol* 76:34–40.
- Cosgrove D, et al. (1991) Mice lacking MHC class II molecules. *Cell* 66:1051–1066.
- Borriello F, et al. (1997) B7-1 and B7-2 have overlapping, critical roles in immunoglobulin class switching and germinal center formation. *Immunity* 6:303–313.
- Brocker T, Riedinger M, Karjalainen K (1997) Targeted expression of major histocompatibility complex (MHC) class II molecules demonstrates that dendritic cells can induce negative but not positive selection of thymocytes in vivo. *J Exp Med* 185:541–550.
- Vremec D, et al. (1992) The surface phenotype of dendritic cells purified from mouse thymus and spleen: Investigation of the CD8 expression by a subpopulation of dendritic cells. *J Exp Med* 176:47–58.
- Vremec D, Shortman K (1997) Dendritic cell subtypes in mouse lymphoid organs: Cross-correlation of surface markers, changes with incubation, and differences among thymus, spleen, and lymph nodes. *J Immunol* 159:565–573.
- Gray DH, Chidgey AP, Boyd RL (2002) Analysis of thymic stromal cell populations using flow cytometry. *J Immunol Methods* 260:15–28.
- Winkler TH, Melchers F, Rolink AG (1995) Interleukin-3 and interleukin-7 are alternative growth factors for the same B-cell precursors in the mouse. *Blood* 85:2045–2051.
- Proietto AI, et al. (2004) Differential production of inflammatory chemokines by murine dendritic cell subsets. *Immunobiology* 209:163–172.
- Berzins SP, Boyd RL, Miller JF (1998) The role of the thymus and recent thymic migrants in the maintenance of the adult peripheral lymphocyte pool. *J Exp Med* 187:1839–1848.

IN THIS ISSUE, PSYCHOLOGY

Correction for the “In This Issue” summary entitled “Universal displays of pride and shame,” which appeared in issue 33, August 19, 2008, of *Proc Natl Acad Sci USA* (105:11587–11588).

The authors note that the figure is copyrighted by Bob Willingham and is reprinted with permission. The online version has been corrected. The figure and its corrected legend appear below.



Blind athletes (Right) show pride in victory like sighted athletes (Left). [Reproduced with permission (Copyright 2004, Bob Willingham).]

www.pnas.org/cgi/doi/10.1073/pnas.0811958106

PERSPECTIVE

Correction for “Chemical Ecology Special Feature: The evolution of gene collectives: How natural selection drives chemical innovation,” by Michael A. Fischbach, Christopher T. Walsh, and Jon Clardy, which appeared in issue 12, March 25, 2008, of *Proc Natl Acad Sci USA* (105:4601–4608; first published January 23, 2008; 10.1073/pnas.0709132105).

The authors note that a reference was inadvertently omitted from their article. On page 4607, right column, in *Conclusion: How Do New Gene Clusters Form?*, line 17, the reference callout “(109–111)” should instead read “(109–111, 113).” The added reference appears below.

113. Balado M, Osorio CR, Lemos ML (2006) A gene cluster involved in the biosynthesis of vancomycin, a chromosome-encoded siderophore produced by *Vibrio anguillarum*. *Microbiology* 152:3517–3528.

www.pnas.org/cgi/doi/10.1073/pnas.0812594106

DEVELOPMENTAL BIOLOGY

Correction for “Genome-wide expression profiling reveals distinct clusters of transcriptional regulation during bovine preimplantation development in vivo,” by W. A. Kues, S. Sudheer, D. Herrmann, J. W. Carnwath, V. Havlicek, U. Besenfelder, H. Lehrach, J. Adjaye, and H. Niemann, which appeared in issue 50, December 16, 2008, of *Proc Natl Acad Sci USA* (105:19768–19773; first published December 8, 2008; 10.1073/pnas.0805616105).

The authors note that due to a printer’s error, the affiliation information for some authors appeared incorrectly. The correct affiliation for V. Havlicek and U. Besenfelder is “Reproduction Centre-Wieselburg, University of Veterinary Medicine, 1210 Vienna, Austria”; and the correct affiliation for H. Lehrach and J. Adjaye is “Department of Vertebrate Genomics, Max Planck Institute for Molecular Genetics, 14195 Berlin, Germany.”

www.pnas.org/cgi/doi/10.1073/pnas.0813350106

APPLIED BIOLOGICAL SCIENCES

Correction for “HDAC2 blockade by nitric oxide and histone deacetylase inhibitors reveals a common target in Duchenne muscular dystrophy treatment,” by Claudia Colussi, Chiara Mozzetta, Aymone Gurtner, Barbara Illi, Jessica Rosati, Stefania Straino, Gianluca Ragone, Mario Pescatori, Germana Zaccagnini, Annalisa Antonini, Giulia Minetti, Fabio Martelli, Giulia Piaggio, Paola Gallinari, Christian Steinkulher, Emilio Clementi, Carmela Dell’Aversana, Lucia Altucci, Antonello Mai, Maurizio C. Capogrossi, Pier Lorenzo Puri, and Carlo Gaetano, which appeared in issue 49, December 9, 2008, of *Proc Natl Acad Sci USA* (105:19183–19187; first published December 1, 2008; 10.1073/pnas.0805514105).

The authors note that the author name **Christian Steinkulher** should have appeared as **Christian Steinkuhler**. The author line has been corrected online. The corrected author line appears below.

Claudia Colussi, Chiara Mozzetta, Aymone Gurtner, Barbara Illi, Jessica Rosati, Stefania Straino, Gianluca Ragone, Mario Pescatori, Germana Zaccagnini, Annalisa Antonini, Giulia Minetti, Fabio Martelli, Giulia Piaggio, Paola Gallinari, Christian Steinkuhler, Emilio Clementi, Carmela Dell’Aversana, Lucia Altucci, Antonello Mai, Maurizio C. Capogrossi, Pier Lorenzo Puri, and Carlo Gaetano

www.pnas.org/cgi/doi/10.1073/pnas.0813311106

IMMUNOLOGY

Correction for “Dendritic cells in the thymus contribute to T-regulatory cell induction,” by Anna I. Proietto, Serani van Dommelen, Penghui Zhou, Alexandra Rizzitelli, Angela D’Amico, Raymond J. Steptoe, Shalin H. Naik, Mireille H. Lahoud, Yang Liu, Pan Zheng, Ken Shortman, and Li Wu, which appeared in issue 50, December 16, 2008, of *Proc Natl Acad Sci USA* (105:19869–19874; first published December 10, 2008; 10.1073/pnas.0810268105).

The authors note that due to a printer’s error, in the Abstract, beginning on line 6, “TDCs include two conventional dendritic cell (DC) subtypes, CD8^{lo}Sirpα^{hi/+} (CD8^{lo}Sirpα⁺) and CD8^{hi}Sirpα^{lo/-} (CD8^{lo}Sirpα⁻), which have different origins. We found that the CD8^{hi}Sirpα⁺ DCs represent a conventional DC subset that originates from the blood and migrates into the thymus” should instead read: “TDCs include two conventional dendritic cell (DC) subtypes, CD8^{lo}Sirpα^{hi/+} (CD8^{lo}Sirpα⁺) and CD8^{hi}Sirpα^{lo/-} (CD8^{hi}Sirpα⁻), which have different origins. We found that the CD8^{lo}Sirpα⁺ DCs represent a conventional DC subset that originates from the blood and migrates into the thymus.”

www.pnas.org/cgi/doi/10.1073/pnas.0813353106

Biological Sciences, Immunology

**Targeting Lymphotoxin-mediated Negative Selection to Prevent Prostate
Cancer in Mice with Genetic Predisposition**

Penghui Zhou¹, Xianfeng Fang², Ping Yu³, Mingzhao Zhu³, Yang-Xin Fu³,
Lizhong Wang¹, Yang Liu¹ and Pan Zheng¹

¹Division of Immunotherapy

Departments of Surgery, Internal Medicine and Pathology

University of Michigan School of Medicine and Cancer Center

Ann Arbor, MI 48109

²Institute of Biophysics, Chinese Academy of Science, Beijing, China

³Department of Pathology, University of Chicago School of Medicine
Chicago, IL 60636

Corresponding Authors:

Pan Zheng (panz@umich.edu) or Yang Liu (yangl@umich.edu).

109 Zina Pitcher Place, Ann Arbor, MI 48109. Tel: (734)-615-3464, Fax: (734)-
763-2162.

Number of pages: 24.

Figures: 6.

Tables: 1.

Abstract

Identification of genetically susceptible individuals calls for preventive measures to minimize the life-long cancer risk of these high risk populations. Immune prevention is made necessary by the anticipated health threat but only possible by predictability of antigens. Lack of enough high affinity of T cells against tumor-associated antigens and unpredictability of tumor antigen make antigen-based immune prevention untenable for cancer. To address this issue, we explored a non-antigen-based cancer immune prevention using the TRAMP mice that spontaneously develop prostate cancer with 100% penetrance. We show that targeted mutation of the *LT α* gene efficiently rescued tumor-reactive T cells, drastically reduced cancer incidence and almost completely ablated metastasis. Remarkably, short-term treatments with LT β Rlg interrupted clonal deletion, reduced the size of primary cancer and completely prevented metastasis later in life, thus providing an easily translatable immune prevention for those with genetic predisposition to cancer.

Introduction

One of the most important advances in cancer research is the identification of individuals with increased susceptibility (1). Broadly speaking, genetic susceptibility can be conferred by inactive alleles of tumor suppressor gene or by hypermorphic alleles of oncogenes (2, 3). In extreme cases, inactivating mutations of tumor suppressor genes such as p53 (4), APC (5, 6) and BRCA1/2 (7-9) resulted in nearly 80% life-long cancer risk. The high penetrance of the high risk allele was responsible for their identification. It is estimated that about 1-5% of cancer cases are caused by dominant familial susceptibility alleles, yet the majority of the genes remains to be identified (10). In addition to the high penetrance cancer susceptibility alleles, recent genetic studies allow identification of numerous susceptibility loci that can be identified by genetic markers (11-16). It is anticipated that increasing numbers of individuals will be diagnosed with high cancer risk, which provides enormous opportunity for cancer prevention. Moreover, family history alone can serve as a powerful tool to identify individual with high risk. For example, a comprehensive studies involving more than 2 million nuclear families reveals that individuals with affected sib and at least one parent can have more than 30-fold higher risk of colon-rectal cancer (17).

Identification of genetically susceptible individuals calls for preventive measures to minimize the life-long cancer risk of these high risk populations, such as prophylactic surgery (18). Given vital importance of many organs,

prophylactic surgery is difficult to implement to those yet to develop cancer. Therefore, other preventive measures are badly needed. The notion of chemoprevention was first demonstrated more than 30 years ago (19). Its efficacy has been demonstrated in several large clinical trials (20-22). Generally speaking, the drug or nutritional supplement must be administered repeatedly over the life time. Therefore, chemoprevention has a high burden of compliance and drug safety. On the other hand, thanks to immunological memory, immunity can last a life time without the stringent requirement of frequent boosting. Unfortunately, we are not aware of any attempt to use immune prevention to reduce both risk and mortality of cancer among the population with high genetic predisposition to cancer.

Immune prevention is made necessary by the anticipated health threat and possible by predictability of antigens carried by pathogens. The classic notion of immune prevention is based on immunization with antigens expressed by the pathogens. The power of immune prevention is best demonstrated by large scale of prevention of various infection diseases, including eradication of smallpox. However, adoption of immune prevention to cancer is limited by several factors. First, compared with pathogens, cancer antigens are poorly defined, unpredictable and more heterogeneous (23-25), which makes it considerably more difficult to design antigen-based vaccine for the purpose of prevention. Second, since cancers are derived from normal tissues, most of high affinity T cells reactive to such peripheral tissue antigens in the cancer cells have

been deleted (26). Lack of high affinity tumor-reactive T cells would in theory makes immune prevention difficult to attain.

Recent studies have demonstrated that clonal deletion of T-cell reactive to peripheral antigens depends on their expression in the thymic medullar epithelial cells (27, 28). Since tumors are comprised of malignantly transformed cells from normal tissues and therefore likely express tissue-specific antigens, it is of interest to determine whether these T cells can be rescued for the purpose of immune prevention. Since lymphotoxin α ($LT\alpha$) gene play a major role in the development and function of medullar epithelial cells (29, 30), especially in the context of clonal deletion of peripheral antigen-reactive T cells, blocking this pathway may allow one to rescue tumor-reactive T cells to prevent the development of cancer. Using mice with targeted mutation of $LT\alpha$ (31), we reveal here a valuable target for rescuing prostate cancer-reactive T cells and for cancer immune prevention. More importantly, transient blockade of $LT\alpha$ significantly reduced the sizes of prostate cancer and eliminated cancer metastasis. To our knowledge, this is the first non-antigen-based immune prevention for cancer and it has a realistic chance to be translated into clinical care of those patients with high genetic risk for cancer.

Results

Targeted mutation of *LT α* limits clonal deletion of SV40 T antigen-specific T cells

One of our groups has recently demonstrated a critical role for *LT α* in clonal deletion of T cells specific for tissue-specific antigens (29). As a first test to determine whether this pathway can be explored for cancer immune prevention, we take a transgenic approach to determine whether this pathway can be explored for rescue of cancer-reactive T cells. We crossed the transgenic mice expressing TCR specific for SV40 large T antigen (Tag-I) (32) to the TRAMP mice expressing SV40 large T antigen under the control of probasin promoter (33), with the null mutation in none, one or two alleles of *LT α* gene. The development of the transgenic T cells was evaluated by flow cytometry.

As shown in Fig. 1a, in the Tag-I/TRAMP double transgenic mice, targeted mutation of one or both allele of the *LT α* gene resulted in significant increase in total thymic cellularity. A dramatic increase in % of DP and a significant decrease in DN% were observed among the transgenic TCR⁺ cells. Targeted mutation of both alleles of *LT α* eliminated the DN while expanded the DP and CD8 SP subsets (Fig. 1b&c). In addition, the numbers of transgenic T cells are greatly increased in the spleens of *LT α* -deficient mice (Fig. 1d, e). Remarkably, partial rescue was observed in the heterozygous mice (Fig. 1). Therefore, *LT α* play a critical role in clonal deletion of SV40-large T antigen-reactive T cells.

Targeted mutation of $LT\alpha$ inhibits development of spontaneous prostate cancer

To test the role for $LT\alpha$ in the onset of prostate cancer, measured the size of prostates at 30 weeks by magnet resonance imaging (MRI) (34). Representative images are shown in Fig. 2a, while the summary data are shown in Fig. 2b. These data demonstrated that the size of prostate was reduced by more than 3-fold in the TRAMP mice with either heterozygous or homologous deletion of $LT\alpha$ (Fig. 2b, c). At 34 weeks, the three groups of mice were sacrificed for double blind histology analyses of the cancer development and metastasis. As shown in Fig. 2c, 100% WT mice developed malignant prostate cancer, with metastasis in 7/12 cases. Among them, one mouse had metastasis in kidney only, while six others had metastasis in the lung including two that also had metastasis in the liver. In mice with homozygous mutation, only 45% (5/11) mice developed malignant tumors. Remarkably, 4/11 mice had normal prostate morphology, while two others had prostate intraepithelial neoplasia (PIN). Only 1/11 mice had metastasis, in both liver and lung. A reduction of cancer incidence 13/16 was also observed in the heterozygous mice. Two heterozygous mice had completely normal prostate and one mouse had PIN. Moreover, only 1 in 16 heterozygous mice show lung metastasis. Since lymph node development is preserved in the heterozygous mice (data not shown), the major reduction of metastasis cannot be attributed to the lack of lymph nodes, which occurred in mice with homozygous $Lt\alpha$ mutation (31). X^2 analysis indicates a gene-dose

dependent reduction both in rate of malignancy ($P=0.0071$) and metastasis ($P=0.0023$). Taken together, our data presented in Figure 1 and 2 demonstrated that targeted mutations of $LT\alpha$ rescued tumor-reactive T cells and increased host resistance to prostate cancer.

The administration of $LT\beta$ Rlg rescues tumor-reactive T cells without provoking autoimmune inflammation

The fact genetic inactivation of $LT\alpha$ conveys host resistance to prostate cancer raised an interesting possibility that $LT\alpha$ may be targeted for the purpose of immune prevention. Since aged $LT\alpha^{-/-}$ mice developed chronic inflammation, one has to be concerned with potential autoimmune side effects of this treatment (29, 30). In order to achieve this goal, we compared the inflammatory response when mice were treated with 3 weekly administration of soluble murine $LT\beta$ Rlg or Human IgGFc, starting at 4, 6 or 11 weeks of age. The mice were sacrificed 4 weeks after completion of the treatments. As shown in Table 1 and Fig. 3, while infiltrates in liver and lung was observed in mice received their first dose at 4 weeks, no inflammation or tissue injury were observed when the treated was initiated at 6 or 11 weeks.

We have recently reported strong clonal deletion in transgenic mice TRAMP/TGB that both express TCR specific for SV40 large T cells and SV40 large T antigen (35, 36). The clonal deletion was characterized by massive reduction of $CD8^+V\beta 8^{hi}$ transgenic T cells (35). These features were recapitulated in the double transgenic mice receiving IgG Fc control (Fig. 4a).

Interestingly, treatment with LT β Rlg resulted in a 6-fold increase in DP and nearly 3-fold increase in the CD8 SP subset (Fig. 4b lower panel and Fig. 4c). Correspondingly, the number of transgenic CD8 T cells was more than doubled in the spleen. In mice lacking the large T antigen, no increase of transgenic T cells in the thymus was conferred by fusion protein (Fig. 4f-h). In contrast the fusion proteins actually reduced the number of transgenic T cell in the thymus. Therefore, the LT β Rlg expand SV40 T antigen-specific T cells only if the antigen was present.

To determine whether LT β Rlg prevented deletion of antigen-specific T cells, we compared % of apoptotic cells by staining with Annexin V. As shown in Fig. 5, LT β Rlg significantly reduced % of apoptotic cells regardless of the subsets of the transgenic thymocytes. This treatment, however, has no effect on apoptosis of T cells in the spleen. Therefore, the increase of transgenic T cells in the TRAMP/TGB mice is likely due to rescue of T cells from clonal deletion in the thymus.

Short-term treatment with LT β Rlg reduces the progression of primary prostate cancer and prevented metastasis

LT β Rlg binds LT α with high affinity. To test whether LT β Rlg treatment can significant affect the progression of prostate cancer, we treated the TRAMP mice with 3 weekly injections of either LT β Ig or control IgG, starting at six weeks. At 30 weeks the volume of the prostate were measured the MRI. As shown in

Fig. 6a, on average, the LT β Rlg treatment at 6 weeks caused greater than 50% reduction in the prostate volume ($P < 0.01$).

We carried out histological analysis to characterize the effect of LT β Rlg treatment on the development of metastasis. As shown in Fig. 6b, 4 of 7 control-Ig treated TRAMP mice developed metastasis in lung and/or liver, consistent with previous reports by others (33). Importantly, none of the LT β Rlg treated mice developed metastasis. Moreover, the lack of autoimmune disease is further supported by lack of inflammation in any of the organ studied (Fig. 6b and data not shown). Therefore, transient treatment of LT β Rlg reduced the site of primary lesion and completely prevented metastasis without provoking lymphocyte infiltration into organs.

Discussion

It is difficult to use cancer vaccine as preventive measures for those with genetic predisposition because of a multitude of mechanisms of immune tolerance, including clonal deletion to tissue-specific antigens (26, 35, 36) and clonal anergy (37) as well as unpredictability of tumor antigens (23-25). Here we devised a non-antigen-based strategy of immune prevention that in theory can be applicable to tumors from a variety of tissue origin. The foundation of the strategy is the critical role for $LT\alpha$ in clonal deletion of T cells specific for peripheral antigen (29, 30). Using TCR transgenic mice as the basic readout, we have demonstrated that short-term treatments with soluble $LT\beta RIg$ rescued cancer-reactive T cells that would be otherwise deleted in the thymus. Corresponding to this, we found that TRAMP mice that received short term treatment of soluble $LT\beta RIg$ at six weeks have significantly reduced sizes at 30 weeks. More importantly, this treatment completely prevented the development of metastasis. Since targeted mutation of $LT\alpha$ limits clonal deletion of SV40 T antigen-specific T cells and inhibits development of spontaneous prostate cancer, prevention by $LT\beta RIg$ is likely due to its binding to $LT\alpha$.

It has been demonstrated that transgenic mice expressing SV40 T antigens developed tumors concomitant with development of T-antigen-specific T cells (38). Therefore, merely priming antigen-specific T cells is insufficient to prevent tumor development. The quality of T cells, such as the antigens recognized and affinity for cancer antigens, also likely matters. Our data

presented in this studies indicated that blockade of $LT\alpha$ can efficiently prevent deletion of two lines of high affinity transgenic T cells specific for an antigen expressed in prostate specific fashion as a transgene.

A major advantage of the $LT\alpha$ -blockade based immune prevention is the potential applicability to a number of different cancer types regardless of tumor antigens involved. Although it remains to be tested whether this strategy is applicable to human, it is of interest to note the association between $LT\alpha$ polymorphism and risk of prostate cancer in man (39-41).

Since the prevention is to be applied to high-risk healthy patients, a primary concern is its potential autoimmune side effect. It has been reported that germline mutation of $LT\alpha$ cause multiple organ infiltration (29). Our extensive analysis of the $LT\beta RIg$ -treated mice indicated no lymphocyte infiltration into organs if the treatment was initiated after 4 weeks. The side effect when treated at 4 weeks of age is probably due to more active thymopoiesis at younger age. Since treatment at six week have significant preventive effect, our data demonstrate that it is possible to identify appropriate window in which cancer immune prevention can be achieved without overt risk of autoimmune diseases. Taken together, this study has opened a new avenue to develop an immune intervention that prevents cancer development. This approach represents a major departure from the principle of cancer vaccine as it alleviates the need to identify tumor antigen. It is envisaged that subjects that carries high risk allele may be treated with reagents to block $LT\alpha$ or other critical pathway for tolerance

to periphery antigen in order to reduce their future cancer risk and improve clinical outcome if they do develop cancer.

Materials and Methods

Experimental animals WT, TRAMP mice expressing the SV40 Tag controlled by rat probasin regulatory elements and $Lt\alpha^{-/-}$ mice, all in the C57BL/6 background, were purchased from the Jackson Laboratory (Bar Harbor, ME). The mice were bred at the animal facilities of the Ohio State University (Columbus, OH) and the University of Michigan (Ann Arbor, MI). Transgenic TGB and TAG-1 mice expressing TCR specific for different epitope of SV40 large T antigen presented by different MHC loci have been described (42) (32).

Generation of TRAMP mice expressing TGB TCR (TGB-TRAMP) was described (35). $Lt\alpha^{+/+}$ TRAMP, $Lt\alpha^{+/-}$ TRAMP and $Lt\alpha^{-/-}$ TRAMP mice were obtained by breeding $Lt\alpha^{+/-}$ mice with $Lt\alpha^{+/-}$ TRAMP mice. The TAG-1 mice were bred with $Lt\alpha^{-/-}$ mice to obtain $Lt\alpha^{+/-}$ TAG-1 mice, which were crossed with the $Lt\alpha^{+/-}$ TRAMP mice to produce $Lt\alpha^{+/+}$ TAG-1TRAMP, $Lt\alpha^{+/-}$ TAG-1TRAMP and $Lt\alpha^{-/-}$ TAG-1TRAMP mice.

LT β RlgFc treatment For cancer prevention, 6 weeks old TRAMP mice were treated with 3 weekly injections of 100 μ g LT β RlgFc or control IgGFc, intraperitoneally. Treated mice were examined at least weekly for palpable tumor at lower abdomen. The prostate volume was measured by MRI at 30 weeks. Mice were euthanized at 32 weeks, and internal organs were collected for histology analysis.

For rescue of clonal deletion, 6 weeks old TRAMP/TGB mice were treated with 3 weekly injection of 100 μ g LT β RlgFc or control IgGFc, intraperitoneally.

Two weeks after the last treatment, the mice were sacrificed and the total thymocytes and splenocytes were harvested and stained with fluorochrome-conjugated anti-CD4 (RM4.5), anti-CD8 (53-6.7), and anti-V β 8.1+8.2 (MR5-2) antibodies and analyzed by flow cytometer LS2 (Becton & Dickinson, Mountainview, CA).

To test potential autoimmune side effects, 4 weeks, 6 weeks and 11 weeks old TRAMP mice were treated with 100 μ g LT β RlgFc or control IgGfc every week, total 3 injections intraperitoneally. Two weeks after the last treatment, the mice were sacrificed and peripheral organs were collected. Tissue sections from peripheral organs were stained with hematoxylin and eosin (H&E).

Histology Mouse organs were fixed with 10% buffered formalin and were paraffin embedded. Tissue sections were stained with hematoxylin and eosin (H&E), and examined under a microscope. All pathological examinations were performed without knowing the treatment and the genotypes of the mice. At least three sections, 25 micron apart, were examined for each organ to ensure comprehensive evaluation.

Magnetic resonance imaging (MRI) of prostate. The progression of prostate cancer in the TRAMP model was measured by MRI as described (34).

Acknowledgement

This study is supported by grants from National Institute of Health (YL) and Department of Defense Prostate Cancer Program (PZ). The authors have no financial conflict of interest.

References

1. Kinzler KW, Vogelstein B (1996) Lessons from hereditary colorectal cancer. *Cell* 87:159-170.
2. Hanahan D (1985) Heritable formation of pancreatic beta-cell tumours in transgenic mice expressing recombinant insulin/simian virus 40 oncogenes. *Nature* 315:115-122.
3. Hanahan D, Weinberg RA (2000) The hallmarks of cancer. *Cell* 100:57-70.
4. Malkin D, *et al.* (1990) Germ line p53 mutations in a familial syndrome of breast cancer, sarcomas, and other neoplasms. *Science* 250:1233-1238.
5. Groden J, *et al.* (1991) Identification and characterization of the familial adenomatous polyposis coli gene. *Cell* 66:589-600.
6. Nishisho I, *et al.* (1991) Mutations of chromosome 5q21 genes in FAP and colorectal cancer patients. *Science* 253:665-669.
7. Easton DF, *et al.* (1997) Cancer risks in two large breast cancer families linked to BRCA2 on chromosome 13q12-13. *Am J Hum Genet* 61:120-128.
8. Ford D, Easton DF, Bishop DT, Narod SA, Goldgar DE (1994) Risks of cancer in BRCA1-mutation carriers. Breast Cancer Linkage Consortium. *Lancet* 343:692-695.
9. Ford D, *et al.* (1998) Genetic heterogeneity and penetrance analysis of the BRCA1 and BRCA2 genes in breast cancer families. The Breast Cancer Linkage Consortium. *Am J Hum Genet* 62:676-689.
10. Eng C, Hampel H, de la Chapelle A (2001) Genetic testing for cancer predisposition. *Annu Rev Med* 52:371-400.
11. Amundadottir LT, *et al.* (2006) A common variant associated with prostate cancer in European and African populations. *Nat Genet* 38:652-658.
12. Gudmundsson J, *et al.* (2007) Genome-wide association study identifies a second prostate cancer susceptibility variant at 8q24. *Nat Genet* 39:631-637.
13. Haiman CA, *et al.* (2007) A common genetic risk factor for colorectal and prostate cancer. *Nat Genet* 39:954-956.
14. Haiman CA, *et al.* (2007) Multiple regions within 8q24 independently affect risk for prostate cancer. *Nat Genet* 39:638-644.
15. Witte JS (2007) Multiple prostate cancer risk variants on 8q24. *Nat Genet* 39:579-580.
16. Yeager M, *et al.* (2007) Genome-wide association study of prostate cancer identifies a second risk locus at 8q24. *Nat Genet* 39:645-649.
17. Dong C, Hemminki K (2001) Modification of cancer risks in offspring by sibling and parental cancers from 2,112,616 nuclear families. *Int J Cancer* 92:144-150.
18. Guillem JG, *et al.* (2006) ASCO/SSO review of current role of risk-reducing surgery in common hereditary cancer syndromes. *J Clin Oncol* 24:4642-4660.
19. Sporn MB (1976) Approaches to prevention of epithelial cancer during the preneoplastic period. *Cancer Res* 36:2699-2702.

20. Dannenberg AJ, Zakim D (1999) Chemoprevention of colorectal cancer through inhibition of cyclooxygenase-2. *Semin Oncol* 26:499-504.
21. Fisher B, *et al.* (1998) Tamoxifen for prevention of breast cancer: report of the National Surgical Adjuvant Breast and Bowel Project P-1 Study. *J Natl Cancer Inst* 90:1371-1388.
22. Klein EA, *et al.* (2003) SELECT: the selenium and vitamin E cancer prevention trial. *Urologic oncology* 21:59-65.
23. Boon T, Cerottini JC, Van den Eynde B, van der Bruggen P, Van Pel A (1994) Tumor antigens recognized by T lymphocytes. *Annu Rev Immunol* 12:337-365.
24. Prehn RT, Main JM (1957) Immunity to methylcholanthrene-induced sarcomas. *J Natl Cancer Inst* 18:769-778.
25. Monach PA, Meredith SC, Siegel CT, Schreiber H (1995) A unique tumor antigen produced by a single amino acid substitution. *Immunity* 2:45-59.
26. Anderson MS, *et al.* (2002) Projection of an immunological self shadow within the thymus by the aire protein. *Science* 298:1395-1401.
27. Hanahan D (1998) Peripheral-antigen-expressing cells in thymic medulla: factors in self- tolerance and autoimmunity. *Curr Opin Immunol* 10:656-662.
28. Kyewski B, Derbinski J, Gotter J, Klein L (2002) Promiscuous gene expression and central T-cell tolerance: more than meets the eye. *Trends Immunol* 23:364-371.
29. Chin RK, *et al.* (2003) Lymphotoxin pathway directs thymic Aire expression. *Nat Immunol* 4:1121-1127.
30. Boehm T, Scheu S, Pfeffer K, Bleul CC (2003) Thymic medullary epithelial cell differentiation, thymocyte emigration, and the control of autoimmunity require lympho-epithelial cross talk via LTbetaR. *J Exp Med* 198:757-769.
31. De Togni P, *et al.* (1994) Abnormal development of peripheral lymphoid organs in mice deficient in lymphotoxin. *Science* 264:703-707.
32. Staveley-O'Carroll K, *et al.* (2003) In vivo ligation of CD40 enhances priming against the endogenous tumor antigen and promotes CD8+ T cell effector function in SV40 T antigen transgenic mice. *J Immunol* 171:697-707.
33. Greenberg NM, *et al.* (1995) Prostate cancer in a transgenic mouse. *Proc Natl Acad Sci U S A* 92:3439-3443.
34. Eng MH, *et al.* (1999) Early castration reduces prostatic carcinogenesis in transgenic mice. *Urology* 54:1112-1119.
35. Zheng X, *et al.* (2002) Clonal deletion of simian virus 40 large T antigen-specific T cells in the transgenic adenocarcinoma of mouse prostate mice: an important role for clonal deletion in shaping the repertoire of T cells specific for antigens overexpressed in solid tumors. *J Immunol* 169:4761-4769.
36. Zheng X, Yin L, Liu Y, Zheng P (2004) Expression of tissue-specific autoantigens in the hematopoietic cells leads to activation-induced cell death of autoreactive T cells in the secondary lymphoid organs. *Eur J Immunol*.

37. Lee PP, *et al.* (1999) Characterization of circulating T cells specific for tumor-associated antigens in melanoma patients. *Nat Med* 5:677-685.
38. Willimsky G, Blankenstein T (2005) Sporadic immunogenic tumours avoid destruction by inducing T-cell tolerance. *Nature* 437:141-146.
39. Gaudet MM, *et al.* (2007) Genetic variation in tumor necrosis factor and lymphotoxin-alpha (TNF-LTA) and breast cancer risk. *Hum Genet* 121:483-490.
40. Takei K, *et al.* (2008) Lymphotoxin-alpha polymorphisms and presence of cancer in 1,536 consecutive autopsy cases. *BMC cancer* 8:235.
41. Wang SS, *et al.* (2006) Common genetic variants in proinflammatory and other immunoregulatory genes and risk for non-Hodgkin lymphoma. *Cancer Res* 66:9771-9780.
42. Geiger T, Gooding LR, Flavell RA (1992) T-cell responsiveness to an oncogenic peripheral protein and spontaneous autoimmunity in transgenic mice. *Proc Natl Acad Sci U S A* 89:2985-2989.

Table 1. Inflammation induced by LTβlg at 4 but not 6 or 11 weeks.

Organs	Liver		Lung		Kidney		Prostate	
treatment	hlg	LTβlg	hlg	LTβlg	hlg	LTβlg	hlg	LTβlg
4W	0/7	6/7	0/7	3/7	0/7	0/7	0/7	0/7
6W	0/3	0/3	0/3	0/3	0/3	0/3	0/3	0/3
11W	0/3	0/3	0/3	0/3	0/3	0/3	0/3	0/3

Figure legends

Fig 1. LT α deficiency prevents clonal deletion of tumor-reactive T cells in the TRAMP mice.

LT α ^{+/+}, LT α ^{+/-} and LT α ^{-/-} Tag-ITRAMP mice were sacrificed at 6 weeks for analyses. Thymocytes (a-c) and splenocytes (d, e) were harvested and analyzed by flow cytometry, using antibodies specific for V β 7 (transgenic TCR β), CD4 and CD8. a. Number of V β 7⁺ cells in the thymus. Data shown are means and SEM of cell numbers (n=8). b, FACS plots depicting the distribution of CD4 and CD8 markers among the V β 7⁺ thymocytes (b, left panels) or CD8 and V β 7 among total thymocytes (b, right panels), and V β 7⁺ splenocytes (d). The data in the left panel are from one representative mouse per group and similar data were obtained in 2 independent experiments, involving a total of 8 mice per group. c. e. Number of different subsets of transgenic V β 7⁺ T cells in the thymi (c) and spleens (e). Data shown are means and SEM of cell numbers (n=8).

Fig. 2. LT α deficiency inhibits development of prostate cancer.

The tumor incidence of *Lt α ^{+/+}TRAMP*, *Lt α ^{+/-}TRAMP* and *Lt α ^{-/-}TRAMP* mice were diagnosed by double blind histology examination by two individuals at 34 weeks; while the prostate volumes were measured by MRI at 30 weeks. a.

Representative local prostate images of *Lt α ^{+/+}TRAMP*, *Lt α ^{+/-}TRAMP* and *Lt α ^{-/-}TRAMP* mice. The prostate were identified with thick white outlines. b. The prostates sizes of *Lt α ^{+/+}TRAMP*, *Lt α ^{+/-}TRAMP* and *Lt α ^{-/-}TRAMP* mice at 30

weeks old. c. Targeted mutation of $LT\alpha$ resulted in reduction of prostate cancer incidence and elimination of distal metastasis. The raw data for incidence are provided on top of bars, while the P value shown in the panels are obtained by X^2 analyses for gene dose effects. The malignancy and metastasis were diagnosed by two independent and double blind evaluations of at least three slides per organ, including, heart, liver, lung, kidney, pancreas and intestine, 25 microns apart.

Fig. 3. Identification of a time window to avoid lymphocyte infiltration

associated with $LT\beta RIg$ treatment. 4, 6 and 11 weeks old C57B6 mice received 3 weekly i.p. injections with 100 μg of either soluble murine $LT\beta RIg$ or Human IgGFc. The mice were sacrificed 4 weeks after the last injection. Peripheral organs were collected for H&E staining. a. Lymphocyte infiltration into liver was only observed when the treatment was initiated at 4 weeks, but not 6 or 11 weeks. b. Infiltration to lung was only observed if the treatment was initiated at 4 weeks of age.

Fig. 4. $LT\beta RIg$ treatment rescued tumor reactive T cells from clonal

deletion in the thymus. TRAMP/TGB (a-e) or TGB (e-j) transgenic mice received 3 weekly injections (i.p.) of 100 μg of either soluble $LT\beta RIg$ or Human IgGFc, starting at 6 weeks of age. The mice were sacrificed 2 weeks after the last injection. Thymocytes (a-c, f-h) and splenocytes (d, e, I, j) were harvested and analyzed by flow cytometry using antibodies specific for CD4, CD8 and $V\beta 8$.

a, f. Number of $V\beta 8^+$ thymocytes. b, d, g, i. Representative plots depicting distribution of CD4, CD8 and transgenic TCR β among thymocytes. FACS plots are from gated $V\beta 8^+$ cells, except for the two right panels in Fig. 4b, which represented that of total thymocytes. Similar data were obtained from two independent experiments, each involving 4 mice per group. The numbers of different subsets of $V\beta 8^+$ transgenic thymocytes (c, h) and splenocytes (e, j) are presented in bar graphs as means and SEM, involving 8 mice per group.

Fig. 5. LT β Rlg reduced apoptosis of transgenic T cells in the TRAMP/TGB transgenic mice. Thymocytes and splenocytes of the TRAMP/TGB mice as described in Fig. 4 legends were stained with antibodies against $V\beta 8$, CD4 and CD8 in conjunction with Annexin V. a. LT β Rlg treatment on TRAMP/TGB mice reduced the percentage of apoptotic cells in the thymus, mainly at the DP stage. b. LT β Rlg had no impact on apoptosis of transgenic T cells in the spleen. Plots depict apoptotic cells among different subsets of thymocytes (a) spleen cells (b). The numbers in the panels are means and SEM of the % of apoptotic cells, summarized from two independent experiments, each with 4 mice per group (n=8).

Fig. 6. LT β Rlg treatment reduces size of prostate cancer and prevented metastasis. a. Prostate volumes as measured by MRI. Male TRAMP mice received 3 weekly i.p. injections with either 100 μ g of soluble murine LT β Rlg or Human IgGFc at 6 weeks old. The prostate volume was measured at 30 weeks.

The upper panels show representative local images of Human IgGFc treated and LT β Rlg treated TRAMP mice. The prostate were identified with thick white outlines. The lower panels depict the sizes of individual prostates (n=7). b. Histological analysis of tumor metastasis. TRAMP mice that received 3 weekly treatment of control Ig or LT β Rlg starting at 6 weeks were sacrificed at 33 weeks after MRI analysis at week 30. H&E sections were examined double blind by a pathologist for metastatic lesions in all internal organs, including liver, lung, kidney, colon, heart and pancreas. Metastases (to lung and/or liver) were found in 4/7 control Ig treated and none of the LT β Rlg-treated mice. The differences in the rate of metastasis is statistically significant (P=0.012).

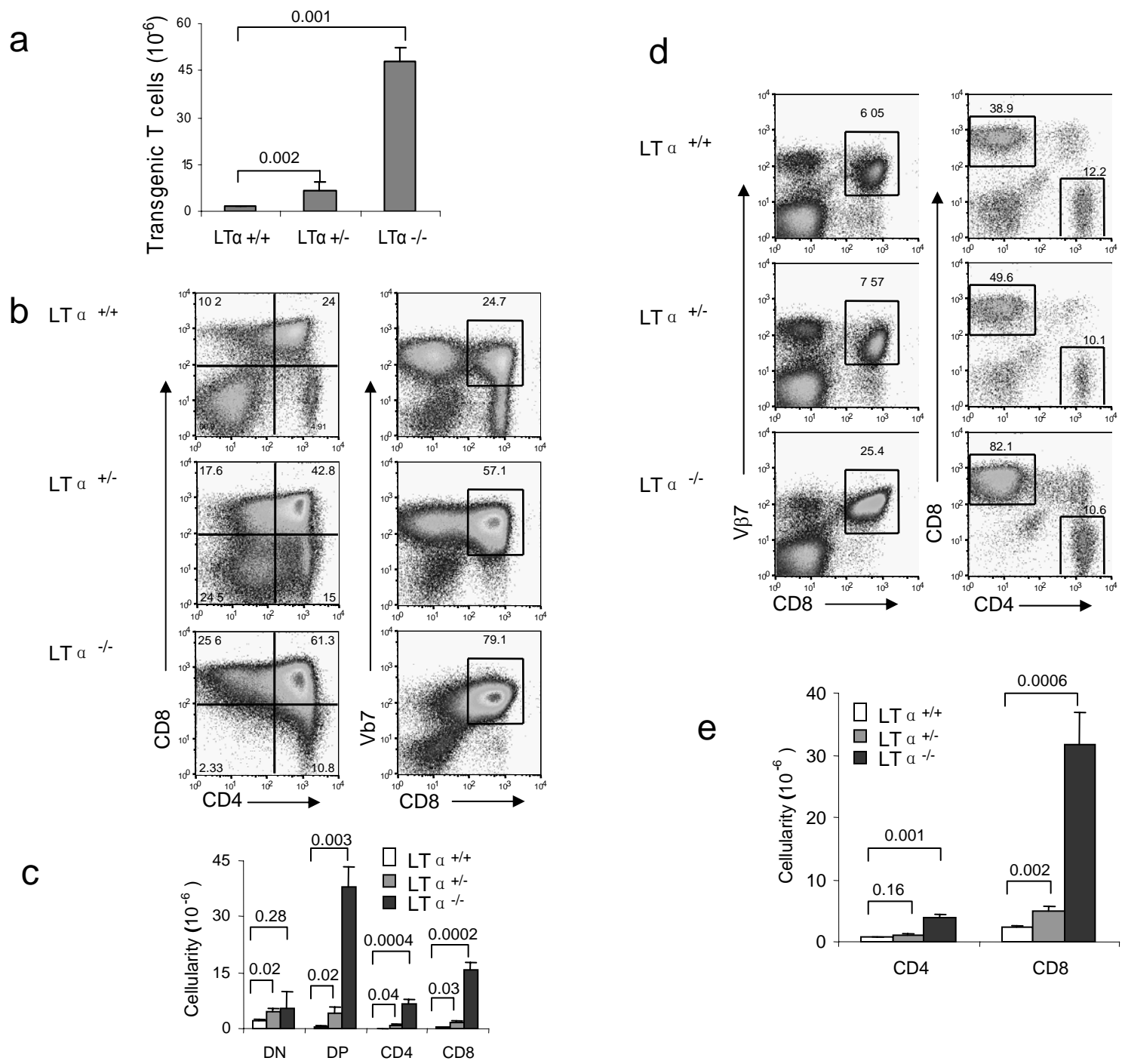


Fig. 1.

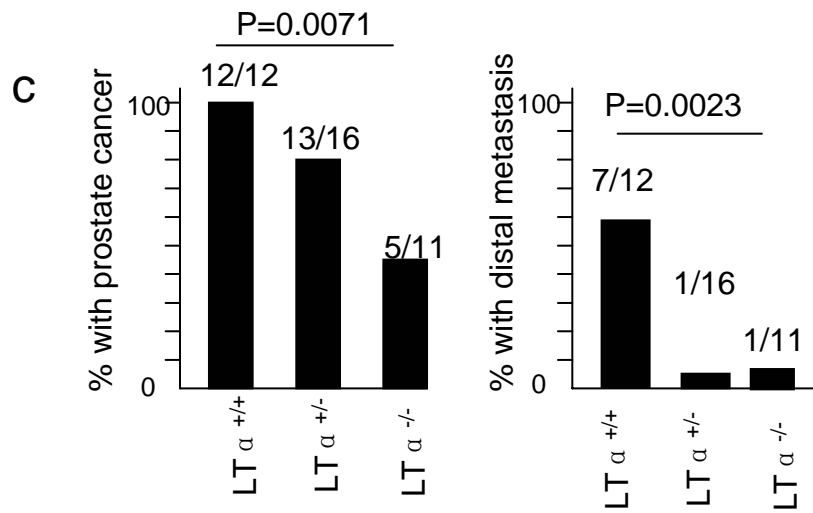
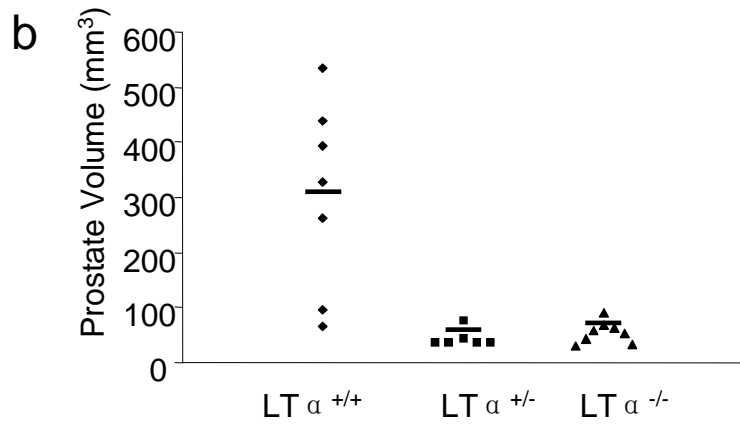
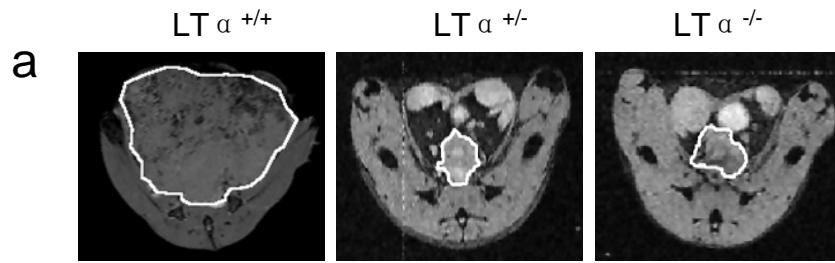


Fig. 2

a. Liver

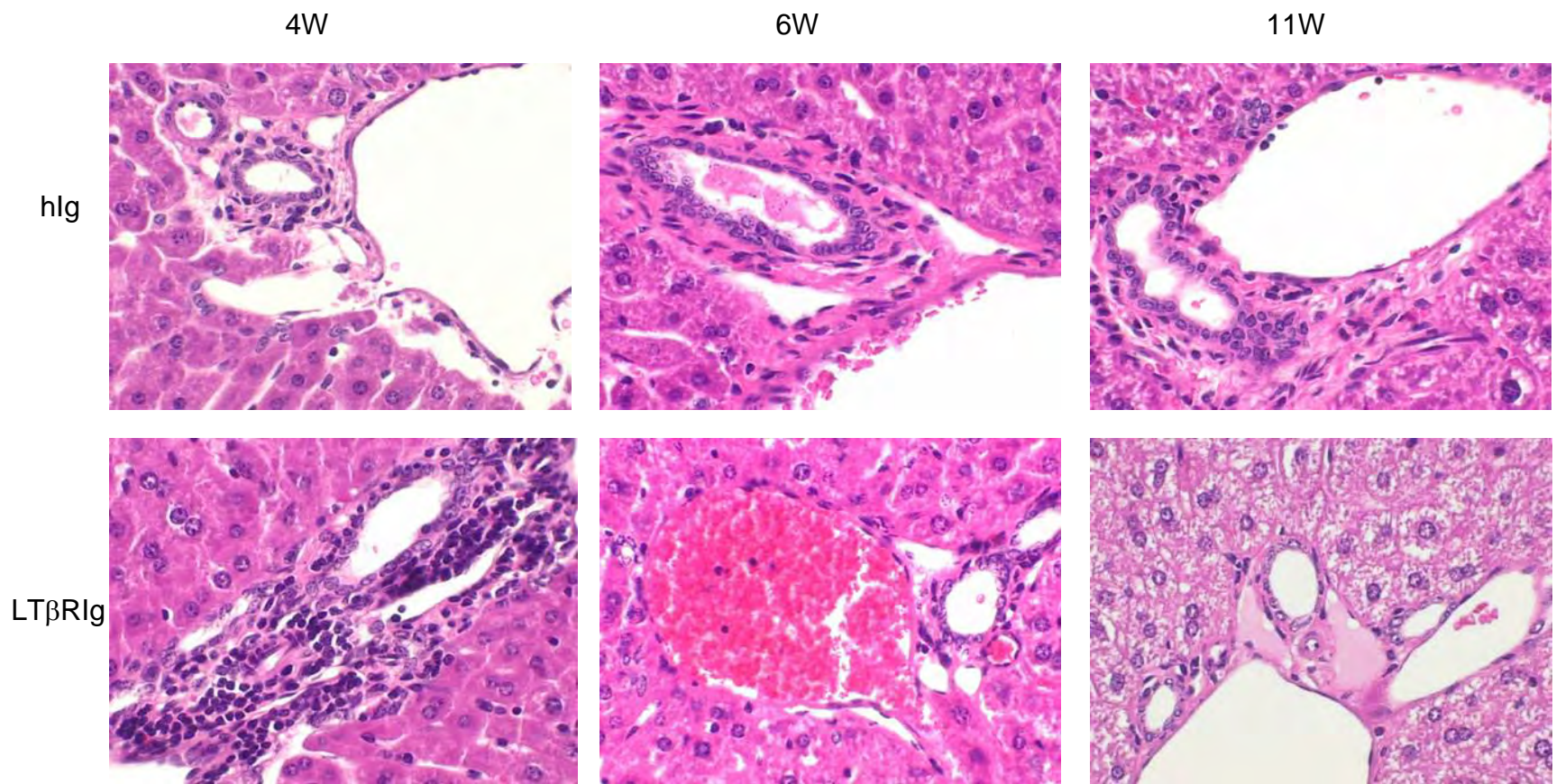


Fig. 3a

b. Lung

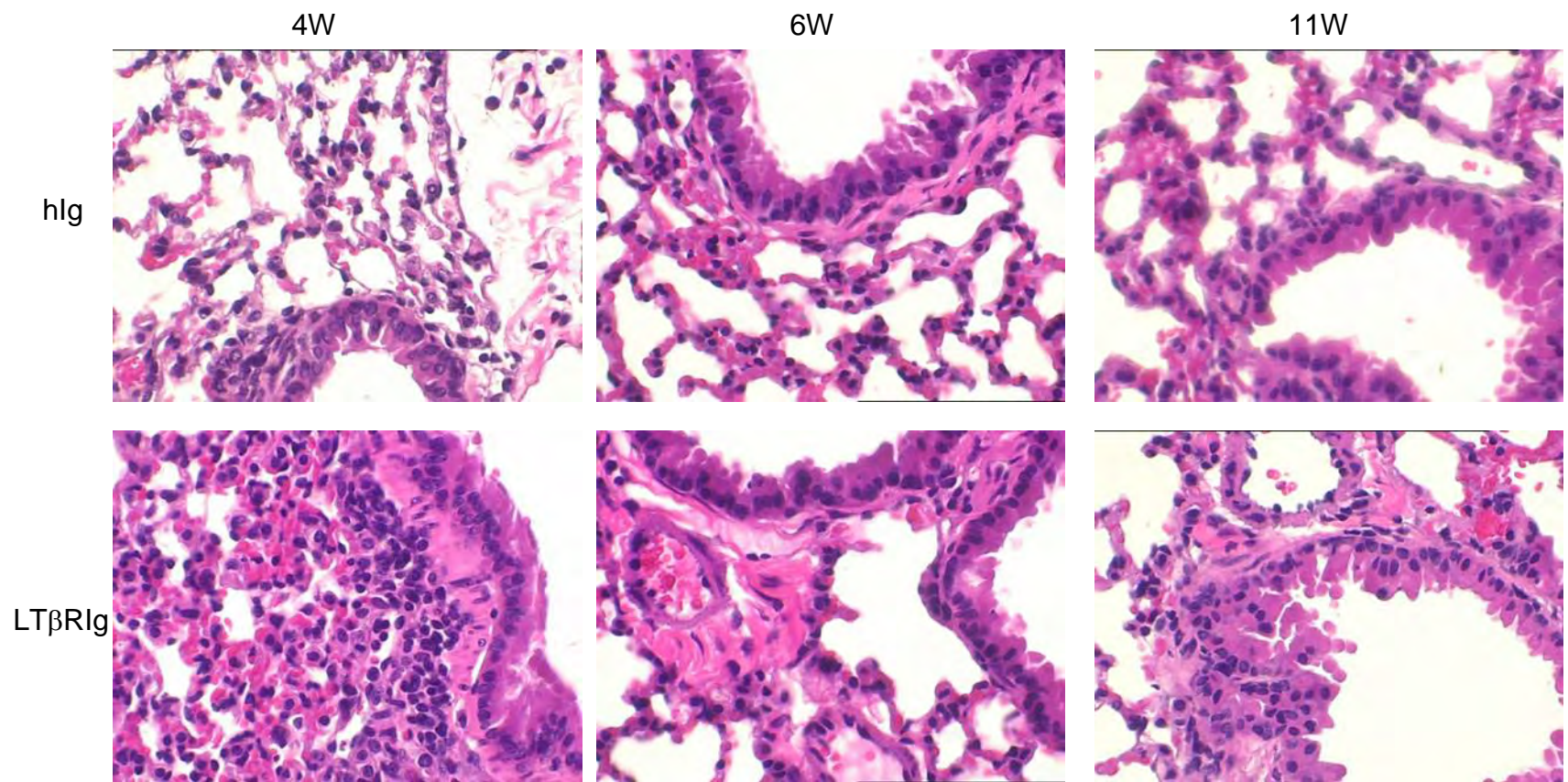


Fig. 3b

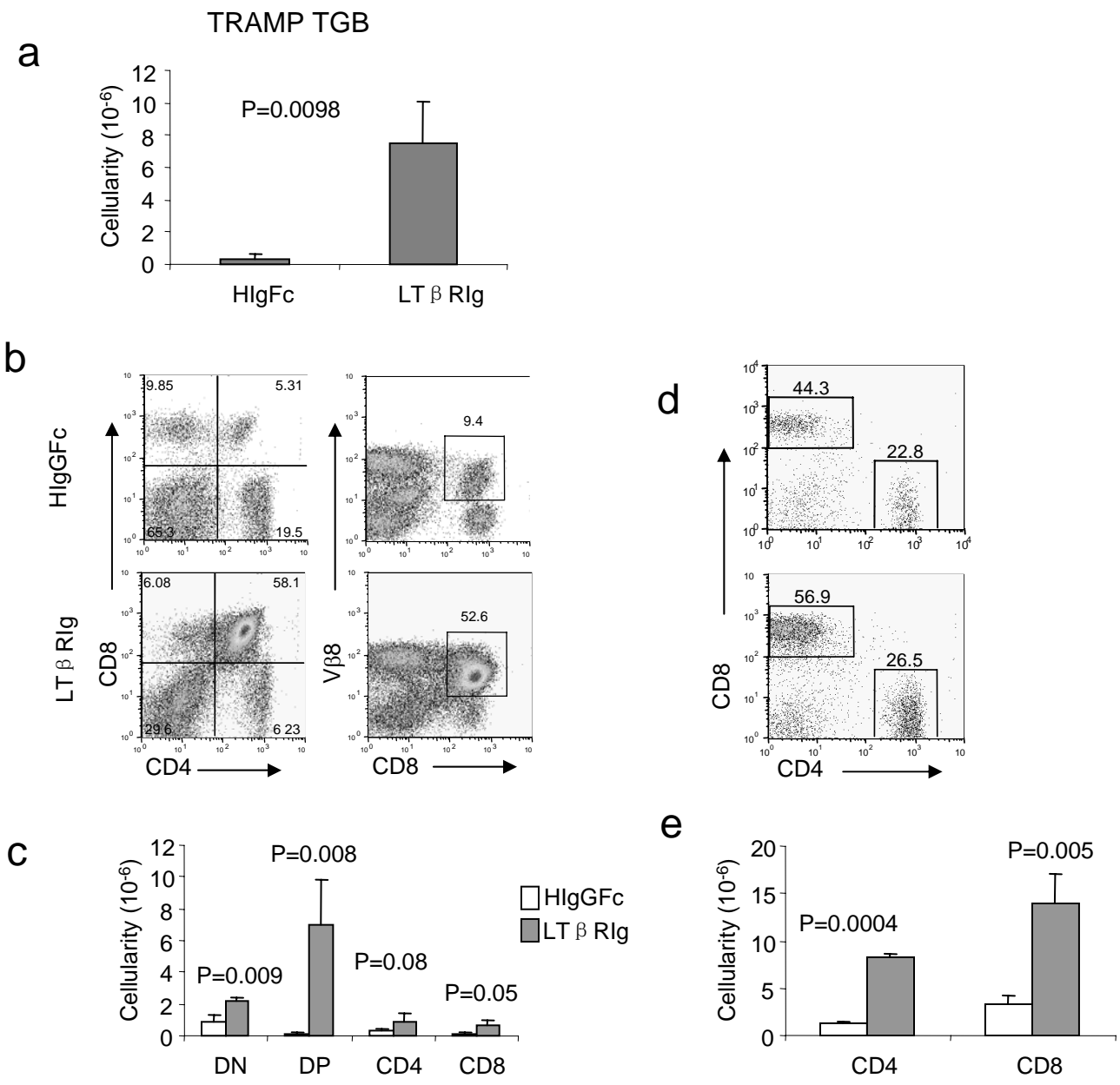


Fig. 4a-e

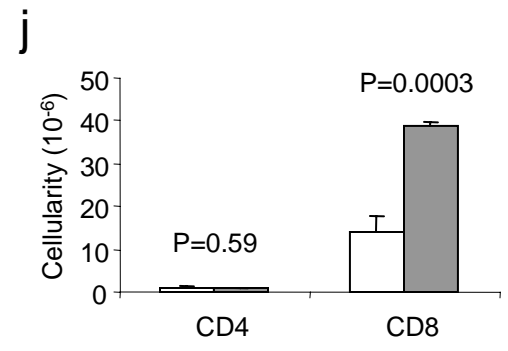
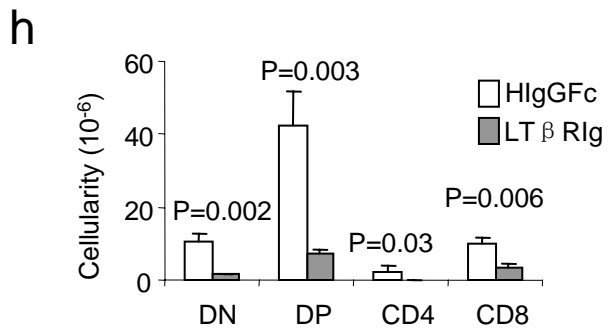
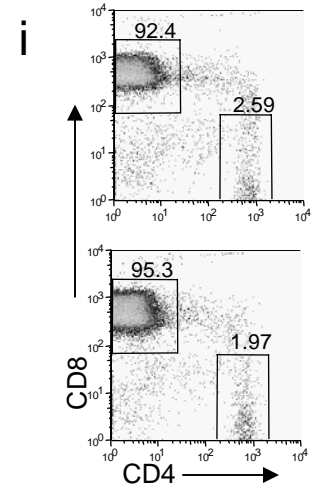
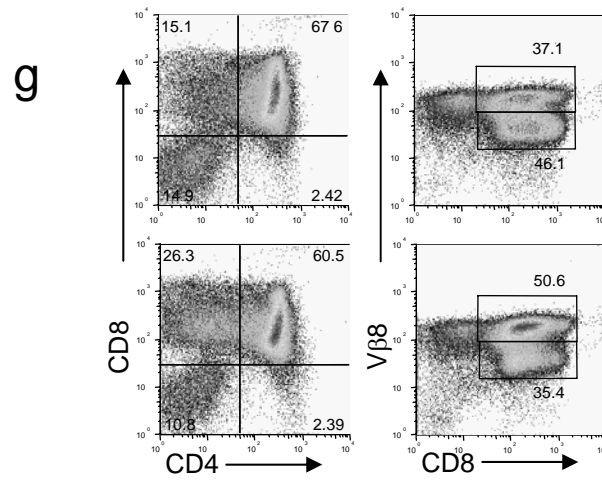
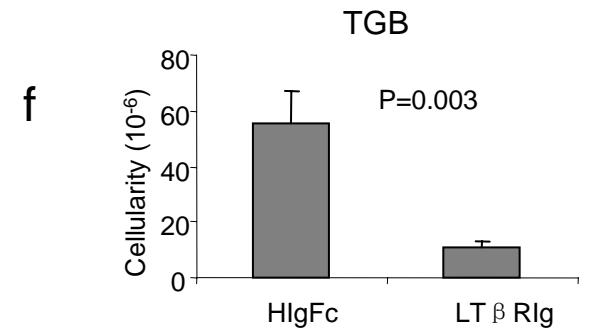


Fig. 4f-j

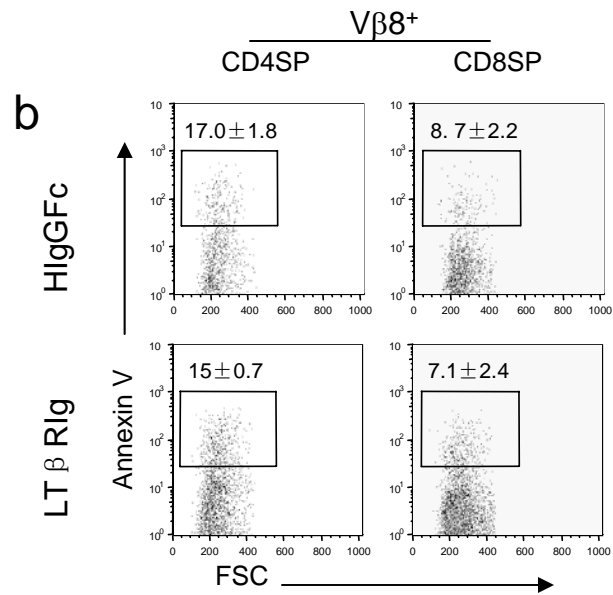
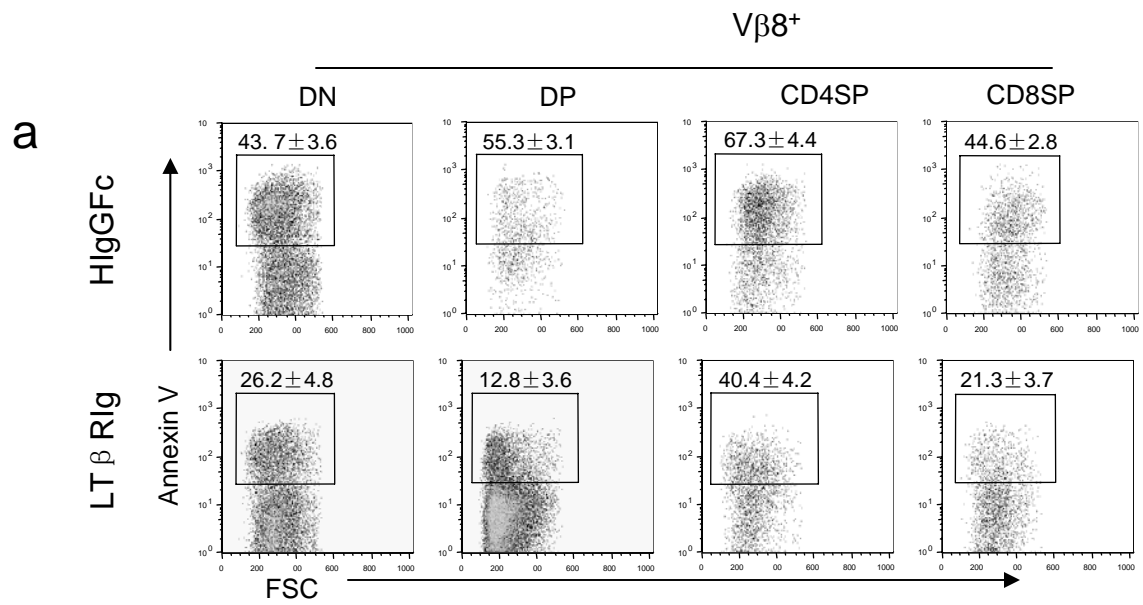


Fig. 5

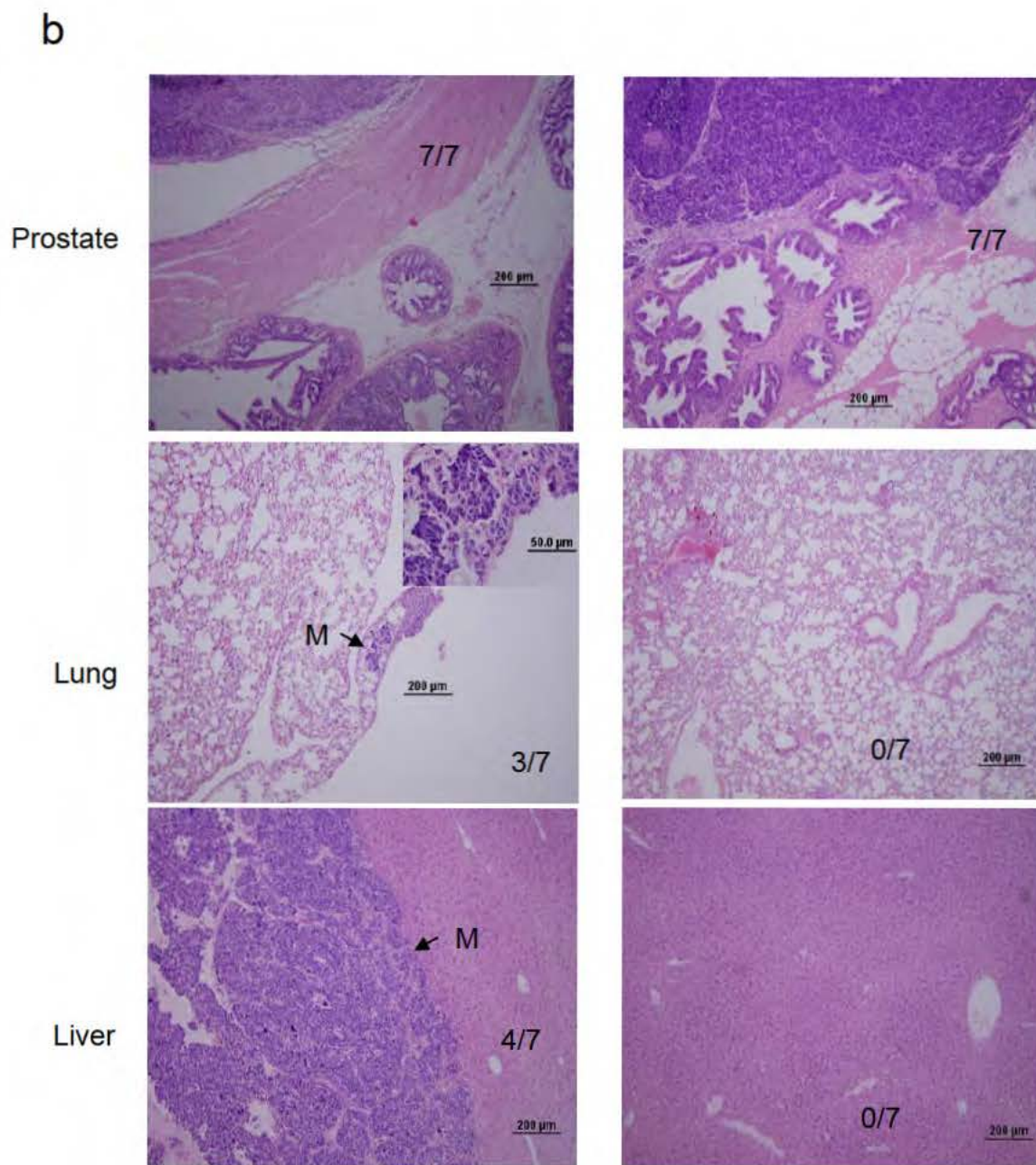
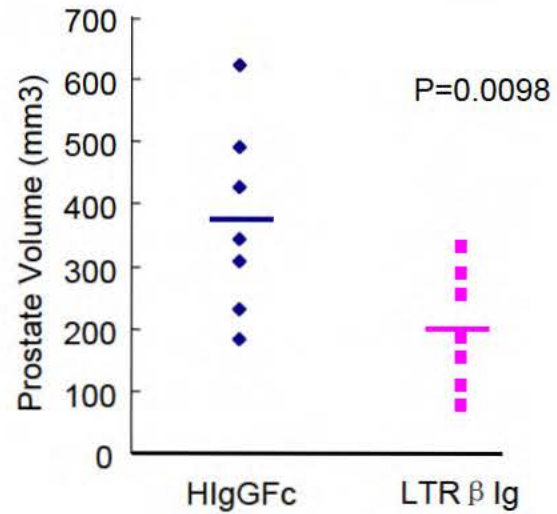
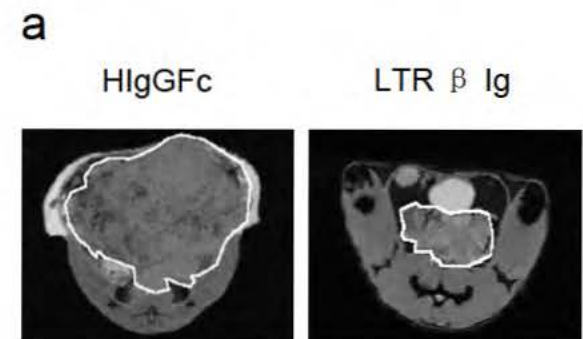


Fig. 6.

Modulation of NKT Cell Development by B7-CD28 Interaction: An Expanding Horizon for Costimulation

Xincheng Zheng^{1,2*}, Huiming Zhang¹, Lijie Yin¹, Chyung-Ru Wang³, Yang Liu¹, Pan Zheng¹

1 Department of Surgery, Comprehensive Cancer Center, Program of Molecular Mechanism of Diseases, University of Michigan, Ann Arbor, Michigan, United States of America, **2** Oncolimmune Ltd., Columbus, Ohio, United States of America, **3** Department of Pathology, University of Chicago, Chicago, Illinois, United States of America

Abstract

It has been demonstrated that the development of NKT cells requires CD1d. The contribution of costimulatory molecules in this process has not been studied. Here we show that in mice with targeted mutations of B7-1/2 and CD28, the TCR β^+ α -Galcer/CD1d⁺ (iV α 14 NKT) subset is significantly reduced in the thymus, spleen and liver. This is mainly due to decreased cell proliferation; although increased cell death in the thymus of CD28-deficient mice was also observed. Moreover, in the B7-1/2- and CD28-deficient mice, we found a decreased percentage of the CD4⁺NK1.1⁺ subset and a correspondingly increased portion of the CD4⁺NK1.1⁻ subset. In addition, the mice with a targeted mutation of either B7 or CD28 had a reduced susceptibility to Con A induced hepatitis, which is known to be mediated by NKT cells. Our results demonstrate that the development, maturation and function of NKT cell are modulated by the costimulatory pathway and thus expand the horizon of costimulation into NKT, which is widely viewed as a bridge between innate and adaptive immunity. As such, costimulation may modulate all major branches of cell-mediated immunity, including T cells, NK cells and NKT cells.

Citation: Zheng X, Zhang H, Yin L, Wang C R, Liu Y, et al. (2008) Modulation of NKT Cell Development by B7 CD28 Interaction: An Expanding Horizon for Costimulation. PLoS ONE 3(7): e2703. doi:10.1371/journal.pone.0002703

Editor: Derya Unutmaz, New York University School of Medicine, United States of America

Received: April 30, 2008; **Accepted:** June 19, 2008; **Published:** July 16, 2008

Copyright: © 2008 Zheng et al. This is an open access article distributed under the terms of the Creative Commons Attribution License, which permits unrestricted use, distribution, and reproduction in any medium, provided the original author and source are credited.

Funding: This work is supported by an NIH grant (AI 51342 to YL) and grants from the Department of Defense (DAMD17 03 1 0013 and W81XWH 07 1 0169 to PZ).

Competing Interests: The authors have declared that no competing interests exist.

* E mail: panz@umich.edu

Introduction

The notion of costimulation was proposed as the signal 2 for the activation of T lymphocytes [1–3]. Over the last two decades, B7 and CD28 families have emerged as the prototypical costimulatory ligands and receptors respectively [4]. Although the main emphasis in the field has been on the role of these interactions in the activation of T cells, accumulating data have demonstrated that this pathway also modulates effector function of T cells in cancer rejection [5–7] and autoimmune diseases [8,9]. Moreover, clear evidence has been reported that support an important role for costimulation in the development of T cells [10]. Thus, the costimulatory pathway can in fact function through the whole life span of T cells. Another interesting development in the field is that the costimulatory molecules ascribed to T cell immunity also modulate innate NK cell immune responses, including both expansion and effector function of NK cells [11]. An interesting issue is whether costimulation modulates the NKT subset, which is generally viewed as the bridge between innate and adaptive immunity.

NKT cells are a unique subset of T cells expressing both TCR and NK cell markers [12–16]. However, unlike NK cells, NKT cells mainly develop in the thymus. In contrast to conventional T cells, NKT cells respond to antigen presented by the nonpolymorphic major histocompatibility complex (MHC) Class I like molecule CD1d [14–16]. The TCR of a major subset of NKT cells is composed almost exclusively of V α 14/J α 18 in the mouse and V α 24/J α 18 in human. In mice the TCR receptor α chain is paired with the V β 8.2, V β 7, or V β 2 TCR β chain. This subset recognize glycolipids presented by CD1d molecules [15,16]. Almost all NKT

cells are either CD4⁺ or CD4⁻CD8⁻ (DN). Upon stimulation through their TCR, the NKT cells rapidly produce substantial amounts of cytokines, such as IL 4 and IFN γ [17,18]. Emerging data demonstrate that it is involved in immunity against infection [19] and tumor [20] and in autoimmune disease [21] by either direct cytotoxicity or secretion of several cytokines.

The developmental relationship between NKT and conventional T cells has been controversial. Two models have been proposed for NKT cell development [22,23]. NKT cells might derive from a distinct precursor that undergoes lineage commitment independently of TCR ligand interactions (pre committed model). Alternatively, they may develop as a byproduct of conventional T cell development at a certain stage, depending on the ligand they recognize (TCR instruction model). Recently, by intrathymic injection, Gapin et al. showed that NKT cells can be produced in the thymus from CD4⁺CD8⁺ DP thymocyte [24]. An intermediate, semi mature CD4⁺NK1.1⁻ stage has been proposed before NKT cells finally develop into NK1.1⁺ cells that are either CD4⁺ or double negative [25–27]. Moreover, the positive and negative selection of NKT cells rely on CD1d being presented by hematopoietic derived DP thymocyte or dendritic cells, respectively [24,28], but not those presented by thymic epithelial cells. The details of this selective process are still largely unknown. A largely unresolved issue is whether the B7/CD28 interaction is involved in the development of NKT cells. In order to address this question, we compared the development of NKT cells in WT mice to that in mice with targeted mutations of B7 1/B7 2 or CD28. Our results demonstrate that the development and function of NKT cells are subject to modulation by costimulatory pathways.

Results

The reduced TCR β^+ NK1.1 $^+$ NKT cells in B7-1/2 and CD28 deficient mice

In order to evaluate the role for costimulatory molecules on NKT development, we compared the percentages of NKT cells in the central and peripheral lymphoid organs of B7 1/2, CD28 mutant mice with those of NKT cells in the same organs of age and sex matched WT mice. In this study, the total NKT cells were defined as NK1.1 $^+$ TCR β^+ cells. As shown in Fig. 1A, TCR β^+ NK1.1 $^+$ cells comprise about 1% of the total thymocytes in WT mice. After dividing the thymocytes into DN, DP and SP subsets, it was clear that NKT cells were largely absent from the DP and CD4 $^+$ CD8 $^+$ subsets, as others have reported [15]. About 5% of DN and 4% of CD4 $^+$ CD8 $^+$ thymocytes expressed the NKT marker in WT mice. A 3–5 fold reduction of the NKT cells was observed in total thymocytes and DN and CD4 subsets from both B7 1/2 and CD28 deficient mice. Thus, B7 CD28 interaction is required for the development of NKT in the thymus.

We also compared the amounts of NKT cells in the spleens and livers of mice deficient for B7 1/2 and CD28 with those of WT mice. As shown in Fig. 1B, total TCR β^+ NK1.1 $^+$ cells in the spleen were decreased somewhat as a result of targeted mutation of B7 and CD28. Among the CD4 $^+$ splenocytes, the NKT subset is reduced by more than 2 fold. However, the reduction in DN NKT was marginal. The liver is known to be populated with a high number of NKT cells [29–31]. However, except for the reduction in NKT among the CD4 $^+$ CD8 $^+$ subset in the CD28 deficient mice, targeted mutation of B7 CD28 did not have a significant impact on the number of TCR β^+ NK1.1 $^+$ NKT cells (Fig. 1C).

Most of the NKT cells recognize glycolipids presented by MHC class I like molecule CD1d, and are referred to as iV α 14 NKT cells for being CD1d restricted NKT bearing the invariant V α 14 rearrangement [32,33]. Although the identity of the endogenous antigen presented by CD1d is still unclear, a synthetic glycolipid antigen derived from marine sponges called alpha galactosyl ceramide (α GalCer) can be recognized by NKT and potently stimulate NKT cells via TCR when presented by CD1d [34]. Recently, the development of α GalCer/CD1d tetramer, which recognizes invariant V α 14 J α 281 TCR, provides another powerful tool to identify iV α 14 NKT cells. α GalCer/CD1d tetramer positive cells comprised about 80% of NK1.1 $^+$ TCR β^+ cells [35,36]. Those α GalCer/CD1d tetramer negative cells were identified as different subsets of NKT cells, which are preferentially localized in spleen and bone marrow and are predominantly of the CD8 $^+$ (or DN) phenotype [23]. In this study, we used the tetramer to further characterize the TCR β^+ NK1.1 $^+$ cells in B7 1/2 and CD28 deficient mice. As shown in Fig. 2, about 90% of the TCR β^+ NK1.1 $^+$ cells in WT thymus bind to α GalCer CD1d tetramer. In B7 and CD28 deficient thymus only about 75% of the TCR β^+ NK1.1 $^+$ NKT bind to the tetramer. The reduction of the α GalCer CD1d tetramer binding cells in the spleen and liver is more severe in the mutant mice. Whereas in WT mice, there were close to 50% of spleen and liver derived TCR β^+ NK1.1 $^+$ NKT cells that bound to the tetramer, and less than 20% of TCR β^+ NK1.1 $^+$ NKT cells in mutant mice showed similar specificity in the spleen, and the tetramer binding cells were reduced by 2 fold in the liver of the mutant mice.

B7-CD28 interaction promotes expansion of NK1.1 on the iV α 14 NKT cells

To further characterize the effect of costimulatory molecules on iV α 14 NKT cell development and activation, we analyzed the number of cells as well as NK1.1, CD44 and CD4 expression

among iV α 14 NKT cells. As shown in Fig. 3A, the number of iV α 14 NKT cells was significantly reduced in total lymphocytes from both the thymus and spleen of B7 1/2 deficient mice. Again, a qualitatively similar but quantitatively more significant reduction was detected in CD28 deficient mice. While a small reduction was observed in the liver of B7 deficient mice, no reduction of iV α 14 NKT was observed in the liver of CD28 deficient mice. Thus, the optimal production of iV α 14 NKT cells in the thymus and their accumulation in the spleens require B7 CD28 interaction.

Recent studies have demonstrated that in normal mice the NK1.1 $^+$ iV α 14 NKT cells are developed from NK1.1 $^+$ iV α 14 NKT cells. Interestingly, in B7 1/2 and CD28 deficient mice, the percentage of NK1.1 $^+$ subsets among iV α 14 NKT cells was significantly reduced, while the NK1.1 $^+$ subsets were significantly increased by 4 fold in the thymus and 2 fold in the spleen and liver (Fig. 3B). The iV α 14 NKT cells could be further divided into three major subsets, NK1.1 $^+$ CD4 $^+$, NK1.1 $^+$ CD4 $^+$ and NK1.1 $^+$ CD4 $^-$. Compared to wild type mice, targeted mutation of both B7 and CD28 caused a significant reduction in the NK1.1 $^+$ CD4 $^+$ subset and a corresponding increase in the NK1.1 $^+$ CD4 $^-$ subset (Fig. 3C). If the reduction of iV α 14 NKT cells from total lymphocytes is considered, the reduction of the NK1.1 $^+$ iV α 14 NKT subset seen in the mutant mice is even more significant when compared to WT mice, and the seemingly observed increase in the NK1.1 $^+$ iV α 14 NKT subset is actually unchanged (Table 1).

Normal generation of immature iV α 14 NKT cells in young B7- and CD28-deficient mice

In the thymus, a low number of iV α 14 NKT cells can be detected by α GalCer/CD1d tetramer as early as 5 days after birth [16,27]. Thereafter, both the percentage and the absolute number of iV α 14 NKT cells increase reaching a peak level at around 6 weeks [24,27]. To determine if B7 CD28 interaction is required for the generation of iV α 14 NKT cells in young mice, we analyzed the number and phenotypes of iV α 14 NKT cells in the thymi and livers of 8 day old mice. As shown in Fig. 4A, the total percents of tetramer binding cells in WT and mutant mice were only around 0.03% in the thymus and 0.2% in the liver. Both the number and the pattern of NK1.1 and CD4 are consistent with that previously observed in WT mice [27]. Pellicci et al. also demonstrated that at day11 of fetal thymus organ culture FTOC, α GalCer/CD1d tetramer NKT cells only account for less than 5% of total NK1.1 $^+$ TCR β^+ cells [27]. Therefore, the percentage of total NKT cells at 8 days of age should be more than the above numbers. In all strains of mice, the majority of iV α 14 NKT cells were immature as they did not yet express NK1.1 (Fig. 4B). Thus, B7 CD28 interaction appears selectively involved in the maturation of NKT cells in adult mice.

B7-CD28 interaction promotes proliferation of NKT cells

The reduced cell number can be explained by increased cell death and/or decreased cell proliferation in the organ. Therefore, we first tested whether B7 and CD28 deficiencies affect the survival of iV α 14 NKT cells. We compared the number of cells undergoing programmed cell death in WT, B7 1/2 and CD28 deficient mice by staining with Annexin V. Since the reduction of iV α 14 NKT cells is limited to the NK1.1 $^+$ subset, we analyzed apoptosis of TCR $^+$ NK1.1 $^+$ NKT cells. As shown in Fig. 5A, in WT mice, there were about 3% Annexin V $^+$ cells in the thymic TCR $^+$ NK1.1 $^+$ cells and 20% in the same subsets from the spleen. While the same amount of Annexin V $^+$ cells was detected in the thymus of B7 1/2 deficient mice, CD28 deficient mice had an increase in Annexin V $^+$ cells in the thymus, but not in the spleen. Thus, while a contribution of CD28 in the survival of NKT cells in

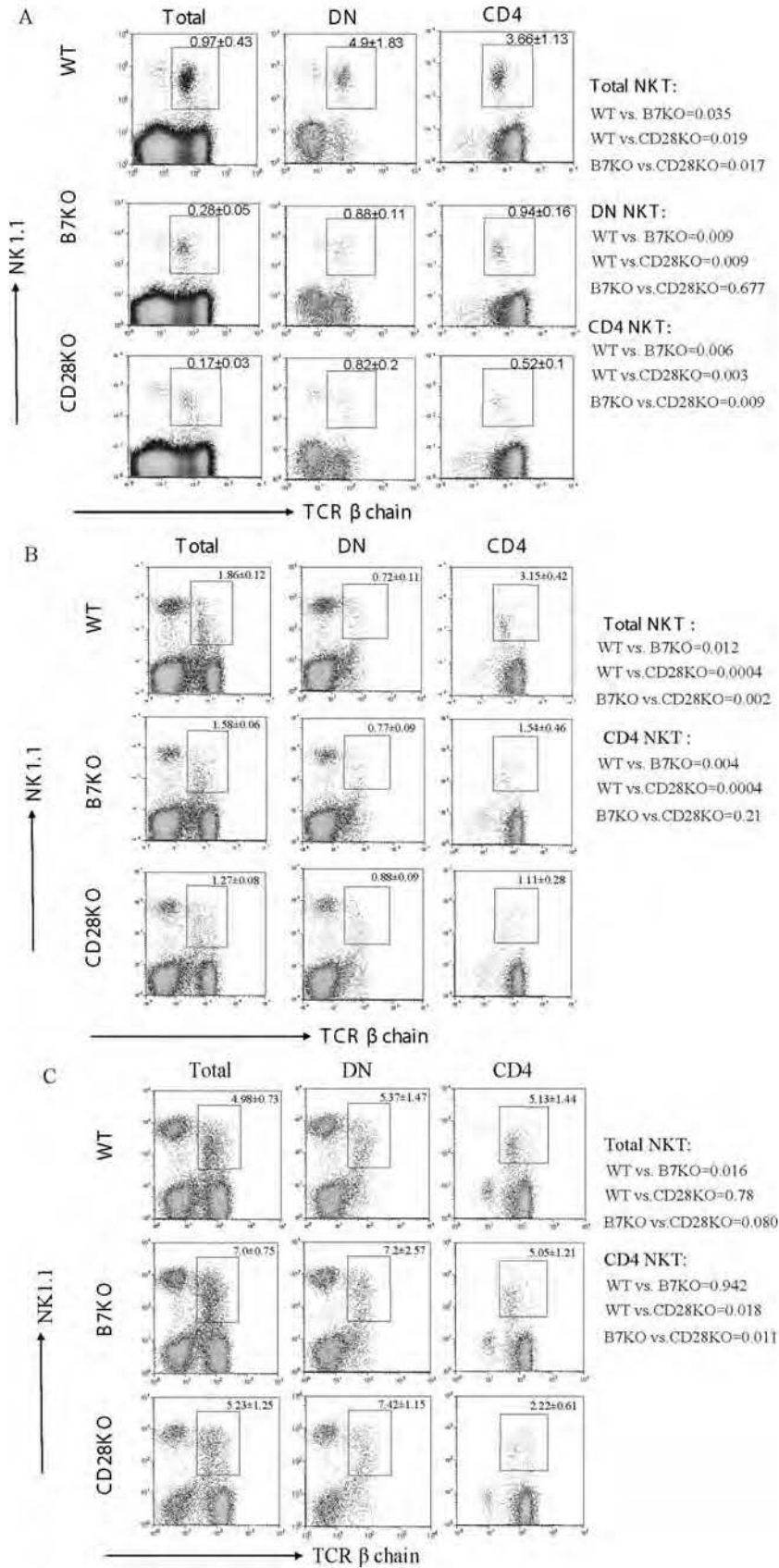


Figure 1. Roles for B7 1/2 CD28 interaction in the accumulation of TCR β^+ NK1.1 $^+$ NKT cells in the thymus (A), spleen (B) and liver (C). B7KO, CD28KO and WT C57BL/6 mice were sacrificed at 8 week of age. Total lymphocytes (left column) from viable cells, CD4 $^-$ CD8 $^-$ DN lymphocytes (middle column) and CD4 $^+$ lymphocytes (right column) were analyzed for the expression of TCR β and NK1.1. One representative profile from each group is presented. The numbers in the panels are percentages (Mean \pm SD) of gated NKT cells (n = 9). The numbers shown on the side of figures are *p* value between two indicated groups.
doi:10.1371/journal.pone.0002703.g001

the thymus cannot be ruled out, decreased survival does not explain the defect in the development of iV α 14 NKT cells.

To investigate whether B7 and CD28 deficiencies affect the proliferation of NKT cells, we pulsed WT, B7 and CD28 deficient mice with BrdU and measured DNA synthesis in TCR $^+$ NK1.1 $^+$ by flow cytometry. As shown in Fig. 5B, about 10% of the TCR $^+$ NK1.1 $^+$ cells were undergoing proliferation in WT mice during the 4h period, the percentages of BrdU $^+$ cells were reduced by 2 fold in B7 1/2 deficient mice and 4 fold in CD28 deficient mice in the thymus. A significant although less pronounced reduction was observed in the spleens of the mutant mice. The more significant inhibition of cell proliferation and somewhat increased cell death of NKT cells in the thymus might

explain the more severe reduction of NKT cells in mice with targeted mutations of CD28.

The defective NKT function in costimulatory molecule deficient mice

Several publications have demonstrated the contribution of liver NKT cells to a Con A induced murine hepatitis model [37,38]. To explore if there is possible defective NKT function due to the reduction of iV α 14 NKT cells in B7 and CD28 deficient mice, we injected Con A into B7 1/2, CD28 deficient mice and WT mice and measured serum AST and ALT levels for liver damage. The liver sections were also examined after H&E staining. As shown in

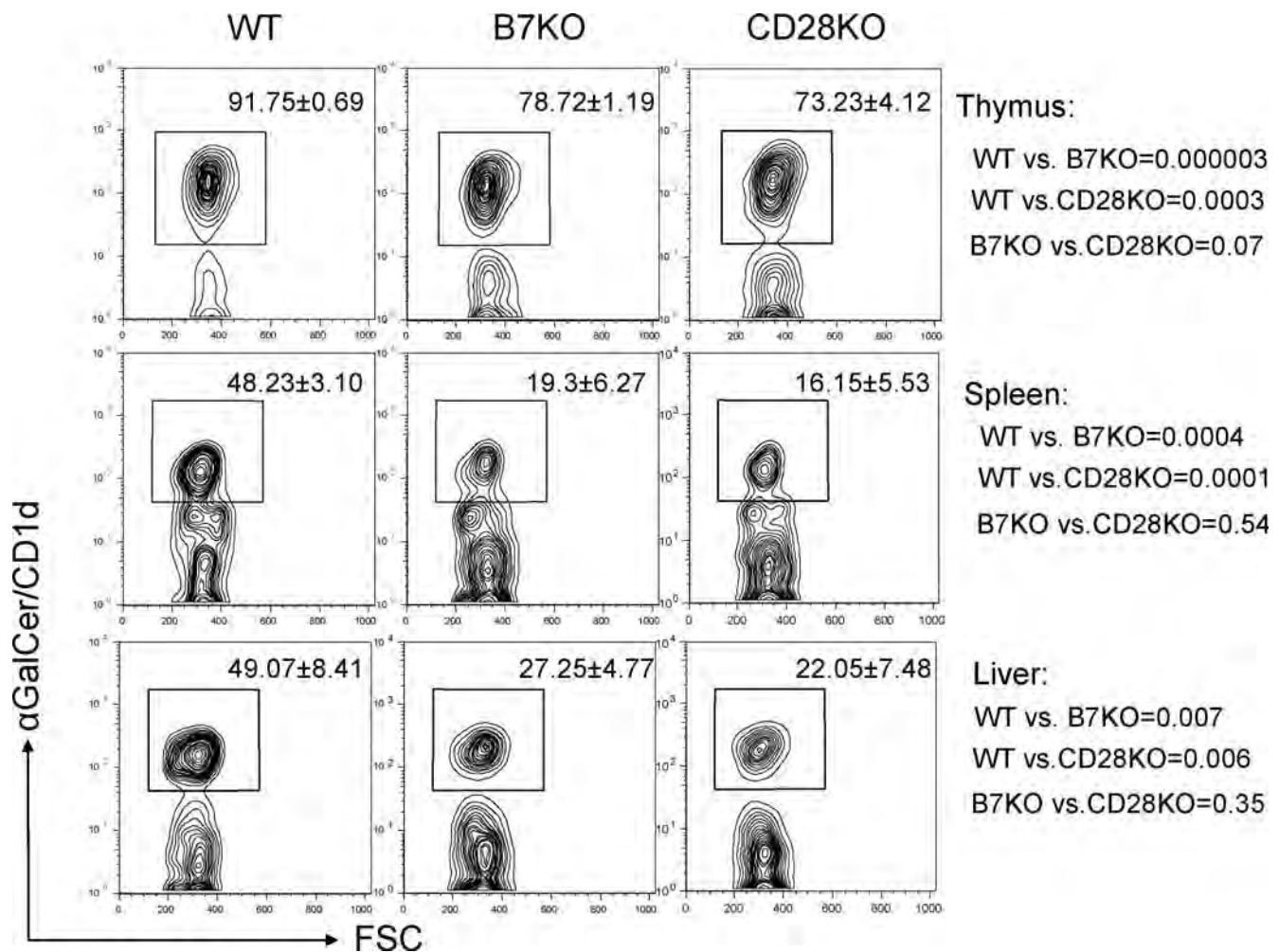


Figure 2. Proportions of iV α 14 NKT cells among TCR β^+ NK1.1 $^+$ cells isolated from the thymus, spleen and liver of WT, B7 1/2 and CD28 deficient mice. Total lymphocytes from the thymus (left), spleen (middle) and liver (right) of 8 week old WT (top), B7 1/2 (center) and CD28 (bottom) deficient mice were stained with TCR β , NK1.1 and α GalCer/CD1d tetramer. The numbers represent the percentage (Mean \pm SD, n = 9) of α GalCer/CD1d $^+$ cells in the TCR β^+ NK1.1 $^+$ population. One representative profile from each group is shown here. The numbers shown on the side of figures are *p* value between two indicated groups.
doi:10.1371/journal.pone.0002703.g002

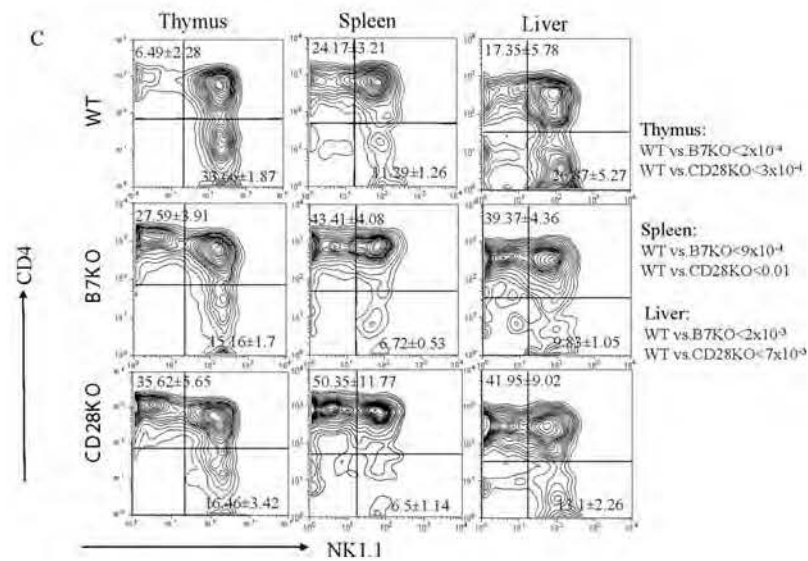
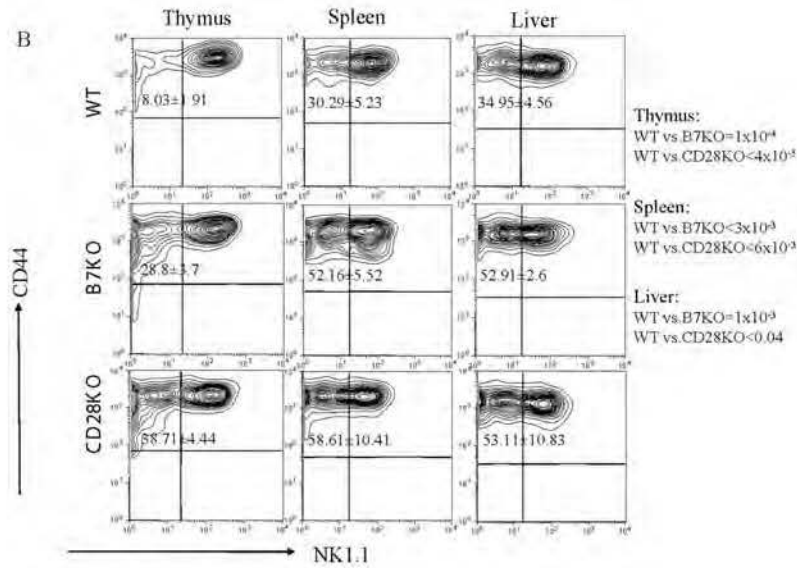
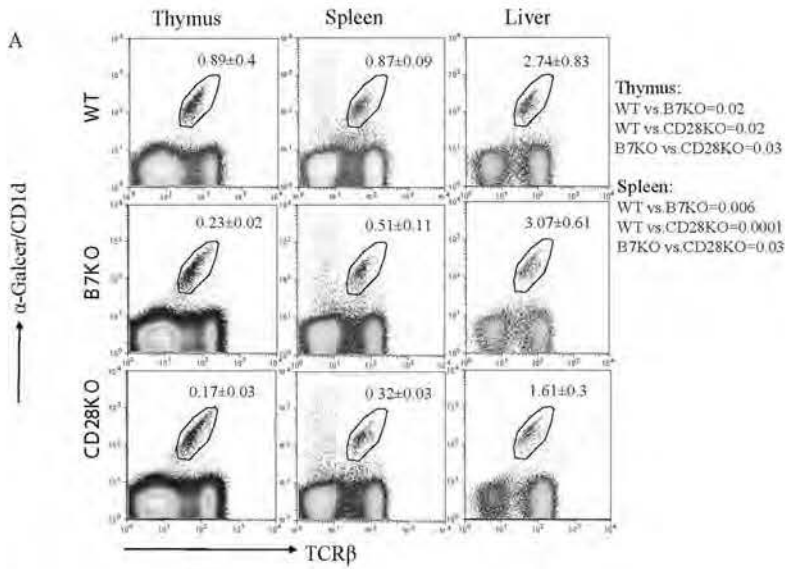


Figure 3. Quantitative and phenotypic variation of $iV\alpha 14$ NKT cells in the thymus, spleen and liver of WT, B7 1/2 and CD28 deficient mice. Total lymphocytes from the thymus (left), spleen (middle) and liver (right) of 8 week old WT (top), B7 1/2 (center) and CD28 (bottom) deficient mice were analyzed. A. The quantification of $iV\alpha 14$ NKT cells. The numbers represent the percentage (Mean \pm SD, n=9) of $iV\alpha 14$ NKT cells. B. The expression of CD44 and NK1.1 among the gated $iV\alpha 14$ NKT cells. The numbers represent the percentage (Mean \pm SD) of NK1.1⁺ $iV\alpha 14$ NKT cells. C. The expression of CD4 and NK1.1 from gated $iV\alpha 14$ NKT cells. The numbers represent the percentage (Mean \pm SD) of NK1.1⁺ CD4⁺ (upper left) and NK1.1⁺ CD4⁻ (lower right) $iV\alpha 14$ NKT cells. One representative profile from each group is shown here. The numbers shown on the side of figures are p value between two indicated groups. doi:10.1371/journal.pone.0002703.g003

Fig. 6, severe liver damage was induced in WT mice as revealed by high serum AST and ALT levels and necrosis of hepatocytes. In the B7 and CD28 deficient mice, serum AST and ALT levels were reduced by more than 2 fold in mutant mice as compared with WT mice (Fig. 6A). Corresponding to this we also observed a 4–5 fold reduction in the necrotic area of the livers from B7 and CD28 deficient mice (Fig. 6B and C).

Reduced level of Con A induced IFN- γ production in B7-1/2 deficient mice

Con A induced hepatitis is a multiple factors disease process. Both Th1 type cytokine IFN γ [39–41] and Th2 type cytokine IL 4 [37,38,42] are crucially involved in the induction of NKT cell mediated liver specific inflammation. Moreover, other immunoregulatory cytokines, such as IL 5 [42,43] and IL 6 [44], had also been demonstrated to mediate the pathogenesis of this disease. We investigated whether the reduced susceptibility to Con A induced hepatitis in B7 1/2 deficient mice is due to defective cytokine production. *Ex vivo* mononuclear cells were analyzed at 6 hours after Con A treatment *in vivo*. As shown in Fig. 7A, compared with Non treated mice, the percentage of total NKT cells was reduced almost 10 fold in the livers of ConA treated WT and B7KO mice. Correspondingly, the conventional T cells, which were identified by NK1.1⁺ TCR β ⁺ cells are relatively increased. Interestingly, those NKT cells reside in the spleen are not affected. Comparable numbers of total NKT cells are detected before and after ConA treatment in the spleens of both strains. This further demonstrated that NKT cells in the liver play a major role inducing acute

hepatitis. In addition, as shown in Fig. 7B, in WT mice, about 20% of the liver NKT cells produced IFN γ and 4% of the NKT cells produced high levels of IL 4. The amount of the same level of IFN γ producing cells was reduced by 50% in B7 1/2 deficient mice, while the amount of high levels of IL 4 producing cells was unchanged. It has been shown that the peak of IL 4 production by NKT cells is earlier than IFN γ [45,46]. We also confirmed that B7 1/2 deficient NKT cells in the spleen produced less IL 4 compared with WT mice at an earlier time point (unpublished observation). However, both IFN γ and IL 4 cytokine secretions in conventional T cells are barely detectable (Fig. 7C). Therefore, reduced severity in Con A induced hepatitis in the B7 deficient mice correlates to decreased IFN γ by NKT cells.

To further confirm the defect of NKT population in B7 mutant mice, we adopted an *in vitro* model to test the reactivity of NKT cells from WT and B7KO mice to its exogenous ligand, α Galactosylceramide (KRN7000). To exclude the effect of weak costimulatory signaling from B7 mutant antigen presenting cells [47], both purified CD4⁺ T cells from WT and B7KO mice was stimulated *in vitro* with purified CD11c⁺ dendritic cells from WT mice. As shown in Fig. 7D, after 48 hours co culture with KRN7000, CD4⁺ T cells from WT have a stronger response, as indicated by more IFN γ and IL 4 secretion. Because KRN7000 can only be recognized by $iV\alpha 14$ NKT cell in CD4⁺ population, this result provided direct evidence of lower number and/or functional defect of NKT cells in B7KO mice.

Discussion

By comparing WT mice with those with targeted mutations of CD28 or B7 1/2, we have demonstrated a major contribution of B7 CD28 interaction in the generation of $iV\alpha 14$ NKT cells in the thymus. Two lines of evidence presented here suggest that B7 CD28 interaction is required for the expansion of more mature NK1.1⁺ $iV\alpha 14$ NKT subsets. First, the number of $iV\alpha 14$ NKT cells in young mice, which are predominantly NK1.1⁺, is unaffected by these mutations. Second, the overall number of NK1.1⁺ $iV\alpha 14$ NKT cell was largely unaffected in the mutant adult mice, while the NK1.1⁺ $iV\alpha 14$ NKT cells were drastically reduced. Since earlier studies demonstrated that NK1.1⁺ $iV\alpha 14$ NKT cells are the precursors of NK1.1⁺ $iV\alpha 14$ NKT [26,27], our data indicated that B7 1/2 CD28 interaction is not required for the generation of NKT cell precursors. The co stimulation dependent expansion of mature NKT is largely due to a critical contribution of B7 CD28 interaction in proliferation of the NKT cells as the incorporation of BrdU into the NK1.1⁺ NKT cells was drastically reduced. However, the percentage of apoptotic cells was unchanged in the B7 1/2 deficient mice and only marginally increased in the CD28 deficient mice.

As a consequence of defective NKT maturation in the thymus, we observed a significant reduction of the mature NKT cells in the spleen and liver, the major residences of the NKT cells. Nevertheless, the defects in the periphery were somewhat less pronounced than what was observed in the thymus. Theoretically, this can be due to increased emigration from the thymus, increased survival and increased proliferation in the mutant mice.

Table 1. Different $iV\alpha 14$ NKT subsets in total lymphocytes of thymus, spleen and liver in WT, B7-1/2 and CD28 deficient mice.

		WT	B7KO	CD28KO
Thymus	NK1.1 ⁻ CD4 ⁺	0.05 \pm 0.02	0.06 \pm 0.01	0.06 \pm 0.01
	NK1.1 ⁺ CD4 ⁺	0.52 \pm 0.23	0.13 \pm 0.02*	0.03 \pm 0.01*
	NK1.1 ⁺ CD4 ⁻	0.3 \pm 0.15	0.03 \pm 0.01*	0.03 \pm 0.01*
Spleen	NK1.1 ⁻ CD4 ⁺	0.21 \pm 0.04	0.22 \pm 0.05	0.16 \pm 0.03
	NK1.1 ⁺ CD4 ⁺	0.53 \pm 0.07	0.23 \pm 0.06**	0.13 \pm 0.05***
	NK1.1 ⁺ CD4 ⁻	0.1 \pm 0.01	0.03 \pm 0.01***	0.02 \pm 0.01***
Liver	NK1.1 ⁻ CD4 ⁺	0.48 \pm 0.26	1.21 \pm 0.29*	0.68 \pm 0.21
	NK1.1 ⁺ CD4 ⁺	1.34 \pm 0.44	1.46 \pm 0.33	0.64 \pm 0.19*
	NK1.1 ⁺ CD4 ⁻	0.72 \pm 0.26	0.3 \pm 0.05*	0.21 \pm 0.05*

Lymphocytes from thymus, spleen and liver of age and sex matched WT, B7 1/2 or CD28 deficient mice were analyzed by flow cytometry. The $iV\alpha 14$ NKT cells were identified based on expressing TCR β and binding to the α Galcer/CD1d tetramer. Data shown are means and SD of the percentage of given subsets in total viable lymphocytes (n=4). Similar data were obtained in another experiment involving 5 mice per group.

*P<0.05,

**P<0.01,

***P<0.001.

doi:10.1371/journal.pone.0002703.t001

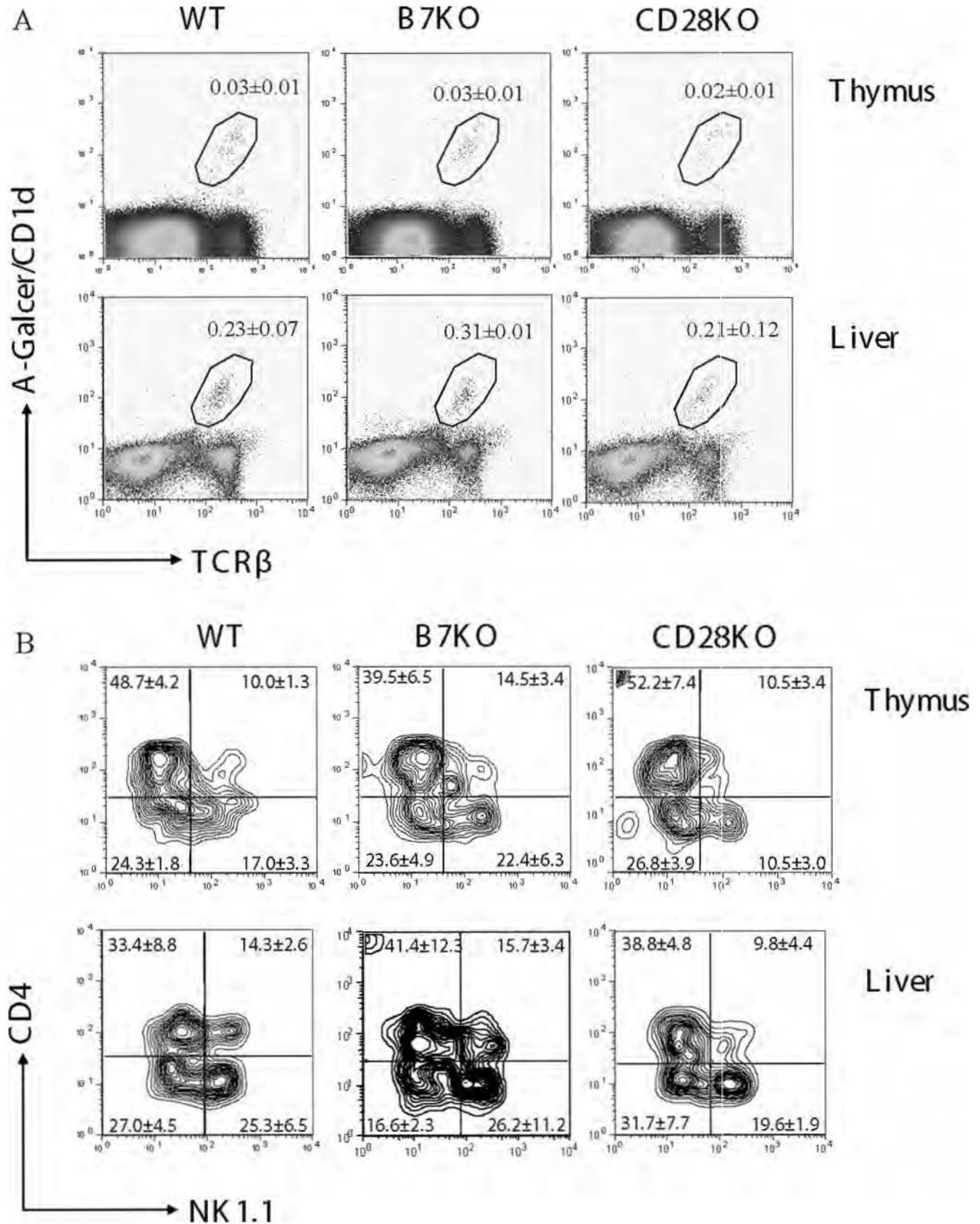


Figure 4. B7 and CD28 deficiency does not affect the generation of immature $iV\alpha 14$ NKT cells in young mice. Total lymphocytes from the thymus (upper panel) and liver (lower panel) of 8 day old WT (left), B7 1/2 (middle) and CD28 (right) deficient mice were analyzed. The numbers represent the percentage (Mean±SD, n=4) of $iV\alpha 14$ NKT cells (A) and the percentage (Mean±SD, n=4) of individual subsets from gated $iV\alpha 14$ NKT cells (B). One representative profile from each group is shown.
doi:10.1371/journal.pone.0002703.g004

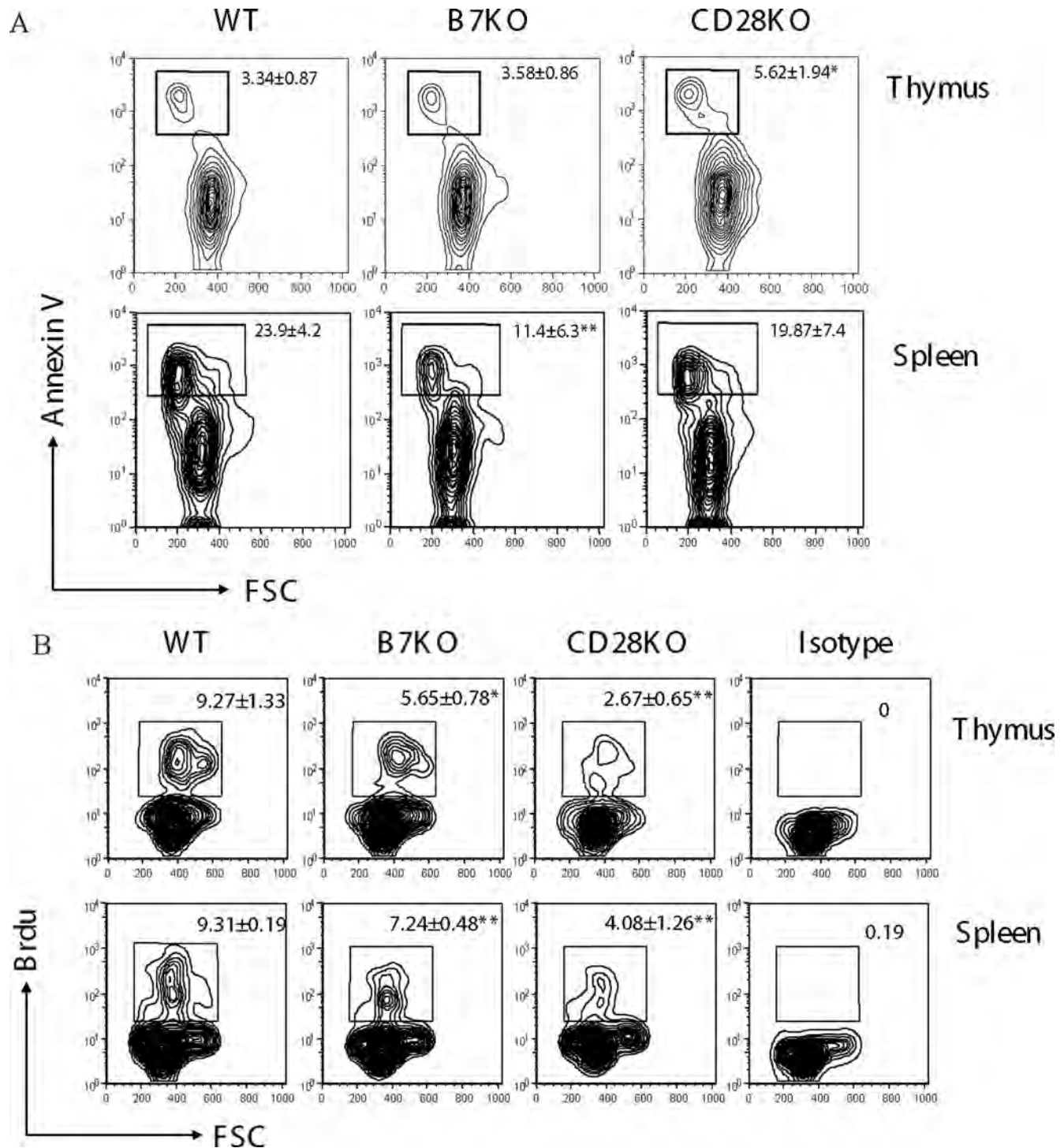


Figure 5. B7 CD28 interaction promotes proliferation but not survival of NKT cells. 5–7 week old WT, B7KO, CD28KO mice received intravenous injection of BrdU. The lymphocytes from the thymus (top) and spleen (bottom) were harvested 4 hours later and stained with antibodies for TCR β , NK1.1 and BrdU or with Annexin V. A. NKT cells that underwent apoptosis. The numbers represent the percentages (Mean±SD) of apoptotic cells among TCR β ⁺NK1.1⁺ cells and summarizing data from 2 independent experiments involving a total of 6 mice in the WT and CD28 mutant group, and 3 in B7 1/2 mutant mice. B. NKT cells undergo proliferation *in vivo* as revealed by incorporation of BrdU. The numbers in the panels indicate means and SD (n=3) of the percentages of NKT cells that have incorporated BrdU in the thymus. FITC conjugated mouse IgG $_{1, \kappa}$ was used as isotype control (right). One representative profile from each group is shown. doi:10.1371/journal.pone.0002703.g005

We have not observed increased proliferation of NKT in the periphery of the mutant mice. In fact, we have observed decreased proliferation of NKT in the mutant mice. However, we have

observed a decreased apoptosis of NKT cells in the spleens of B7 deficient mice. A similar trend was also observed in the CD28 deficient mice. The increased survival explains the lack of 1:1

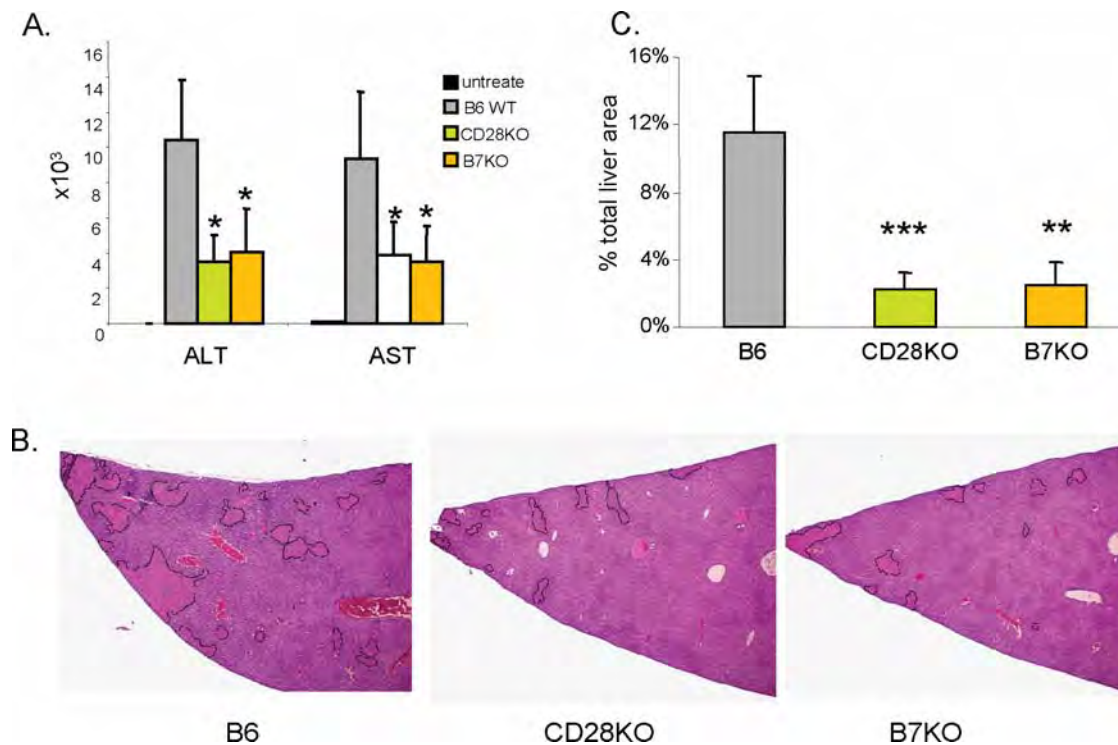


Figure 6. Con A induced hepatitis is alleviated in B7 and CD28 deficient mice. Eight week old B7KO, CD28KO and C57BL/6 mice received intravenous injection of Con A at a dose of 20 mg/kg. Sixteen hours later, serum and liver tissues from individual mice were harvested. A. Serum ALT and AST levels. B. One representative section from each group showing the pattern of liver injury. C. Average percentages of area with injuries from 3–4 sections per mouse and 4–5 mice per group. doi:10.1371/journal.pone.0002703.g006

correlation between the reduction in the thymus and that in the spleen and liver. Another unexplained observation is the more severe phenotype observed in CD28 deficient mice as compared to B7 deficient mice. Since B7 1/2 interacts with both CD28 and CTLA 4, it is theoretically possible to explain the discrepancies between B7 1/2 deficient mice and CD28 deficient mice by invoking an opposite function of these two receptors. The fact that the deficiency was observed in older mice and that the CTLA 4 deficient mice do not survive to adulthood have made it difficult to test this hypothesis.

Concanavalin A induced (ConA induced) hepatitis in mice is a well characterized model of T cell mediated inflammatory liver disease. Recently, it has been demonstrated that invariant NKT (iNKT) cells play a key role in the development of ConA induced hepatitis. Both $J\alpha 18^{-/-}$ and $CD1d^{-/-}$ mice that lack iNKT cells are resistant to ConA induced hepatic injury [37,38,48]. In addition, the adoptive transfer of hepatic mononuclear cells from wild type mice, but not from CD1 deficient mice, sensitized *gld* mice to Con A induced hepatitis [37]. The later results demonstrated that NKT cell, other than other cell, is the major mediator of the disease process. Here we demonstrated that the B7 1/2 and CD28 deficient mice are more resistant to the disease. In this model, IL 4 secreted by mainly $NK1.1^{+}iV\alpha 14$ NKT cells, was demonstrated to play a crucial role in causing NKT cells to express FasL and to contribute to Fas/FasL mediated liver injury in an autocrine fashion [37,38,42]. Although our presented data appear to refute a role for IL 4 production by NKT cells, this is likely due to the fact that the data presented was obtained at 6 hours when the peak of IL 4 production had waned [45,46]. In addition, IFN γ produced by $NK1.1^{+}iV\alpha 14$ NKT cells is also very important in mediating the disease process. IFN γ can activate

resident Kupffer cells and recruit macrophages to produce TNF α , which subsequently causes liver injury [37], induces proliferation and cytotoxicity of NK cells [40] and regulates IL 4 signaling as well as its own signaling through induced suppressor of cytokine signaling (SOCS 1) [41]. Thus, the significant reduction of $NK1.1^{+}iV\alpha 14$ NKT cells may alleviate Con A induced hepatitis in B7 and CD28 deficient mice by abrogating the production of IFN γ . This hypothesis is supported by our analysis of ex vivo NKT cells, which revealed reduced IFN γ producing cells following in vivo Con A stimulation.

Costimulatory pathways were traditionally viewed as critical modulators for the induction of T cell responses in peripheral lymphoid organs [49]. Subsequent studies in tumor [5–7] and autoimmune disease [8] models have revealed a critical contribution to the effector phase of T cell immunity. More recent studies expand its contribution to differentiation of immature thymocytes and negative selection of T cells [10,50]. In addition, the function of costimulatory molecules may extend beyond adaptive immunity, as several groups have suggested a role for the activation of NK cells [11]. Our data presented here demonstrate a role for T cell costimulation in both the development and function of NKT cells, which is widely regarded as a bridge between adaptive and innate immunity. Taken together, it is possible that costimulatory molecules modulate all major branches of cell mediated immunity, including T cells, NK cells and NKT cells.

Materials and Methods

Experimental animals

Wild type C57BL/6j, B7 1/2 double knockout and CD28 knockout mice on C57BL/6j background were purchased from

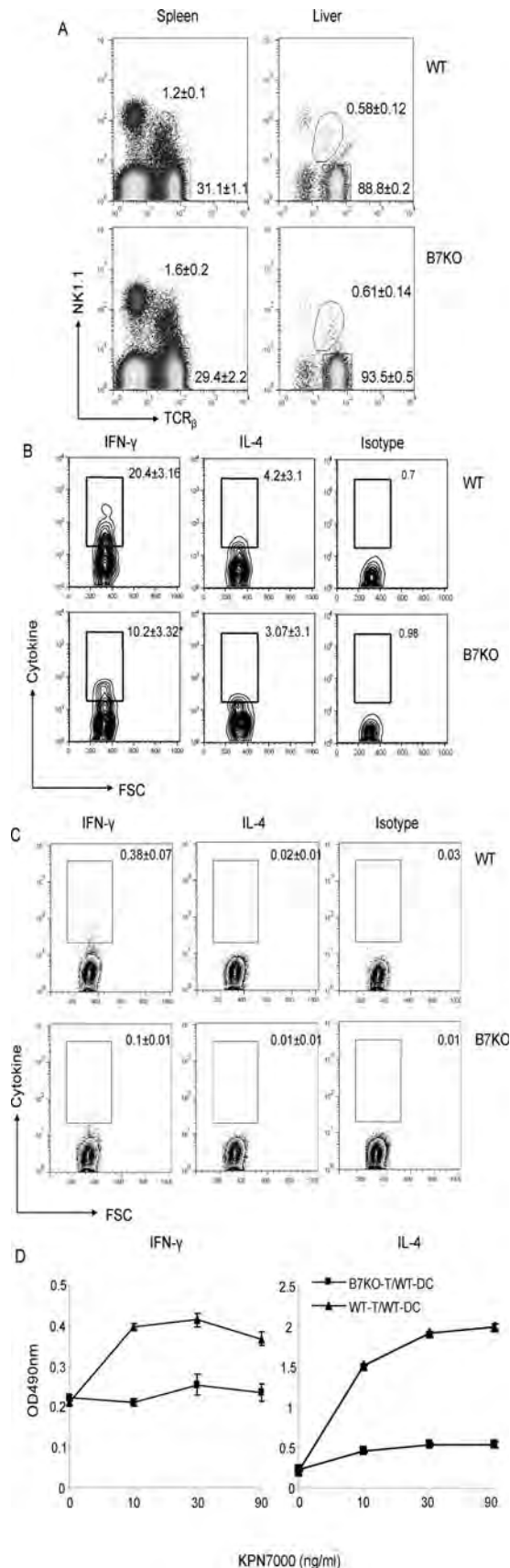


Figure 7. The reduction of IFN γ production among TCR β ⁺NK1.1⁺ cells isolated from the liver of B7 1/2 deficient mice.

Eight week old WT (top) and B7 1/2 (bottom) deficient mice received intravenous injection of Con A (25mg/kg). The mice were sacrificed six hours later. After perfusion the total number of mononuclear cells from the liver and spleen were stained with TCR β , NK1.1, anti mouse IFN γ or IL 4 mAbs, or fluorescence conjugated isotype control. A. The percentage of total NKT cells (NK1.1⁺TCR β ⁺) and conventional T cells (NK1.1⁻TCR β ⁺) in the spleen and liver from Non treated (left) and ConA treated mice (right). B. The percentage of cytokine producing cells among the NK1.1⁺TCR β ⁺ population. C. The percentage of cytokine producing cells among the NK1.1 TCR β ⁺ population. The numbers represent the percentage (Mean \pm SD) of one representative profile from each group is shown. The experiment was repeated twice; 7–8 mice were included in each group. D. Cytokine secretion of purified CD4 T cells from WT and B7KO mice stimulated by KRN7000. The numbers represent the profile of purified CD4 T cells from 3 mice in each group. The experiment was repeated twice. doi:10.1371/journal.pone.0002703.g007

the Jackson Laboratory (Bar Harbor, ME, USA). Different strains of Mice were maintained in the University Laboratory Animal Research Facility at The Ohio State University and The University of Michigan under specific pathogen free conditions. All animal experimental procedures were reviewed and approved by The Ohio State University and University of Michigan Institutional Animal Care and Use Committees.

Cell Preparation

Single cell suspensions from the thymus and spleen were prepared by mechanical disruption in cold, serum free RPMI 1640 medium. The liver was perfused with 1xPBS via portal vein. Then, the liver fragments were incubated with 1mg/ml Collagenase type IV (Sigma, C5138) in 10mM Hepes NaOH buffer (150 mM NaCl, 5 mM KCl, 1 mM MgCl₂ and 1.8 mM CaCl₂, pH 7.4) for 1 h at 37°C and gently dissociated. The whole material was passed through a syringe several times to get a single cell suspension. The liver mononuclear cells were recovered from the interface of 40% and 60% percoll after centrifugation. Red blood cells from single cell suspensions were removed by brief hypotonic lysis before cell surface staining.

Antibodies and flow cytometry

Both cell surface markers and intracellular staining were analyzed by flow cytometry (Becton Dickinson, Mountain View, CA). The fluorescein conjugated antibodies anti CD4 (GK1.5), anti CD8 (53 6.7), anti TCR β chain (H57 597), anti CD44 (IM7), anti CD25 (PC61) and anti NK1.1 (PK136) were purchased from BD Pharmingen (San Diego, CA, USA). Phycoerythrin conjugated α GalCer loaded CD1d tetramer was prepared as described [28,36]. The fixation and permeabilization solution kit (Cytofix/CytopermTM, BD Pharmingen) was used for intracellular staining according to the manufacturer's protocol. The samples were analyzed by flow cytometry. Data acquisition was performed on a FACSCalibur instrument with CELLQUEST software (Biosciences, Mountain View, CA), and data were analyzed using FLOWJO software (Tree Star, Inc., Ashland, OR).

Cell death and proliferation assay

The apoptotic lymphocytes were determined by their binding to Annexin V. After cell surface staining, the cells were resuspended in Annexin V (BD Pharmingen), dissolved in 10 mM Hepes, 140mM NaCl, 2.5mM CaCl₂ and stained at room temperature for 15 minutes and then analyzed within an hour. To measure the proliferation of lymphocytes *in vivo*, mice were injected intraperitoneally (i.p.) with BrdU (1 mg/mouse in 100 μ l PBS). Four hours later, the mice were sacrificed and single lymphocytes were

prepared. BrdU incorporation was detected by flow cytometry with a BrdU Flow Kit, as described by manufacturer (BD PharMingen).

Induction of ConA induced hepatitis

Con A (Sigma, C0412) was dissolved in pyrogen free PBS and i.v. injected into mice through the tail vein at a dose of 20mg/kg. Sera from individual mice were obtained 16 h after Con A injection. Alanine aminotransferase (ALT) and aspartate amino transferase (AST) activities were measured by the standard photometric method using Hitachi type 911 automatic analyzer (Tokyo). 25mg/kg Con A was used for short term stimulation, and the splenocytes and hepatocytes were harvested 6 hours later for intracellular cytokine staining.

Histological Examination

The livers from Con A treated mice were harvested after 16 h and then fixed in 10% formalin, embedded in paraffin, sectioned and stained with hematoxylin and eosin for histological examination. Specimens were examined under a light microscope. 3–4 images were collected from each section and the injured area was measured with MCID Analysis 7.0 (Imaging Research Inc., Ontario, Canada).

In vitro stimulation of purified CD4 cells with α -Galactosylceramide

Spleens were harvested from 10–12 weeks old WT C57BL/6 and B7 1/2 mutant mice. Single cell suspension were treated for 45 min with 400 U ml⁻¹ collagenase type IV and 50 μ g ml⁻¹ DNase I (Boehringer, Mannheim, Germany) before were

incubated with anti CD11c coated magnetic beads. CD11c⁺ cells were positively selected according to the manufacturer's procedure (Miltenyi Biotec, Bergisch Gladbach, Germany). Then all the flow through was depleted with antibody mixture containing rat monoclonal antibodies against mouse CD45R (B220), CD11b (Mac1), CD16/32(2.4G2), CD11c (HB224) and CD8 (TIB210) according to manufacturer's manual (DYNAL, Oslo, Norway). Cell suspensions contained about 90% of CD11c⁺ cells and CD4⁺ cells respectively. After purification, 7 \times 10⁵ CD4 cells from either WT C57BL/6 or B7 1/2 mutant mice were co cultured with 3 \times 10⁵ CD11c⁺ cells in 1ml Bruff's medium containing different concentration of α Galactosylceramide (KRN7000). 48 hours later, the supernatant was harvest for the detection of secreted INF γ and IL 4 with ELISA. The relative amounts of cytokines were shown by absorbance read at 490nm (OD490nm).

Statistical Analysis

Data were statistically analyzed with two tailed student T test. P<0.05 is significant and p<0.01 is highly significant.

Acknowledgments

We thank Lynde Shaw for her editorial assistance. Part of the study was carried out while the authors were at The Ohio State University.

Author Contributions

Conceived and designed the experiments: XZ YL PZ. Performed the experiments: XZ HZ LY. Analyzed the data: XZ YL PZ. Contributed reagents/materials/analysis tools: CRW. Wrote the paper: XZ YL PZ.

References

- Norton SD, Zuckerman L, Urdahl KB, Shefner R, Miller J, et al. (1992) The CD28 ligand, B7, enhances IL-2 production by providing a costimulatory signal to T cells. *J Immunol* 149: 1556–1561.
- Harding FA, Allison JP (1993) CD28-B7 interactions allow the induction of CD8⁺ cytotoxic T lymphocytes in the absence of exogenous help. *J Exp Med* 177: 1791–1796.
- Harding FA, McArthur JG, Gross JA, Raulat DH, Allison JP (1992) CD28-mediated signalling co-stimulates murine T cells and prevents induction of anergy in T-cell clones. *Nature* 356: 607–609.
- Carreno BM, Collins M (2002) The B7 family of ligands and its receptors: new pathways for costimulation and inhibition of immune responses. *Annu Rev Immunol* 20: 29–53.
- Ramarathinam L, Castle M, Wu Y, Liu Y (1994) T cell costimulation by B7/BB1 induces CD8 T cell-dependent tumor rejection: an important role of B7/BB1 in the induction, recruitment, and effector function of antitumor T cells. *J Exp Med* 179: 1205–1214.
- Sarma S, Guo Y, Guilloux Y, Lee C, Bai X-F, et al. (1999) Cytotoxic T lymphocytes to an unmutated tumor antigen P1A: normal development but restrained effector function. *J Exp Med* 189: 811–820.
- Bai XF, Bender J, Liu J, Zhang H, Wang Y, et al. (2001) Local costimulation reinvigorates tumor-specific cytolytic T lymphocytes for experimental therapy in mice with large tumor burdens. *J Immunol* 167: 3936–3943.
- Chang TT, Jabs C, Sobel RA, Kuchroo VK, Sharpe AH (1999) Studies in B7-deficient mice reveal a critical role for B7 costimulation in both induction and effector phases of experimental autoimmune encephalomyelitis. *J Exp Med* 190: 733–740.
- Dong C, Juedes AE, Temann UA, Shrestha S, Allison JP, et al. (2001) ICOS costimulatory receptor is essential for T-cell activation and function. *Nature* 409: 97–101.
- Zheng X, Gao JX, Chang X, Wang Y, Liu Y, et al. (2004) B7-CD28 interaction promotes proliferation and survival but suppresses differentiation of CD4-CD8⁺ T cells in the thymus. *J Immunol* 173: 2253–2261.
- Gao JX, Liu X, Wen J, Caligiuri MA, Stroynowski I, et al. (2003) Two-signal requirement for activation and effector function of natural killer cell response to allogeneic tumor cells. *Blood*.
- Taniguchi M, Seino K, Nakayama T (2003) The NKT cell system: bridging innate and acquired immunity. *Nat Immunol* 4: 1164–1165.
- Taniguchi M, Harada M, Kojima S, Nakayama T, Wakao H (2003) The regulatory role of Valpha14 NKT cells in innate and acquired immune response. *Annu Rev Immunol* 21: 483–513.
- Bendelac A, Lantz O, Quimby ME, Yewdell JW, Bennink JR, et al. (1995) CD1 recognition by mouse NK1+ T lymphocytes. *Science* 268: 863–865.
- Bendelac A, Rivera MN, Park SH, Roark JH (1997) Mouse CD1-specific NK1 T cells: development, specificity, and function. *Annu Rev Immunol* 15: 535–562.
- Kronenberg M, Gapin L (2002) The unconventional lifestyle of NKT cells. *Nat Rev Immunol* 2: 557–568.
- Matsuda JL, Gapin L, Baron JL, Sidobre S, Stetson DB, et al. (2003) Mouse V alpha 14 natural killer T cells are resistant to cytokine polarization in vivo. *Proc Natl Acad Sci U S A* 100: 8395–8400.
- Stetson DB, Mohrs M, Reinhardt RL, Baron JL, Wang ZE, et al. (2003) Constitutive cytokine mRNAs mark natural killer (NK) and NK T cells poised for rapid effector function. *J Exp Med* 198: 1069–1076.
- Van Dommelen SL, Degli-Esposti MA (2004) NKT cells and viral immunity. *Immunol Cell Biol* 82: 332–341.
- Swann J, Crowe NY, Hayakawa Y, Godfrey DI, Smyth MJ (2004) Regulation of antitumor immunity by CD1d-restricted NKT cells. *Immunol Cell Biol* 82: 323–331.
- Van Kaer L (2004) Natural killer T cells as targets for immunotherapy of autoimmune diseases. *Immunol Cell Biol* 82: 315–322.
- MacDonald HR (2002) Immunology. T before NK. *Science* 296: 481–482.
- MacDonald HR (2002) Development and selection of NKT cells. *Curr Opin Immunol* 14: 250–254.
- Gapin L, Matsuda JL, Surh CD, Kronenberg M (2001) NKT cells derive from double-positive thymocytes that are positively selected by CD1d. *Nat Immunol* 2: 971–978.
- Pellicci DG, Uldrich AP, Kyparissoudis K, Crowe NY, Brooks AG, et al. (2003) Intrathymic NKT cell development is blocked by the presence of alpha-galactosylceramide. *Eur J Immunol* 33: 1816–1823.
- Benlagha K, Kyin T, Beavis A, Teyton L, Bendelac A (2002) A thymic precursor to the NK T cell lineage. *Science* 296: 553–555.
- Pellicci DG, Hammond KJ, Uldrich AP, Baxter AG, Smyth MJ, et al. (2002) A natural killer T (NKT) cell developmental pathway involving a thymus-dependent NK1.1(-)CD4(+) CD1d-dependent precursor stage. *J Exp Med* 195: 835–844.
- Chun T, Page MJ, Gapin L, Matsuda JL, Xu H, et al. (2003) CD1d-expressing dendritic cells but not thymic epithelial cells can mediate negative selection of NKT cells. *J Exp Med* 197: 907–918.
- Emoto M, Kaufmann SH (2003) Liver NKT cells: an account of heterogeneity. *Trends Immunol* 24: 364–369.

30. Crispe IN (2003) Hepatic T cells and liver tolerance. *Nat Rev Immunol* 3: 51–62.
31. Exley MA, Koziel MJ (2004) To be or not to be NKT: natural killer T cells in the liver. *Hepatology* 40: 1033–1040.
32. Eberl G, Lees R, Smiley ST, Taniguchi M, Grusby MJ, et al. (1999) Tissue-specific segregation of CD1d-dependent and CD1d-independent NK T cells. *J Immunol* 162: 6410–6419.
33. Hammond KJ, Pelikan SB, Crowe NY, Randle-Barrett E, Nakayama T, et al. (1999) NKT cells are phenotypically and functionally diverse. *Eur J Immunol* 29: 3768–3781.
34. Kawano T, Cui J, Koezuka Y, Toura I, Kaneko Y, et al. (1997) CD1d-restricted and TCR-mediated activation of valpha14 NKT cells by glycosylceramides. *Science* 278: 1626–1629.
35. Benlagha K, Weiss A, Beavis A, Teyton L, Bendelac A (2000) In vivo identification of glycolipid antigen-specific T cells using fluorescent CD1d tetramers. *J Exp Med* 191: 1895–1903.
36. Matsuda JL, Naidenko OV, Gapin L, Nakayama T, Taniguchi M, et al. (2000) Tracking the response of natural killer T cells to a glycolipid antigen using CD1d tetramers. *J Exp Med* 192: 741–754.
37. Takeda K, Hayakawa Y, Van Kaer L, Matsuda H, Yagita H, et al. (2000) Critical contribution of liver natural killer T cells to a murine model of hepatitis. *Proc Natl Acad Sci U S A* 97: 5498–5503.
38. Kaneko Y, Harada M, Kawano T, Yamashita M, Shibata Y, et al. (2000) Augmentation of Valpha14 NKT cell-mediated cytotoxicity by interleukin 4 in an autocrine mechanism resulting in the development of concanavalin A-induced hepatitis. *J Exp Med* 191: 105–114.
39. Kusters S, Gantner F, Kunstle G, Tiegs G (1996) Interferon gamma plays a critical role in T cell-dependent liver injury in mice initiated by concanavalin A. *Gastroenterology* 111: 462–471.
40. Eberl G, MacDonald HR (2000) Selective induction of NK cell proliferation and cytotoxicity by activated NKT cells. *Eur J Immunol* 30: 985–992.
41. Naka T, Tsutsui H, Fujimoto M, Kawazoe Y, Kohzaki H, et al. (2001) SOCS-1/SSI-1-deficient NKT cells participate in severe hepatitis through dysregulated cross-talk inhibition of IFN-gamma and IL-4 signaling in vivo. *Immunity* 14: 535–545.
42. Jaruga B, Hong F, Sun R, Radaeva S, Gao B (2003) Crucial role of IL-4/STAT6 in T cell-mediated hepatitis: up-regulating eotaxins and IL-5 and recruiting leukocytes. *J Immunol* 171: 3233–3244.
43. Louis H, Le Moine A, Flamand V, Nagy N, Quertinmont E, et al. (2002) Critical role of interleukin 5 and eosinophils in concanavalin A-induced hepatitis in mice. *Gastroenterology* 122: 2001–2010.
44. Sun R, Tian Z, Kulkarni S, Gao B (2004) IL-6 prevents T cell-mediated hepatitis via inhibition of NKT cells in CD4+ T cell- and STAT3-dependent manners. *J Immunol* 172: 5648–5655.
45. Sass G, Heinlein S, Agli A, Bang R, Schumann J, et al. (2002) Cytokine expression in three mouse models of experimental hepatitis. *Cytokine* 19: 115–120.
46. Hayakawa Y, Takeda K, Yagita H, Van Kaer L, Saiki I, et al. (2001) Differential regulation of Th1 and Th2 functions of NKT cells by CD28 and CD40 costimulatory pathways. *J Immunol* 166: 6012–6018.
47. Issa-Chergui B, Goldner-Sauve A, Colle E, Prud'homme GJ, Lapchak PH, et al. (1988) Class I and II major histocompatibility complex gene product expression by a rat insulinoma cell line in vitro following exposure to gamma interferon. *Diabetologia* 31: 675–680.
48. Diao H, Kon S, Iwabuchi K, Kimura C, Morimoto J, et al. (2004) Osteopontin as a mediator of NKT cell function in T cell-mediated liver diseases. *Immunity* 21: 539–550.
49. Frauwirth KA, Thompson CB (2002) Activation and inhibition of lymphocytes by costimulation. *J Clin Invest* 109: 295–299.
50. Gao J-X, Zhang H, Bai XF, Wen J, Zheng X, et al. (2002) Peripheral blockade of B7-1 and B7-2 inhibits clonal deletion of highly pathogenic autoreactive T cells. *J Exp Med* 195: 959–971.